

A QUINTIC \mathbb{Z}_2 -EQUIVARIANT LIÉNARD SYSTEM ARISING FROM THE COMPLEX GINZBURG-LANDAU EQUATION: (II)

HEBAI CHEN¹, XINGWU CHEN², MAN JIA¹ AND YILEI TANG³

ABSTRACT. We continue to study a quintic \mathbb{Z}_2 -equivariant Liénard system $\dot{x} = y$, $\dot{y} = -(a_0x + a_1x^3 + a_2x^5) - (b_0 + b_1x^2)y$ with $a_2b_1 \neq 0$, arising from the complex Ginzburg-Landau equation. Global dynamics of the system have been studied in [*SIAM J. Math. Anal.*, **55**(2023) 5993-6038] when the sum of the indices of all equilibria is -1 , i.e., $a_2 < 0$. The aim of this paper is to study the global dynamics of this quintic Liénard system when the sum of the indices of all equilibria is 1 , i.e., $a_2 > 0$.

1. INTRODUCTION AND MAIN RESULTS

With the aid of appropriate traveling wave transformations, numerous nonlinear partial differential equations (PDEs) can be transformed into manageable nonlinear ordinary differential equations (ODEs). Among these transformed equations, Liénard equations occupy a significant position. Named after the French mathematician Liénard, these ODEs are characterized by the form:

$$\ddot{x} + f(x)\dot{x} + g(x) = 0$$

where x represents the dependent variable, \dot{x} denotes its derivative with respect to an independent variable (often time), and $f(x)$ and $g(x)$ are nonlinear functions of x . Liénard equations are a significant class of ODEs, extensively utilized in various fields such as electrical mechanics, mechanical engineering, physics, finance systems and biomedical systems, providing crucial insights into system behaviors. These equations are particularly valuable because many complex mathematical models can be transformed into a Liénard-type system, allowing researchers to study their dynamic behaviors more effectively. This transformation facilitates a deeper understanding of the underlying principles governing these systems, making the Liénard equations a powerful tool in theoretical and applied research. For further insights and detailed studies on the applications and transformations involving Liénard equations, one can refer to sources such as [1, 5, 6, 7, 16, 18, 22, 24] and the references therein.

In this paper, we continue our study of global dynamics for the quintic \mathbb{Z}_2 -equivariant Liénard system

$$(1) \quad \begin{aligned} \dot{x} &= y, \\ \dot{y} &= -(a_0x + a_1x^3 + a_2x^5) - (b_0 + b_1x^2)y \end{aligned}$$

where $(a_0, a_1, a_2, b_0, b_1) \in \mathbb{R}^5$ and $a_2b_1 \neq 0$. Feng [12, 13] proved that certain uniformly translating solutions of the complex Ginzburg-Landau equation

$$\begin{aligned} u_t &= \alpha u + (b_1 + ic_1)u_{xx} - (b_2 - ic_2)|u|^2u - (b_3 - ic_3)|u|^4u \\ &\quad + (b_4 + ic_4)(|u|^2u)_x + (b_5 + ic_5)(|u|^2)_xu \end{aligned}$$

can be converted to solutions of the Liénard system (1). The Ginzburg-Landau equation, a classic nonlinear PDE, has garnered significant attention from researchers, see [2, 14, 15, 17, 19, 20, 21, 23] and the references therein. As demonstrated in [5], system (1) is also a versal unfolding of the following degenerate system $\dot{x} = y$, $\dot{y} = -a_2x^5 - b_1x^2y$ within the \mathbb{Z}_2 -equivariant class for sufficiently small $|a_0|$, $|a_1|$ and $|b_0|$.

2010 *Mathematics Subject Classification.* 34C29, 34C25, 47H11.

Key words and phrases. Ginzburg-Landau equation; Liénard system; limit cycle; bifurcation; global phase portrait.

For system (1), we have completely investigated its global dynamics in [5] for the case $a_2 < 0$ (saddle case), i.e, the sum of the indices of all equilibria is -1 . In this paper, our focus shifts to the case $a_2 > 0$ focus case), i.e., the sum of the indices of all equilibria is $+1$. With a linear transformation $(x, y) \rightarrow (a_2^{-1/4}x, a_2^{-1/4}y)$, system (1) is rewritten as

$$(2) \quad \begin{aligned} \dot{x} &= y, \\ \dot{y} &= -(\mu_1 x + \mu_2 x^3 + x^5) - (\mu_3 + bx^2)y =: -g(x) - f(x)y, \end{aligned}$$

where $(\mu_1, \mu_2, \mu_3, b) = (a_0, a_1 a_2^{-1/2}, b_0, b_1 a_2^{-1/2}) \in \mathbb{R}^4$ and $b \neq 0$. Since system (2) is invariant under the transformation $(y, t, \mu_3, b) \rightarrow (-y, -t, -\mu_3, -b)$, we only need to study the case $b > 0$.

For system (2), Dangelmayr et al. [9] gave some cross sections of local bifurcation diagram in a small neighborhood of $(\mu_1, \mu_2, \mu_3) = (0, 0, 0)$ and some local phase portraits near the origin, without a detailed quantitative analysis. Actually, one can find that the quantitative proof is indeed non-trivial in a small neighborhood of $(\mu_1, \mu_2, \mu_3) = (0, 0, 0)$ as shown in this paper. For the convenience to read, we present the main results of this paper here.

Clearly, system (2) has a unique equilibrium as (μ_1, μ_2) belongs to the region

$$\mathcal{G}_1 := \{(\mu_1, \mu_2) \in \mathbb{R}^2 : \mu_2^2 - 4\mu_1 < 0, \mu_2 < 0\} \cup \{(\mu_1, \mu_2) \in \mathbb{R}^2 : \mu_1 \geq 0, \mu_2 \geq 0\}$$

and at least three equilibria as (μ_1, μ_2) belongs to the region

$$\mathcal{G}_2 := \{(\mu_1, \mu_2) \in \mathbb{R}^2 : \mu_2^2 - 4\mu_1 \geq 0, \mu_2 < 0\} \cup \{(\mu_1, \mu_2) \in \mathbb{R}^2 : \mu_1 < 0, \mu_2 \geq 0\}.$$

Theorem 1. *System (2) has a unique equilibrium if and only if $(\mu_1, \mu_2) \in \mathcal{G}_1$. Furthermore, system (2) has a unique limit cycle as $\mu_3 < 0$ and no limit cycles as $\mu_3 \geq 0$, and all global phase portraits in the Poincaré disc are shown in Figure 1.*

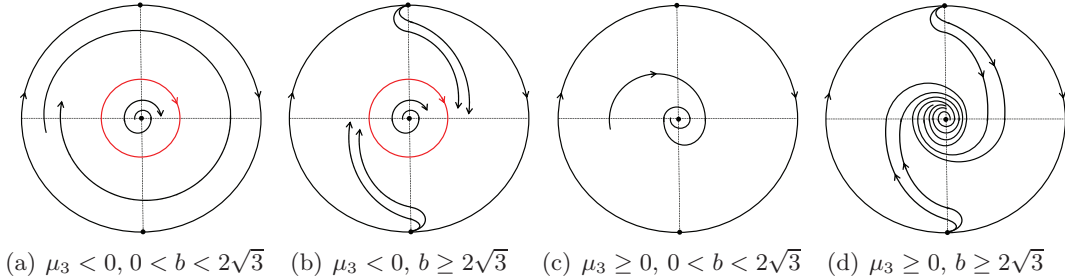


FIGURE 1. Global phase portraits of (2) in \mathcal{G}_1 .

Consider $(\mu_1, \mu_2) \in \mathcal{G}_2$. By the following scaling transformation

$$(3) \quad (x, y, t) \rightarrow \left(sx, s^3 y, \frac{1}{s^2} t \right),$$

system (2) is changed into

$$(4) \quad \begin{aligned} \dot{x} &= y, \\ \dot{y} &= -x(a_1 + x^2)(-1 + x^2) - \delta(a_2 + x^2)y =: -\hat{g}(x) - \hat{f}(x)y, \end{aligned}$$

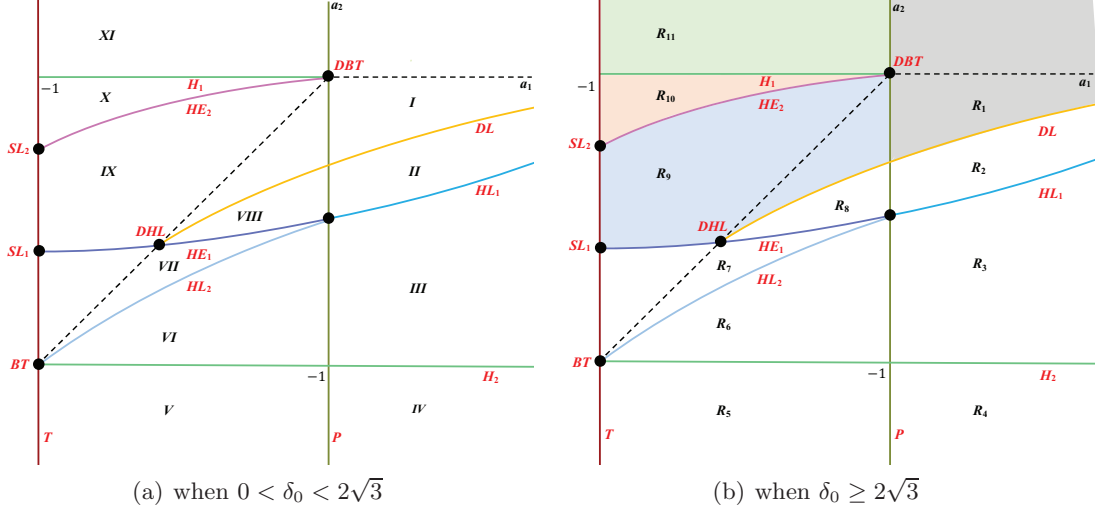
where

$$(a_1, a_2, \delta) := \left(\frac{\mu_2}{s^2} + 1, \frac{\mu_3}{b s^2}, b \right) \in [-1, +\infty) \times (-\infty, +\infty) \times (0, +\infty) =: \Omega$$

and

$$s := \sqrt{\frac{-\mu_2 + \sqrt{\mu_2^2 - 4\mu_1}}{2}} \neq 0.$$

It is clear that system (4) has three equilibria $\hat{E}_{l2} := (-1, 0)$, $\hat{E}_0 := (0, 0)$, $\hat{E}_{r2} := (1, 0)$, and two additional equilibria $\hat{E}_{l1} := (-\sqrt{-a_1}, 0)$, $\hat{E}_{r1} := (\sqrt{-a_1}, 0)$ if $-1 < a_1 < 0$.


 FIGURE 2. The slice $\delta = \delta_0$ of bifurcation diagram of (4).

Theorem 2. Given $\delta = \delta_0 > 0$, the cross-section of the global bifurcation diagram of system (4) is given in Figure 2. Bifurcation diagram of system (4) consists of the following bifurcation sets:

(i): There is a pitchfork bifurcation surface

$$P := \{(a_1, a_2, \delta) \in \Omega \mid a_1 = 0\}.$$

(ii): There is a transcritical bifurcation surface

$$T := \{(a_1, a_2, \delta) \in \Omega \mid a_1 = -1\}$$

for \hat{E}_{l2} and \hat{E}_{r2} .

(iii): There are a supcritical Hopf bifurcation surface

$$H_1 := \{(a_1, a_2, \delta) \in \Omega \mid -1 \leq a_1 < 0 \text{ and } a_2 = 0\}$$

for \hat{E}_0 and a subcritical Hopf bifurcation surface

$$H_2 := \{(a_1, a_2, \delta) \in \Omega \mid a_1 > -1 \text{ and } a_2 = -1\}$$

for \hat{E}_{l2} and \hat{E}_{r2} .

(iv): There is a degenerate Bogdanov-Takens bifurcation curve

$$DBT := \{(a_1, a_2, \delta) \in \Omega \mid a_1 = a_2 = 0\}$$

for \hat{E}_0 , which is the intersection of H_1 and P .

(v): There is a Bogdanov-Takens bifurcation curve

$$BT := \{(a_1, a_2, \delta) \in \Omega \mid a_1 = a_2 = -1\}$$

for \hat{E}_{l2} and \hat{E}_{r2} , which is the intersection of H_2 and T .

(vi): There is a degenerate equilibrium bifurcation surface

$$DE := \{(a_1, a_2, \delta) \in \Omega \mid \delta = 2\sqrt{3}\}$$

for equilibria at infinity.

(vii): There are two homoclinic bifurcation surfaces

$$HL_1 := \{(a_1, a_2, \delta) \in \Omega \mid a_2 = \varphi_1(a_1, \delta), a_1 \geq 0\},$$

$$HL_2 := \{(a_1, a_2, \delta) \in \Omega \mid a_2 = \varphi_2(a_1, \delta), -1 < a_1 < 0\},$$

where φ_1, φ_2 are continuous, $\varphi_1(a_1, \delta) \in (-1, -1/3)$ and $\varphi_2(a_1, \delta) \in (-1, \min\{-1/3, a_1\})$.

(viii): There are two 2-saddle loop bifurcation surfaces

$$\begin{aligned} HE_1 &:= \{(a_1, a_2, \delta) \in \Omega \mid a_2 = \varphi_3(a_1, \delta), -1 < a_1 < 0\}, \\ HE_2 &:= \{(a_1, a_2, \delta) \in \Omega \mid a_2 = \varphi_4(a_1, \delta), -1 < a_1 < 0\}, \end{aligned}$$

where $\varphi_3(a_1, \delta) \in (\varphi_2(a_1, \delta), 0)$ and $\varphi_4(a_1, \delta) \in (\max\{\varphi_3(a_1, \delta), -1/3\}, 0)$ are continuous.

(ix): There is a double limit cycle bifurcation surface

$$DL := \{(a_1, a_2, \delta) \in \Omega \mid a_2 = \varphi_5(a_1, \delta), a_1 > a^*\},$$

where $\varphi_5(a^*, \delta) = \varphi_3(a^*, \delta) = a^* < -1/3$, $\varphi_5(a_1, \delta) \in (\varphi_3(a_3, \delta), \min\{-1/3, a_1\})$ for $a^* < a_1 < 0$ and $\varphi_5(a_1, \delta) \in (\varphi_1(a_3, \delta), -1/3)$ for $a_1 \geq 0$.

(x): There are infinitely many heteroclinic bifurcation surfaces $SC_{1,i}$, $SC_{2,i}$ for \hat{E}_0 and equilibria at infinity, given by

$$SC_{k,i} := \{(a_1, a_2, \delta) \in \Omega \mid a_2 = \psi_{k,i}(a_1, \delta), a_1 \geq 0, \delta \geq 2\sqrt{3}\},$$

for $k = 1, 2$ and $i \in \mathbb{N}$ respectively, where $\psi_{1,i}, \psi_{2,i}$ ($i \in \mathbb{N}$) are continuous, $\psi_{1,i}(a_1, \delta) > \psi_{2,i}(a_1, \delta) > \psi_{1,i+1}(a_1, \delta) > \psi_{2,i+1}(a_1, \delta) > \varphi_5(a_1, \delta)$.

(xi): There are infinitely many heteroclinic bifurcation surfaces $SC_{3,i}$, $SC_{4,i}$, $SC_{5,i}$, $SC_{6,i}$ for the stable manifolds \hat{E}_{r1} , \hat{E}_{l1} and equilibria at infinity, given by

$$SC_{k,i} := \{(a_1, a_2, \delta) \in \Omega \mid a_2 = \psi_{k,i}(a_1, \delta), -1 \leq a_1 < 0, \delta \geq 2\sqrt{3}\}$$

for $k = 3, 4, 5, 6$ and $i \in \mathbb{N}$ respectively, where $\psi_{3,i}, \psi_{4,i}, \psi_{5,i}, \psi_{6,i}$ ($i \in \mathbb{N}^*$) are continuous, $\psi_{3,i}(a_1, \delta) > \psi_{4,i}(a_1, \delta) > \psi_{5,i}(a_1, \delta) > \psi_{6,i}(a_1, \delta) > \psi_{3,i+1}(a_1, \delta) > \psi_{4,i+1}(a_1, \delta) > \psi_{5,i+1}(a_1, \delta) > \psi_{6,i+1}(a_1, \delta)$.

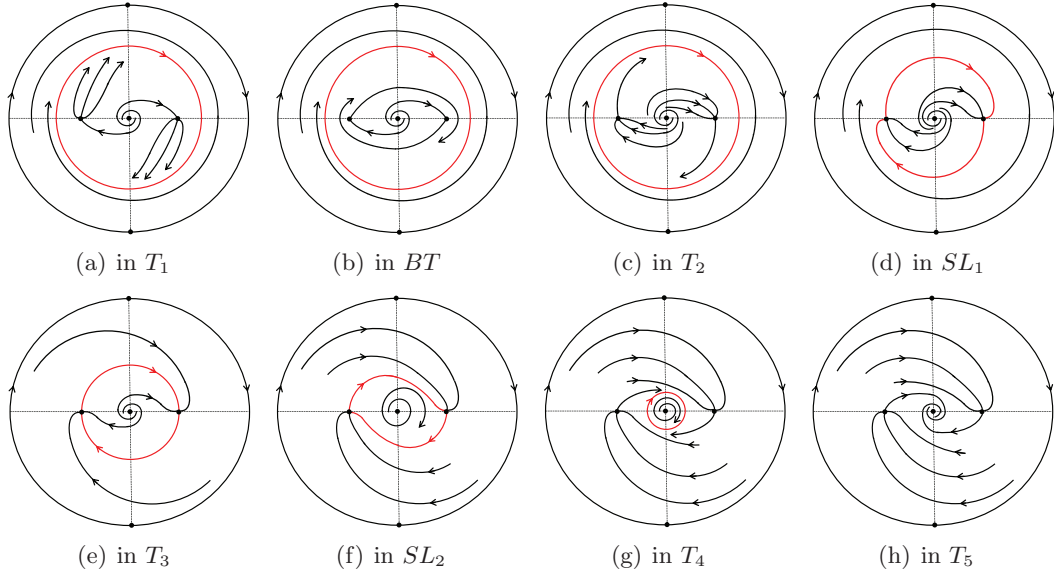


FIGURE 3. Global phase portraits of (4) for $0 < \delta_0 < 2\sqrt{3}$ and $a_1 = -1$.

Theorem 3. Given $\delta = \delta_0 > 0$, all global phase portraits in the Poincaré disc of system (4) are given in Figures 3–8, where the parameter regions for characterizing different global phase portraits are presented in Appendix A. Moreover, system (4) has at most four limit cycles.

In Theorem 3, we get an upper bound 4 of the number of limit cycles for system (4). However, by the numerical simulations we obtain a unique large limit cycle when there are two small limit cycles, and two large limit cycles when there is no small ones. Associated with symmetry of system (4), we conjecture that the maximum number of limit cycles is exactly 3.

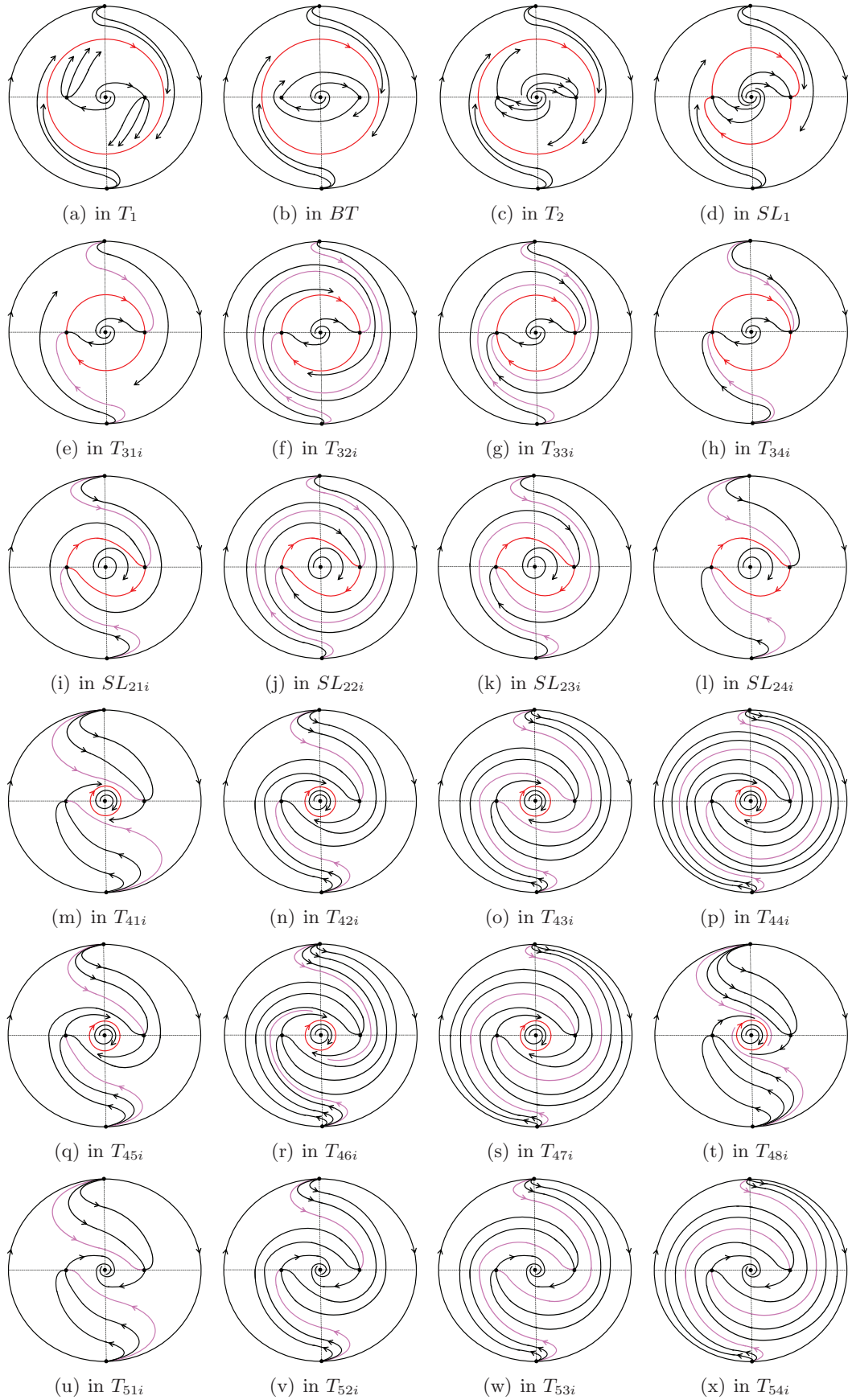


FIGURE 4. Global phase portraits of (4) for $\delta_0 \geq 2\sqrt{3}$ and $a_1 = -1$.

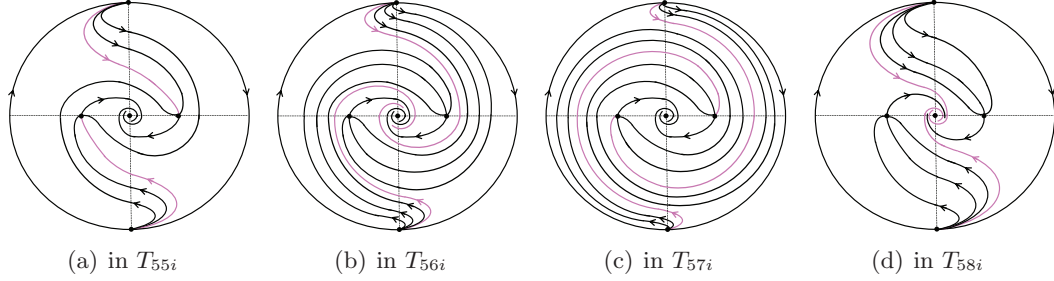
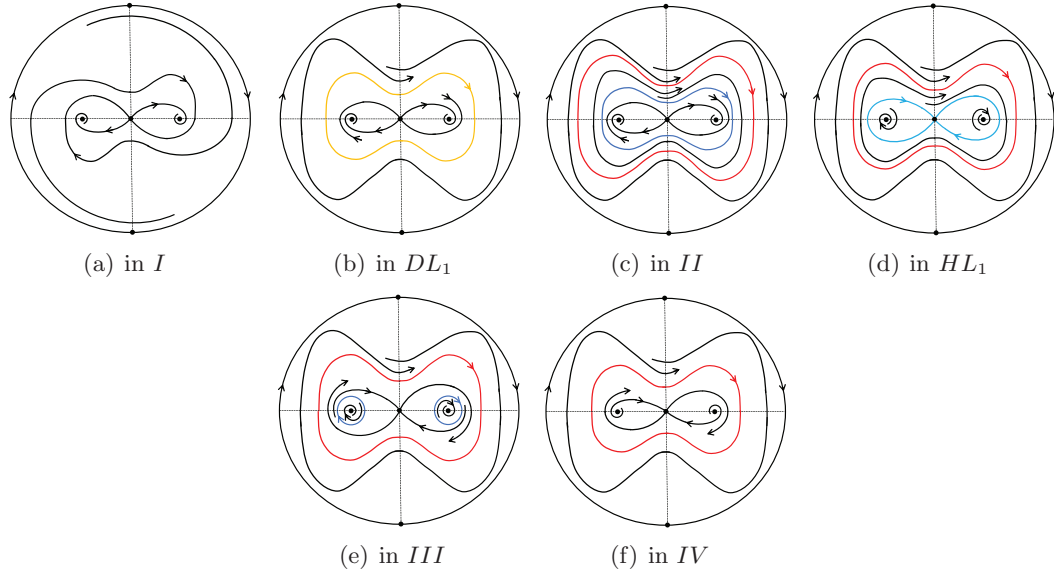


FIGURE 4. Continued.

FIGURE 5. Global phase portraits of (4) for $0 < \delta_0 < 2\sqrt{3}$ and $a_1 \geq 0$.

The remainder of this paper is organized as follows. We study the qualitative properties of equilibria and local bifurcation of system (2) in Section 2. Section 3 is devoted to the research of limit cycles, heteroclinic loops and homoclinic loops of system (2). The proofs of our main Theorems 1-3 are presented in Section 4 as well as some numerical examples.

2. LOCAL BIFURCATION

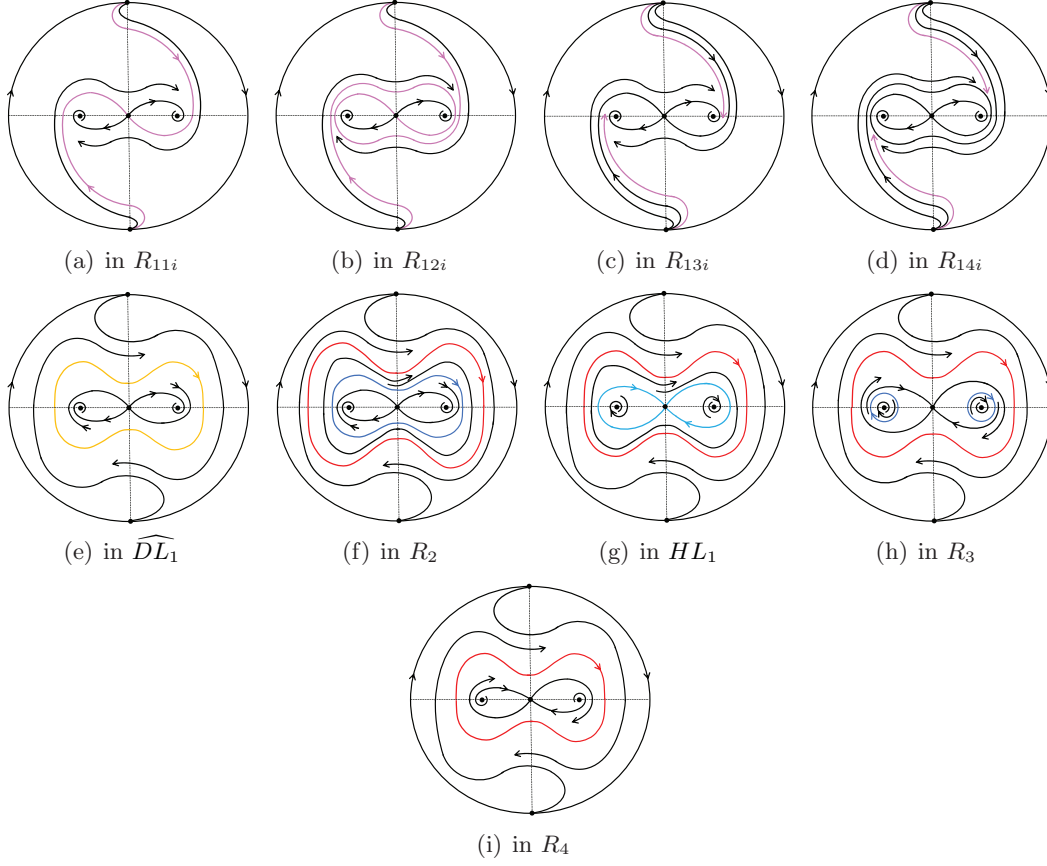
We firstly give the qualitative properties of equilibria of system (2) and please refer to Appendix B for a comprehensive proof.

Lemma 4. *For any $(\mu_1, \mu_2, \mu_3, b) \in \mathbb{R}^3 \times \mathbb{R}^+$, equilibria of system (2) and their properties are given in Table 1, where $E_0 := (0, 0)$ and*

$$E_{l2} := \left(-\sqrt{\frac{-\mu_2 + \sqrt{\mu_2^2 - 4\mu_1}}{2}}, 0 \right), \quad E_{l1} := \left(-\sqrt{\frac{-\mu_2 - \sqrt{\mu_2^2 - 4\mu_1}}{2}}, 0 \right),$$

$$E_{r1} := \left(\sqrt{\frac{-\mu_2 - \sqrt{\mu_2^2 - 4\mu_1}}{2}}, 0 \right), \quad E_{r2} := \left(\sqrt{\frac{-\mu_2 + \sqrt{\mu_2^2 - 4\mu_1}}{2}}, 0 \right).$$

Note that the qualitative properties of equilibria of system (4) are easily obtained by the scaling transformation (3). We find the following local bifurcations in system (2).


 FIGURE 6. Global phase portraits of (4) for $\delta_0 \geq 2\sqrt{3}$ and $a_1 \geq 0$.

Proposition 5. For any $(\mu_1, \mu_2, \mu_3, b) \in \mathbb{R}^3 \times \mathbb{R}^+$, system (2) includes the following bifurcation surfaces.

(i): There are two pitchfork bifurcation surfaces P_1 and P_2 , given by

$$\mu_1 = 0 \text{ and } \mu_2 > 0$$

and

$$\mu_1 = 0 \text{ and } \mu_2 < 0,$$

respectively. For $\mu_1 < 0$, there are three equilibria E_{l2}, E_0 and E_{r2} , E_0 is a saddle, while E_{l2} and E_{r2} are antisaddles. For $0 < \mu_1 < \varepsilon$ and $\mu_2 > 0$ ($\varepsilon > 0$ is small), there is a unique equilibrium E_0 which is an antisaddle. For $0 < \mu_1 < \varepsilon$ and $\mu_2 < 0$, there are five equilibria $E_{l1}, E_{l2}, E_0, E_{r1}$ and E_{r2} , E_0, E_{l2} and E_{r2} are antisaddles, while E_{l1} and E_{r1} are saddles.

(ii): There is a saddle-node bifurcation surface SN , given by

$$\mu_2 = -2\sqrt{\mu_1} > 0.$$

(iii): There is a Hopf bifurcation surface H_1 about E_0 , given by

$$\mu_1 > 0 \text{ and } \mu_3 = 0$$

and a Hopf bifurcation surface H_2 about E_{l2} and E_{r2} , given by

$$\mu_1 < \mu_2^2/4 \text{ and } \mu_3 = b(\mu_2 - \sqrt{\mu_2^2 - 4\mu_1})/2.$$

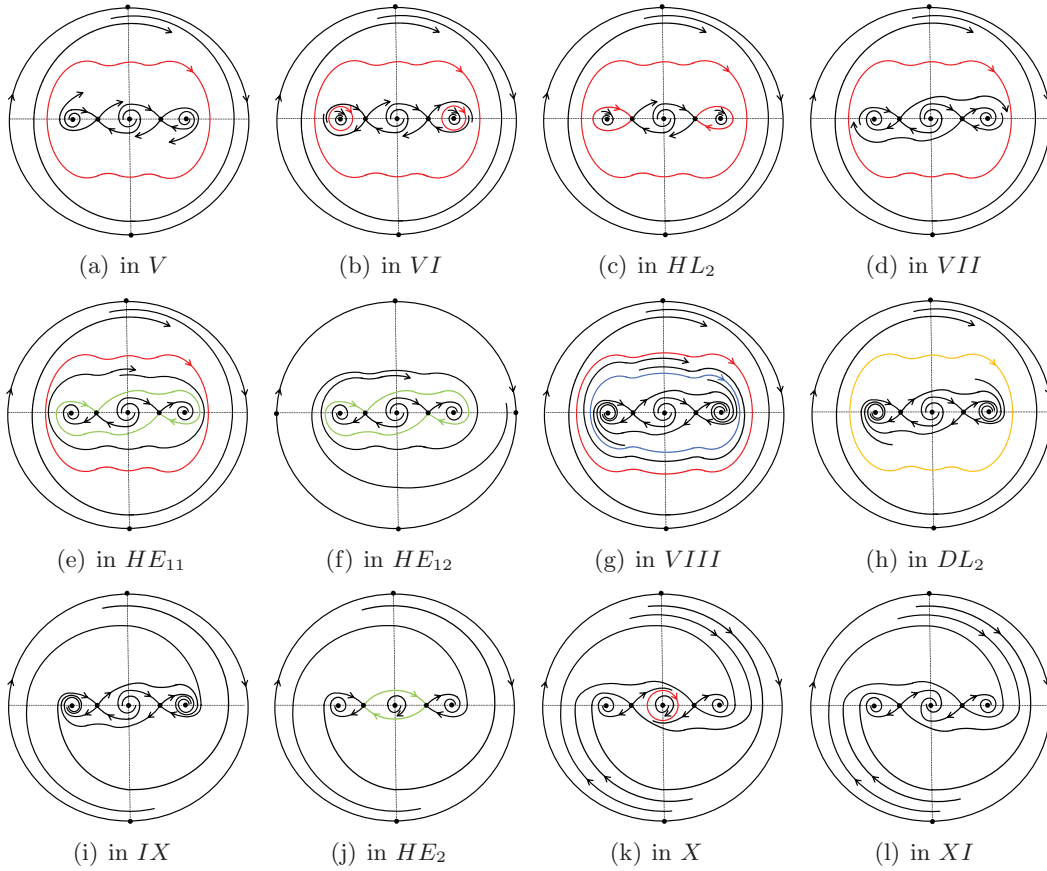


FIGURE 7. Global phase portraits of (4) for $0 < \delta_0 < 2\sqrt{3}$ and $-1 < a_1 < 0$.

(iv): The intersection of H_1 with P_1 and P_2 , respectively, defines with two dBT_1 and dBT_2 of degenerate Bogdanov-Takens bifurcation surfaces, given by

$$\mu_1 = \mu_3 = 0 \text{ and } \mu_2 > 0$$

and

$$\mu_1 = \mu_3 = 0 \text{ and } \mu_2 < 0.$$

(v): The intersection of H_2 with SN , respectively, defines with one BT of Bogdanov-Takens bifurcation surface, given by

$$\mu_1 = \mu_2^2/4 \text{ and } \mu_2 < 0,$$

and

$$\mu_3 = b\mu_2/2.$$

Proof. (i) It is obvious that the equilibria of system (2) are given by $y = 0$ and $\mu_1 x + \mu_2 x^3 + x^5 = 0$. Then the result can be easily proven.

(ii) The equation $\mu_1 x + \mu_2 x^3 + x^5 = 0$ has the discriminant $\Delta := \mu_2^2 - 4\mu_1$, and then the result follows.

(iii) The necessary condition that a Hopf bifurcation occurs at an antisaddle is the divergence equaling zero. The divergence at E_0 is

$$\text{div}(y, -\mu_1 x - \mu_2 x^3 - x^5 - \mu_3 y - bx^2 y) = -\mu_3 - bx^2 = -\mu_3$$

and it is zero for $\mu_3 = 0$. Moreover, E_0 is an antisaddle for $\mu_1 > 0$. Thus, the Hopf bifurcation H_1 is given. It follows from Lemma 4 that E_0 is a stable weak focus of order one when $\mu_1 > 0$

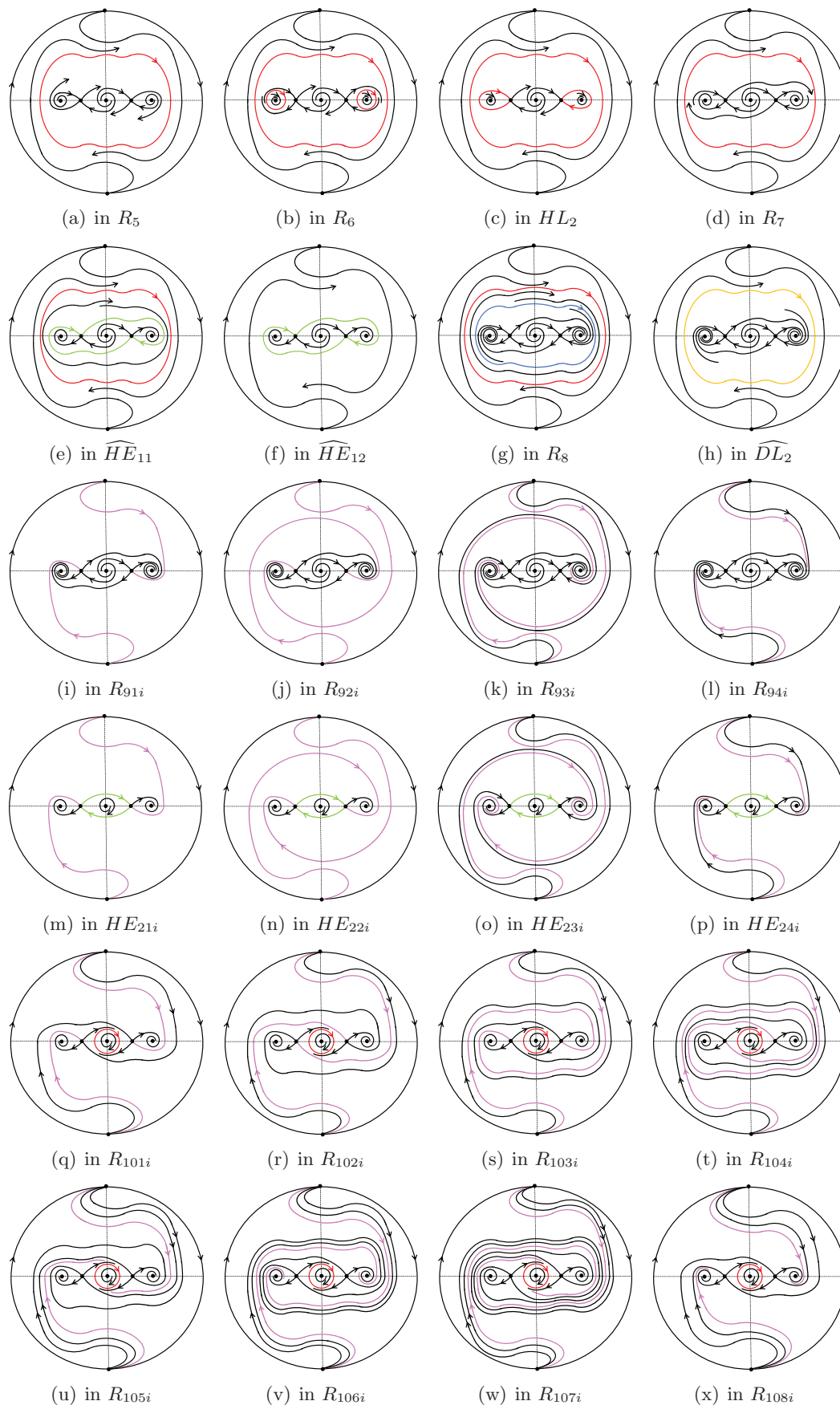


FIGURE 8. Global phase portraits of (4) for $\delta_0 \geq 2\sqrt{3}$ and $-1 < a_1 < 0$.

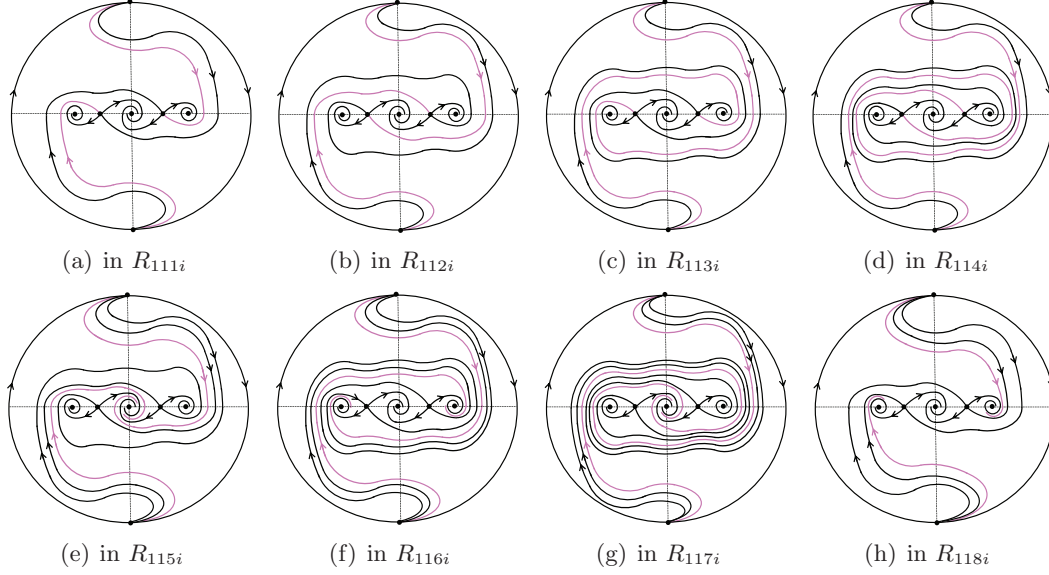


FIGURE 8. Continued.

and $\mu_3 = 0$. Therefore, the Hopf bifurcation H_1 is of order one. The divergence at both E_{l2} and E_{r2} is

$$\operatorname{div}(y, -\mu_1 x - \mu_2 x^3 - x^5 - \mu_3 y - b x^2 y) = -\mu_3 + b(\mu_2 - \sqrt{\mu_2^2 - 4\mu_1})/2$$

and it is zero for $\mu_3 = b(\mu_2 - \sqrt{\mu_2^2 - 4\mu_1})/2$. Moreover, both E_{l2} and E_{r2} are antisaddles for $\mu_1 < \mu_2^2/4$. Thus, the Hopf bifurcation H_2 is given. By Lemma 4 again, we obtain that E_{l2} and E_{r2} are unstable weak foci of order one. Thus, the Hopf bifurcation H_2 is of order one.

(iv) Degenerate Bogdanov-Takens bifurcation with symmetry occur when the divergence vanishes at a cubic point, that is, $\mu_1 = \mu_3 = 0$ and $\mu_2 \neq 0$ hold simultaneously. When $\mu_1 = \mu_3 = 0$ and $\mu_2 < 0$, by [8, p.259], the normal form of (2) is $\dot{x} = y, \dot{y} = -\varepsilon_1 x - \varepsilon_2 y + x^3 - x^2 y$, where ε_1 and ε_2 are small real parameters. When $\mu_1 = \mu_3 = 0$ and $\mu_2 > 0$, by [8, p.259], the normal form of (2) is $\dot{x} = y, \dot{y} = -\varepsilon_1 x - \varepsilon_2 y - x^3 - x^2 y$, where ε_1 and ε_2 are small real parameters.

(v) Bogdanov-Takens bifurcation occurs when the divergence vanishes at a quadratic point, that is, $\mu_1 = \mu_2^2/4, \mu_3 = b\mu_2/2$ and $\mu_2 < 0$ hold simultaneously. Further, the normal form of (2) is $\dot{x} = y, \dot{y} = -\varepsilon_1 - \varepsilon_2 y + x^2 - xy$ by [8, p.259], where ε_1 and ε_2 are small real parameters. \square

In order to study the global dynamics of system (2), we perform a study of equilibria at infinity.

Proposition 6. *For any $(\mu_1, \mu_2, \mu_3, b) \in \mathbb{R}^3 \times \mathbb{R}^+$, the dynamics of system (2) near infinity in the Poincaré disc is as sketched in Figure 9. In particular, the periodic orbit of system (2) at infinity is repulsive when $0 < b < 2\sqrt{3}$.*

Proof. With a scaling transformation $(y, t) \rightarrow (by, t/b)$, system (2) becomes

$$\begin{aligned} \dot{x} &= y, \\ \dot{y} &= -\frac{1}{b^2}(\mu_1 x + \mu_2 x^3 + x^5) - \left(\frac{\mu_3}{b} + x^2\right)y. \end{aligned}$$

By [10], we directly obtain the dynamics near infinity of system (2), as shown in Figure 9.

Besides, we claim that the periodic orbit of system (2) at infinity is repulsive when $0 < b < 2\sqrt{3}$. Using the transformation $(x, y) \rightarrow (x, y - F(x))$, system (2) can be written as

$$(5) \quad \begin{aligned} \dot{x} &= y - \mu_3 x - \frac{b}{3}x^3 =: y - F(x), \\ \dot{y} &= -\mu_1 x - \mu_2 x^3 - x^5 =: -g(x). \end{aligned}$$

possibilities of (μ_1, μ_2, μ_3, b)		location of equilibria	types and stability	
$\mu_1 > 0$	$\mu_2 > -2\sqrt{\mu_1}$	$\mu_3 > 0$	E_0 E_0 sink	
		$\mu_3 = 0$	E_0 E_0 stable weak focus of order one	
		$\mu_3 < 0$	E_0 E_0 source	
	$\mu_2 = -2\sqrt{\mu_1}$	$\mu_3 > 0$	E_{l2}, E_0, E_{r2} E_0 sink; E_{l2}, E_{r2} saddle-nodes with stable nodal sector	
		$\mu_3 = 0$	E_{l2}, E_0, E_{r2} E_0 stable weak focus of order one; E_{l2}, E_{r2} saddle-nodes with stable nodal sector	
		$b\mu_2/2 < \mu_3 < 0$	E_{l2}, E_0, E_{r2} E_0 source; E_{l2}, E_{r2} saddle-nodes with stable nodal sector	
		$\mu_3 = b\mu_2/2$	E_{l2}, E_0, E_{r2} E_0 source; E_{l2}, E_{r2} cusps	
		$\mu_3 < b\mu_2/2$	E_{l2}, E_0, E_{r2} E_0 source; E_{l2}, E_{r2} saddle-nodes with unstable nodal sector	
		$\mu_2 < -2\sqrt{\mu_1}$	$\mu_3 > 0$	$E_{l2}, E_{l1}, E_0, E_{r1}, E_{r2}$ E_0, E_{l2}, E_{r2} sinks; E_{l1}, E_{r1} saddles
	$\mu_3 = 0$		$E_{l2}, E_{l1}, E_0, E_{r1}, E_{r2}$ E_0 stable weak focus of order one; E_{l2}, E_{r2} sinks; E_{l1}, E_{r1} saddles	
	$\frac{b(\mu_2 - \sqrt{\mu_2^2 - 4\mu_1})}{2} < \mu_3 < 0$		$E_{l2}, E_{l1}, E_0, E_{r1}, E_{r2}$ E_0 source; E_{l2}, E_{r2} sinks; E_{l1}, E_{r1} saddles	
	$\mu_3 = \frac{b(\mu_2 - \sqrt{\mu_2^2 - 4\mu_1})}{2}$		$E_{l2}, E_{l1}, E_0, E_{r1}, E_{r2}$ E_0 source; E_{l1}, E_{r1} saddles; E_{l2}, E_{r2} unstable weak foci of order one	
	$\mu_3 < \frac{b(\mu_2 - \sqrt{\mu_2^2 - 4\mu_1})}{2}$		$E_{l2}, E_{l1}, E_0, E_{r1}, E_{r2}$ E_0, E_{l2}, E_{r2} sources; E_{l1}, E_{r1} saddles	
	$\mu_1 = 0$	$\mu_2 > 0$	$\mu_3 > 0$	E_0 E_0 stable degenerate node
			$\mu_3 = 0$	E_0 E_0 stable focus
$\mu_3 < 0$			E_0 E_0 unstable degenerate node	
$\mu_2 = 0$		$\mu_3 > 0$	E_0 E_0 stable degenerate node	
		$\mu_3 = 0$	E_0 stable focus for $b \in (0, 2\sqrt{3})$ degenerate node for $b \in [2\sqrt{3}, +\infty)$	
		$\mu_3 < 0$	E_0 E_0 unstable degenerate node	
$\mu_2 < 0$		$\mu_3 > 0$	E_{l2}, E_0, E_{r2} E_0 degenerate saddle; E_{l2}, E_{r2} sinks	
		$\mu_3 = 0$	E_{l2}, E_0, E_{r2} E_0 degenerate saddle; E_{l2}, E_{r2} unstable weak foci of order one	
		$\mu_3 < 0$	E_{l2}, E_0, E_{r2} E_0 degenerate saddle; E_{l2}, E_{r2} sources	
$\mu_1 < 0$	$\mu_2 \in \mathbb{R}$	$\mu_3 > \frac{b(\mu_2 - \sqrt{\mu_2^2 - 4\mu_1})}{2}$	E_{l2}, E_0, E_{r2} E_0 saddle; E_{l2}, E_{r2} sinks	
		$\mu_3 = \frac{b(\mu_2 - \sqrt{\mu_2^2 - 4\mu_1})}{2}$	E_{l2}, E_0, E_{r2} E_0 saddle; E_{l2}, E_{r2} unstable weak foci of order one	
		$\mu_3 < \frac{b(\mu_2 - \sqrt{\mu_2^2 - 4\mu_1})}{2}$	E_{l2}, E_0, E_{r2} E_0 saddle; E_{l2}, E_{r2} sources	

TABLE 1. Equilibria in finite planes of (2).

Set a generalized Filippov transformation $z(x) := \int_0^x h(s)ds$. Then, from system (5) we get $z(x) = \mu_1 x^2/2 - \mu_2 x^4/4 + x^6/6$. Denote $x_1(z)$ and $x_2(z)$ as the branches of the inverse of $z(x)$ for $x \geq 0$ and $x < 0$, respectively. Transformation $z = z(x)$ changes system (5) into

$$\frac{dz}{dy} = \frac{z'(x)dx}{dy} = \frac{h(x)dx}{dy} = F_1(z) - y, \quad \frac{dz}{dy} = \frac{z'(x)dx}{dy} = \frac{h(x)dx}{dy} = F_2(z) - y$$

for $x \geq 0$ and $x < 0$ separately, where $F_1(z) := F(x_1(z))$ and $F_2(z) := F(x_2(z))$. By the monotonicity, it is clear that there exists a value z^* such that $F_1(z) > F_2(z)$ for every $z \in (z^*, +\infty)$. Although system (2) has equilibria at infinity when $0 < b < 2\sqrt{3}$ and Proposition 3.3

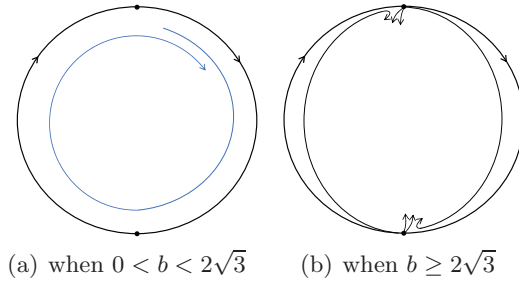


FIGURE 9. Dynamics near infinity in the Poincaré disc of (2).

of [6] holds for a general Liénard system satisfying that there are no equilibria at infinity, we can easily show that Proposition 3.3 of [6] holds for system (2). Therefore, the assertion is proved by Proposition 3.3 of [6]. The proof is completed. \square

3. LIMIT CYCLES, HOMOCLINIC LOOPS AND HETEROCLINIC LOOPS

In this section we study the existences of limit cycles, homoclinic loops and heteroclinic loops of system (2). Moreover, the exact number of limit cycles is obtained if they exist. For simplicity, let a *large limit cycle* be a limit cycle surrounding more than one equilibrium and a *small limit cycle* be a limit cycle surrounding a single equilibrium.

Lemma 7. *For any $(\mu_1, \mu_2, \mu_3, b) \in \mathbb{R}^3 \times \mathbb{R}^+$, system (2) has no limit cycles when $\mu_3 \geq 0$.*

Proof. When $\mu_3 \geq 0$, it is clear that

$$\operatorname{div}(y, -\mu_1 x - \mu_2 x^3 - x^5 - \mu_3 y - bx^2 y) = -\mu_3 - bx^2 < 0$$

for $x \neq 0$. By the Bendixson-Dulac Criterion, system (2) has no limit cycles. \square

As follows, we study the number of limit cycles of system (2) for $\mu_3 < 0$. For simplicity, based on the number of equilibria of system (2), we give the following subsections.

3.1. System (2) with only one equilibrium. By Lemma 4, system (2) has exactly one equilibrium if and only if $(\mu_1, \mu_2) \in \{(\mu_1, \mu_2) \in \mathbb{R}^2 : \mu_2^2 - 4\mu_1 < 0, \mu_2 < 0\} \cup \{(\mu_1, \mu_2) \in \mathbb{R}^2 : \mu_1 \geq 0, \mu_2 \geq 0\} =: \mathcal{G}_1$.

Lemma 8. *When $(\mu_1, \mu_2) \in \mathcal{G}_1$, $\mu_3 < 0$ and $b > 0$, system (2) has a unique limit cycle, which is stable.*

Proof. With a Liénard transformation $(x, y) \rightarrow (x, y - F(x))$, system (2) can be changed into

$$(6) \quad \begin{aligned} \dot{x} &= y - F(x), \\ \dot{y} &= -g(x), \end{aligned}$$

where $F(x) := \int_0^x f(s)ds = \mu_3 x + bx^3/3$. And E_0 of system (2) becomes \bar{E}_0 of system (6). When $(\mu_1, \mu_2) \in \mathcal{G}_1$, system (6) has the following properties:

- (i): $g(x)$ is odd and $xg(x) > 0$ for $x \neq 0$,
- (ii): $F(x)$ is odd, $F(x) < 0$ for $0 < x < \sqrt{-3\mu_3/b}$ and $F(x) > 0$ for $x > \sqrt{-3\mu_3/b}$,
- (iii): $F(+\infty) = \int_0^{+\infty} f(s)ds = +\infty$,
- (iv): f and g are C^∞ .

Therefore, all conditions of [18, section 4] or [24, Theorem 4.1] hold, implying that system (6) or its equivalent system (2) has a unique limit cycle, which is stable. \square

3.2. System (2) with three equilibria. By Lemma 4, system (2) has exactly three equilibria if and only if either $a_1 = -1$ or $a_1 \geq 0$ for its equivalent system (4). In the following, we only need to study limit cycles for simplified system (4) and we discuss in two subcases: $a_1 = -1$ and $a_1 \geq 0$. Moreover, limit cycles exist only if $a_2 < 0$ by Lemma 7.

3.2.1. The case: $a_1 = -1$.

Lemma 9. *When $a_1 = -1$, system (4) has a unique generalized limit cycle (including singular closed orbit) for $a_2 < 0$, which is stable. There are two continuous functions $p_1(\delta)$ and $p_2(\delta)$ satisfying $-1/3 < p_2(\delta) < p_1(\delta) < 0$ such that*

- (i): *system (4) has a unique limit cycle that is small when $p_1(\delta) < a_2 < 0$;*
- (ii): *system (4) has one saddle-node loop when $p_2(\delta_1) \leq a_2 \leq p_1(\delta)$;*
- (iii): *system (4) has a unique limit cycle that is large when $a_2 < p_2(\delta_1)$.*

Proof. By Lemma 4, we know that \hat{E}_0 is an anti-saddle, and both \hat{E}_{l2} and \hat{E}_{r2} are saddle-nodes or cusps for system (4). Thus, the index of \hat{E}_0 is +1 and the indices of \hat{E}_{l2} and \hat{E}_{r2} are 0 by [24, Chapter 3]. Then, any limit cycle of system (4) must surround \hat{E}_0 if it exists. By the symmetry of system (4) about the origin, \hat{E}_{l2} must lie in the interior of a limit cycle if \hat{E}_{r2} lies in it.

With a Liénard transformation $(x, y) \rightarrow (x, y - \hat{F}(x))$, system (4) is changed into

$$(7) \quad \begin{aligned} \dot{x} &= y - \delta(a_2x + \frac{x^3}{3}) =: y - \hat{F}(x), \\ \dot{y} &= -x(-1 + x^2)(a_1 + x^2). \end{aligned}$$

We firstly prove that the two points $(-\sqrt{-3a_2}, 0)$ and $(\sqrt{-3a_2}, 0)$ lie in the interior region surrounded by the limit cycle of system (7) if it exists for $a_2 < 0$. Let

$$(8) \quad E(x, y) := \int_0^x \hat{g}(s)ds + \frac{y^2}{2}.$$

It is obvious that

$$(9) \quad \frac{dE}{dt} |_{(\gamma)} = -\hat{g}(x)\hat{F}(x).$$

When $|x| \leq \sqrt{-3a_2}$, we can obtain $\hat{g}(x)\hat{F}(x) \leq 0$. Assume that system (7) has a limit cycle γ in the strip $x \in [-\sqrt{-3a_2}, \sqrt{-3a_2}]$. Then, we have

$$0 = \oint_{\gamma} dE = \oint_{\gamma} -\hat{g}(x)\hat{F}(x)dt > 0.$$

This is a contradiction. Thus, there is no limit cycles in the strip $x \in [-\sqrt{-3a_2}, \sqrt{-3a_2}]$. In other words, if system (7) has a limit cycle, it has to surround the two points $(-\sqrt{-3a_2}, 0)$ and $(\sqrt{-3a_2}, 0)$.

We secondly show that system (7) has at most one limit cycle. Assume that system (7) exhibits at least two closed orbits γ_1 and γ_2 , where γ_1 lies in the interior region surrounded by γ_2 , as shown in Figure 10. Note that

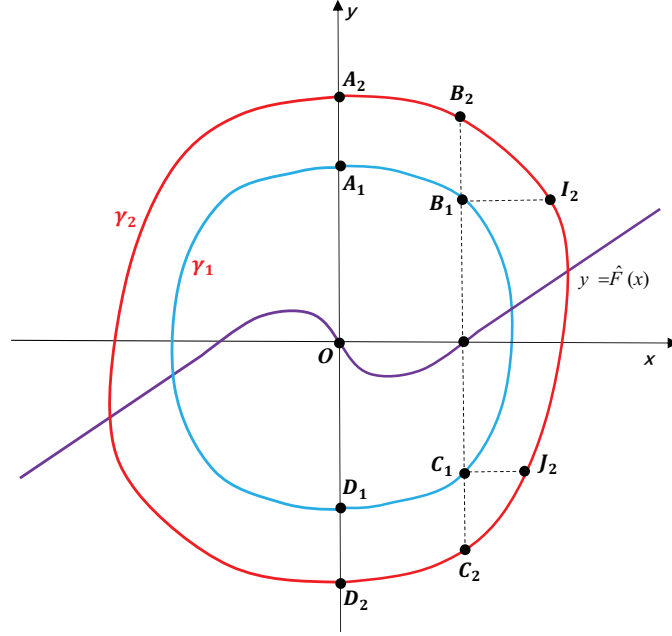
$$(10) \quad \oint_{\gamma_1} dE = \oint_{\gamma_2} dE = 0.$$

By the symmetry of system (7) about the origin, it follows that

$$(11) \quad \oint_{\gamma_1} dE = \frac{1}{2} \int_{\widehat{A_1B_1D_1}} dE \text{ and } \oint_{\gamma_2} dE = \frac{1}{2} \int_{\widehat{A_2B_2D_2}} dE.$$

Let $y = y_1(x)$ and $y = y_2(x)$ be $\widehat{A_1B_1}$ and $\widehat{A_2B_2}$, respectively. Then, we have

$$\int_{\widehat{A_1B_1}} dE - \int_{\widehat{A_2B_2}} dE = - \int_0^{\sqrt{-3a_2}} \frac{\hat{g}(x)\hat{F}(x)}{y_1 - \hat{F}(x)} dx + \int_0^{\sqrt{-3a_2}} \frac{\hat{g}(x)\hat{F}(x)}{y_2 - \hat{F}(x)} dx$$

FIGURE 10. Two closed orbits γ_1 and γ_2 of (7).

$$\begin{aligned}
 &= \int_0^{\sqrt{-3a_2}} \frac{\hat{g}(x)\hat{F}(x)(y_1 - y_2)}{(y_1 - \hat{F}(x))(y_2 - \hat{F}(x))} dx \\
 (12) \quad &> 0.
 \end{aligned}$$

Similarly, we obtain

$$(13) \quad \int_{\widehat{C_1D_1}} dE - \int_{\widehat{C_2D_2}} dE > 0.$$

Let $x = x_1(y)$ and $x = x_2(y)$ be $\widehat{B_1C_1}$ and $\widehat{I_2J_2}$, respectively. It is obvious that $x_1(y) < x_2(y)$ for $y_{C_1} < y < y_{B_1}$. On the one hand, the function $y = \hat{F}(x)$ is increasing for $x > \sqrt{-3a_2}$. Then, we have

$$(14) \quad \int_{\widehat{B_1C_1}} dE - \int_{\widehat{I_2J_2}} dE = \int_{y_{B_1}}^{y_{C_1}} (\hat{F}(x_1) - \hat{F}(x_2)) dy > 0.$$

On the other hand, the function $\hat{F}(x) > 0$ for $x > \sqrt{-3a_2}$. Then, we obtain

$$(15) \quad \int_{y_{B_2}}^{y_{I_2}} \hat{F}(x) dy < 0 \text{ and } \int_{y_{J_2}}^{y_{C_2}} \hat{F}(x) dy < 0.$$

It follows from (11)–(15) that

$$\oint_{\gamma_1} dE > \oint_{\gamma_2} dE,$$

which contradicts (10). Therefore, either system (7) or its equivalent system (4) has at most one limit cycle.

We thirdly prove that system (4) has a unique limit cycle that is large when $a_2 \leq -1/3$. It follows from Lemma 4 that \hat{E}_{l_2} and \hat{E}_{r_2} are saddle-nodes with one stable nodal part when $a_2 > -1$, cusps when $a_2 = -1$ and saddle-nodes with one unstable nodal part when $a_2 < -1$. If $a_2 \leq -1/3$, then \hat{E}_{l_2} and \hat{E}_{r_2} lie in the strip $[-\sqrt{-3a_2}, \sqrt{-3a_2}]$. By the aforementioned analysis, we know that system (4) has no limit cycles lying in the strip $[-\sqrt{-3a_2}, \sqrt{-3a_2}]$. Evidently, system (4) has no small limit cycles when $a_2 \leq -1/3$. We claim that the relative location of stable and unstable manifolds of \hat{E}_{l_2} and \hat{E}_{r_2} is shown in Figure 11 when $a_2 \leq -1/3$. If the

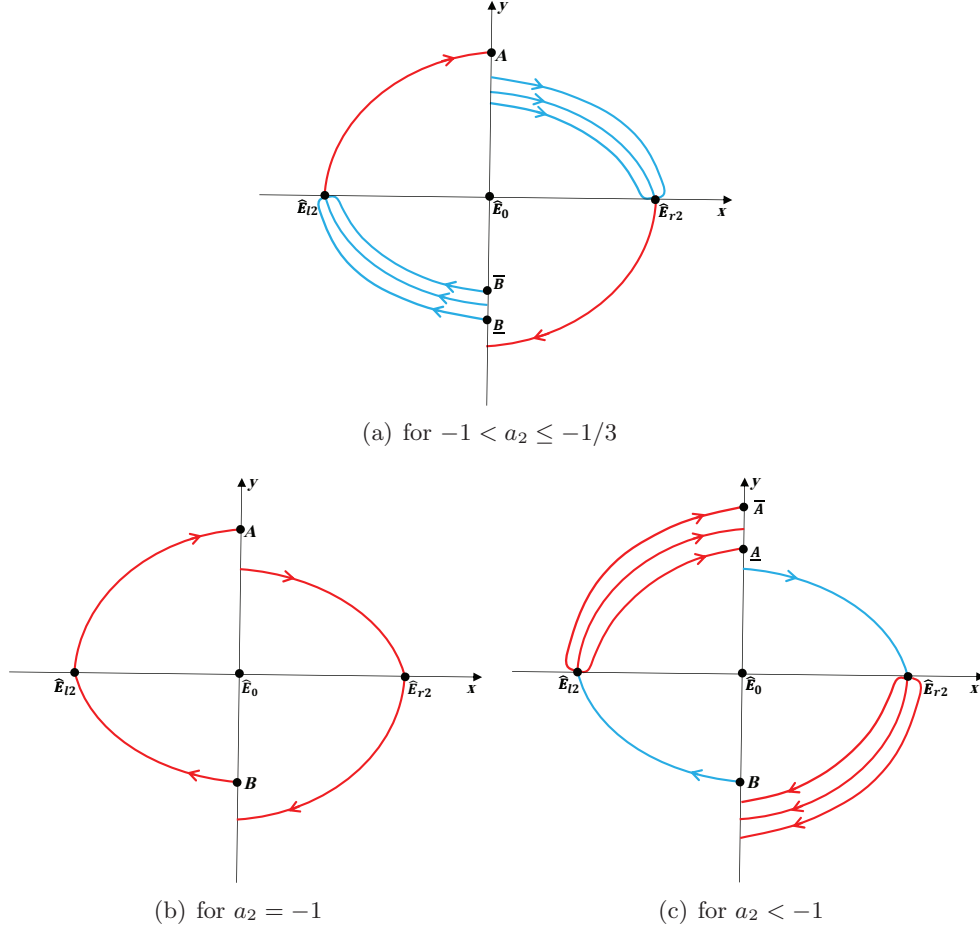


FIGURE 11. Relative location of stable and unstable manifolds of \hat{E}_{l_2} and \hat{E}_{r_2} of (7).

relative location of stable and unstable manifolds of \hat{E}_{l_2} and \hat{E}_{r_2} is not shown in Figure 11, we will obtain that system (4) has a heteroclinic loop or a small limit cycle by the Poincaré-Bendixson Theorem. This is a contradiction. The assertion is proven. Therefore, system (4) has at least one limit cycle that is large when $a_2 \leq -1/3$ by Proposition 6 and Poincaré-Bendixson Theorem. Then, the uniqueness of limit cycles of system (4) is proven and it is large when $a_2 \leq -1/3$.

We finally discuss the remainder case $-1/3 < a_2 < 0$. Since \hat{E}_{l_2} is a saddle-node with one stable nodal part when $a_2 = -1/3$, denote the intersection point of the unstable (resp. stable) manifold of \hat{E}_{l_2} and the positive (resp. negative) y -axis by A (resp. B), as shown in Figure 11(a). Let the coordinate of a general point P be (x_P, y_P) . As proved in Lemma 3.3 of [3], we can similarly prove that $y_A + y_B$ is increasing as μ_3 decreases. On the one hand, $y_A + y_B > 0$ when $a_2 = -1/3$. Since \hat{E}_{l_2} is a saddle-node with one stable nodal part when $-1 < a_2 \leq -1/3$, denote the intersection point of the unstable (resp. the left-most stable; the right-most stable) manifold of \hat{E}_{l_2} and the positive (resp. negative) y -axis by A (resp. \underline{B} ; \bar{B}). On the other hand, we claim that $y_A + y_{\bar{B}} < 0$ when $\mu_3 = 0$. By Hopf bifurcation, system (4) occurs a small limit cycle when $-\varepsilon < a_2 < 0$, where $\varepsilon > 0$ is small. It is clear that $y_A + y_{\bar{B}} = 0$ is impossible. If $y_A + y_{\bar{B}} > 0$, system (4) has at least one large limit cycle by the Poincaré-Bendixson Theorem, which contradicts the uniqueness of closed orbit. By the Intermediate Value Theorem, there exist respectively two values $a_2 = p_1(\delta)$ and $a_2 = p_2(\delta)$ such that $y_A + y_{\underline{B}} = 0$ and $y_A + y_{\bar{B}} = 0$, where $-\sqrt{\delta}/3 < p_2(\delta) < p_1(\delta) < 0$. Here, system (2) has a unique small limit cycle when

$p_1(\delta) < a_2 < 0$, one saddle-node heteroclinic loop when $p_2(\delta) \leq a_2 \leq p_1(\delta)$, and one large limit cycle when $-1/3 < a_2 < p_2(\delta)$. Then, the proof is finished. \square

3.2.2. *The case: $a_1 \geq 0$.* The existence of small limit cycles is only meaningful for a small limit cycle surrounding \hat{E}_{r2} or \hat{E}_{l2} , because \hat{E}_0 is a degenerate saddle for $a_1 = 0$ or a saddle for $a_1 > 0$ by Lemma 4. The existence of large limit cycles is only meaningful for a large limit cycle surrounding E_0 , \hat{E}_{r2} and \hat{E}_{l2} , because the vector field of system (4) is symmetric about the origin.

Lemma 10. *System (4) has no limit cycles when $-1/3 \leq a_2 < 0$.*

Proof. Assume that system (7) exhibits a limit cycle Γ_0 when $a_2 = -1/3$. Consider energy function $E(x, y)$ again, as shown in (8). Clearly, $\oint_{\Gamma_0} dE = 0$. However, from (9) we can show that $\oint_{\Gamma_0} dE = \oint_{\Gamma_0} -\delta x^2(a_1 + x^2)(-1 + x^2)^2 dx/3 < 0$ for $a_2 = -1/3$. This is a contradiction. Therefore, both system (7) and system (4) have no limit cycles when $a_2 = -1/3$.

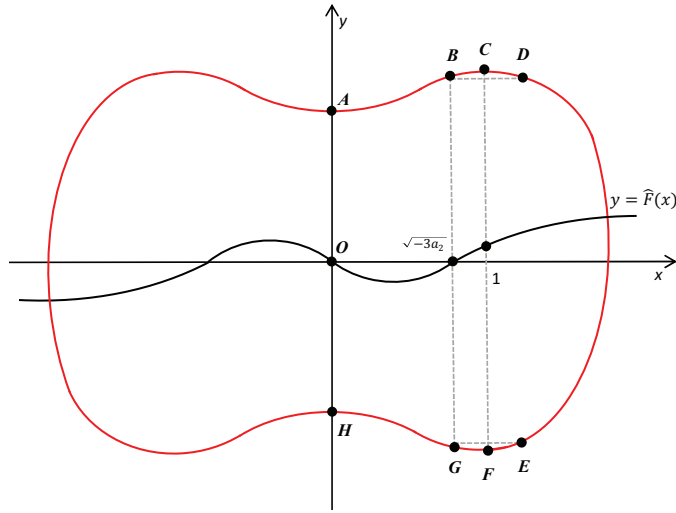


FIGURE 12. Large limit cycle of (7) for $-1/3 \leq a_2 < 0$.

Assume that system (7) exhibits a small limit cycle Γ surrounding the equilibrium $(1, \hat{F}(1))$ for $a_2 \in (-1/3, 0)$. Let

$$\hat{E}(x, y) = \int_0^x \hat{g}(s) ds + \frac{(y - \hat{F}(1))^2}{2}.$$

Then, we have

$$\frac{d\hat{E}(x, y)}{dt} \Big|_{(7)} = -\hat{g}(x)(\hat{F}(x) - \hat{F}(1)) = -\frac{\delta}{3}(x+1)(x-1)^2(x^2 + a_1)(x^2 + x + 1 + 3a_2)x < 0$$

for $x \in (0, 1) \cup (1, +\infty)$. However, we can show that $\oint_{\Gamma} d\hat{E} = \oint_{\Gamma} -\hat{g}(x)(\hat{F}(x) - \hat{F}(1)) dx = 0$ for $a_2 = -1/3$. This is a contradiction. Therefore, system (7) has no small limit cycles when $-1/3 < a_2 < 0$. So does system (4). Assume that system (7) exhibits a large limit cycle Γ surrounding the point $(1, \hat{F}(1))$ for $a_2 = c \in (-1/3, 0)$, where c is a constant. See Figure 12, where A, H (resp., B, G ; C, F ; D, E) are intersection points between Γ and the y -axis (resp., $x = \sqrt{-3a_2}$; $x = 1$; $y = y_B$; $y = y_G$) and y_B, y_G are respectively ordinates of B, G . By the symmetry of system (7), we have $2 \int_{\widehat{ABH}} dE = \oint_{\Gamma} dE$. Then, we obtain

$$\int_{\widehat{AB}} dE = \int_{\widehat{AB}} -\hat{g}(x)\hat{F}(x) dt < 0.$$

It is similar to prove that

$$\int_{\widehat{DE}} dE < 0 \text{ and } \int_{\widehat{GH}} dE < 0.$$

Let $x = x_1(y)$ and $x = x_2(y)$ represent the segment orbits \widehat{BC} and \widehat{CD} , respectively. Since $\hat{F}(x)$ is strictly increasing for $x > \sqrt{-3a_2}$, we have $\hat{F}(x_1(y)) - \hat{F}(x_2(y)) < 0$. Further, we obtain

$$\int_{\widehat{BCD}} dE = \int_{y_B}^{y_C} d(\hat{F}(x_1(y)) - \hat{F}(x_2(y)))y < 0.$$

Similarly, we can prove $\int_{\widehat{EFG}} dE < 0$. Thus, we have $\oint_{\Gamma} dE < 0$, which contradicts $\oint_{\Gamma} dE = 0$. Therefore, neither system (7) nor system (4) can have large limit cycles when $-1/3 \leq a_2 < 0$. \square

Lemma 11. *System (4) has exactly one limit cycle when $a_2 = -1$, which is stable, hyperbolic and large.*

Proof. Firstly, we discuss small limit cycles of system (7), which is equivalent to system (4). When $a_2 = -1$, with transformation

$$(16) \quad (x, y) \rightarrow (x + 1, y + \hat{F}(1)),$$

we move $(1, \hat{F}(1))$ of system (7) to the origin of the following system

$$(17) \quad \begin{aligned} \dot{x} &= y - \hat{F}(x + 1) + \hat{F}(1) =: y - \tilde{F}(x), \\ \dot{y} &= -\hat{g}(x + 1) =: -\tilde{g}(x), \end{aligned}$$

where $\tilde{F}(x) = \delta(x^3/3 + x^2)$, $\tilde{g}(x) = x^5 + 5x^4 + (9 + a_1)x^3 + (7 + 3a_1)x^2 + 2(a_1 + 1)x$ and $\tilde{f}(x) := \tilde{F}'(x) = \delta(x + x^2)$. It is clear that $\tilde{F}(0) = 0$, $x\tilde{g}(x) > 0$ for $x \in (-1, 0) \cup (0, +\infty)$, $\tilde{f}(x) < 0$ for $-1 < x < 0$ and $\tilde{f}(x) > 0$ for $x > 0$. Thus, the conditions **(i)**-**(iii)** of Proposition 9 of [7] hold. Assume that there exist x_1 and x_2 such that

$$(18) \quad \hat{F}(x_1) = \hat{F}(x_2) \text{ and } \frac{\hat{f}(x_1)}{\hat{g}(x_1)} = \frac{\hat{f}(x_2)}{\hat{g}(x_2)},$$

where $0 < x_1 < 1 < x_2$. By the first equality of (18), we have that

$$(19) \quad -3 + x_1^2 + x_1x_2 + x_2^2 = 0.$$

It follows from the second equality of (18) that

$$(20) \quad a_1 + x_1^2 + x_1x_2 + x_2^2 = 0.$$

According to (19) and (20), we obtain $a_1 = -3$, which contradicts to $a_1 \geq 0$. It means that there are no solutions for equations (18) with $\hat{F} = \tilde{F}$, $\hat{f} = \tilde{f}$ and $\hat{g} = \tilde{g}$, where $-1 < x_1 < 0 < x_2$. It follows from Corollary 10 of [7] that system (17) has no limit cycles in the zone $x > -1$, i.e., system (4) has no small limit cycles.

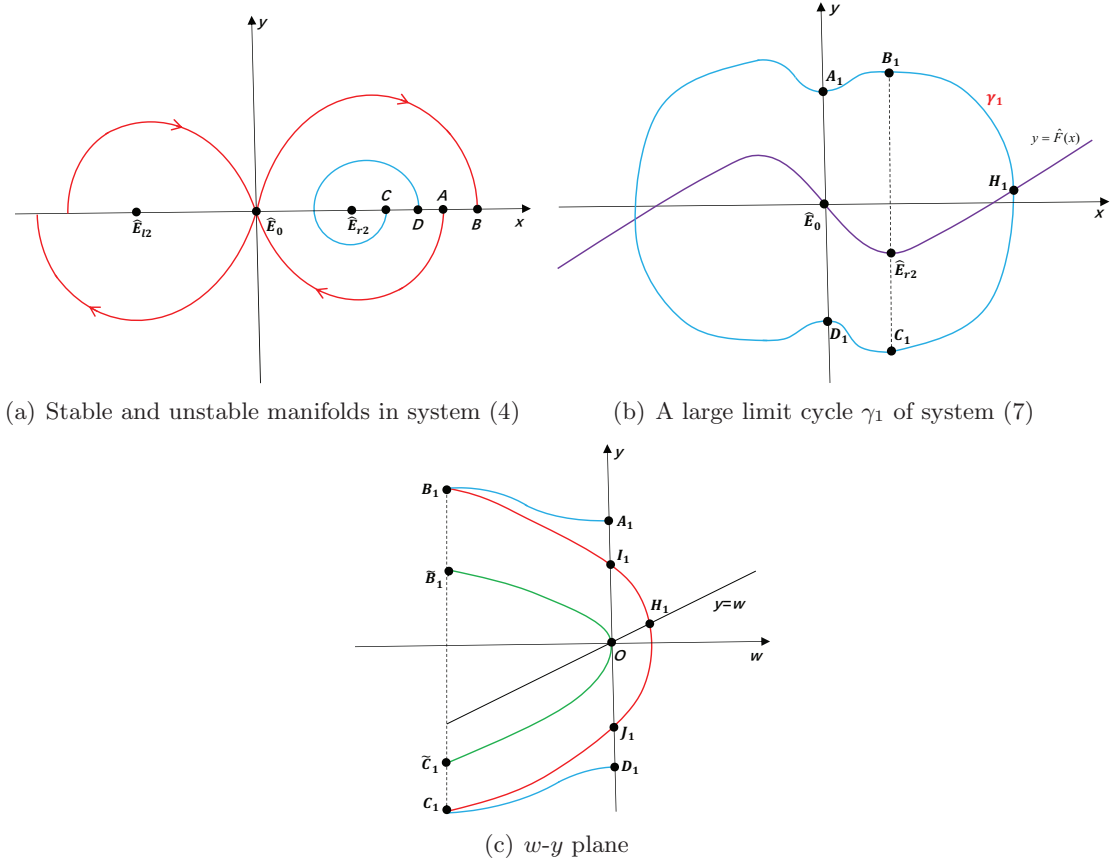
Secondly, we discuss large limit cycles of system (7). Denote $A := (x_A, 0)$ and $B := (x_B, 0)$ be respectively the first intersection points of the stable and unstable manifold of the right-hand side of \hat{E}_0 and the x -axis. Let $D := (x_D, 0)$ be the first intersection point of an orbit crossing $C := (x_C, 0)$ and the x -axis, where $x_C \in (x_{\hat{E}_{r_2}}, x_{\hat{E}_{r_2}} + \varepsilon)$ and $\varepsilon > 0$ is sufficiently small. According to the stability of \hat{E}_{r_2} and the nonexistence of small limit cycles, it is clear that $x_A < x_B$ and $x_C < x_D$ when $a_2 = -1$, see Figure 13(a). By $x_A < x_B$, Proposition 6 and Poincaré-Bendixson Theorem, system (2) has at least one large limit cycle when $a_2 = -1$. Assume that $\gamma_1 := A_1B_1\widehat{H_1C_1D_1}A_1$ is a large limit cycle of system (6), where $x_{A_1} = x_{D_1} = 0$, $x_{B_1} = x_{C_1} = x_{\hat{E}_{r_2}}$ and $y_{H_1} = \hat{F}(x_{H_1})$, as shown in Figure 13(b). Next, we will show that

$$(21) \quad \oint_{\gamma_1} \hat{f}(x)dt > 0.$$

By the symmetry, we can obtain

$$(22) \quad \int_{A_1B_1D_1} \hat{f}(x)dt = \frac{1}{2} \oint_{\gamma_1} \hat{f}(x)dt.$$

From $\hat{F}(x) = \delta(-x + x^3/3)$, we know that $y = \hat{F}(x)$ has two inverse functions $x_1(w)$ and $x_2(w)$

FIGURE 13. Orbits for the case $a_2 = -1$.

for $x > 0$, where $x_1(w) \in (0, 1)$ and $x_2(w) \in (1, \infty)$ when $a_2 = -1$. By changing variable x of system (7) to the variable $w = \hat{F}(x)$, we obtain two equations

$$(23) \quad \frac{dy}{dw} = \frac{\lambda_i(w)}{w - y},$$

where $\lambda_i(w) = \hat{g}(x_i(w))/\hat{f}(x_i(w))$ and $i = 1, 2$. By (19) and (20), we have $\lambda_2(w) > \lambda_1(w)$. Let $y = y_1(w)$, $y = y_2(w)$, $y = z_1(w)$ and $y = z_2(w)$ represent $\widehat{B_1H_1}$, $\widehat{B_1A_1}$, $\widehat{C_1H_1}$ and $\widehat{C_1D_1}$, respectively. By the Comparison Theorem, it follows that $y_2 > y_1$ and $z_2 < z_1$. We claim that $y_{H_1} > 0$. Otherwise, assume that $y_{H_1} \leq 0$. Let \mathcal{D} be the interior region of γ_1 , see Figure 13(b). Set \mathcal{D}_1 be the interior region surrounding by $\widehat{B_1H_1C_1}$ and $w = \hat{F}(1)$, \mathcal{D}_2 be the interior region surrounding by $\widehat{A_1B_1}$, $\widehat{C_1D_1}$, $w = 0$ and $w = \hat{F}(1)$, see Figure 13(c). It is clear that $\mathcal{D}_1 \subset \mathcal{D}_2$. By Green's Formula, it follows that

$$\begin{aligned} \oint_{\gamma_1} [-\hat{g}(x)dx + (\hat{F}(x) - y)]dy &= \iint_{\mathcal{D}} \hat{f}(x)dx dy \\ &= 2 \left(\iint_{\mathcal{D}_1} dw dy - \iint_{\mathcal{D}_2} dw dy \right) \\ &< 0, \end{aligned}$$

which contradicts $\oint_{\gamma_1} [-\hat{g}(x)dx + (\hat{F}(x) - y)]dy = 0$. This proves the assertion $y_{H_1} > 0$.

When $a_2 = -1$, we obtain

$$\frac{(\hat{F}(x) - \hat{F}(1))\hat{f}(x)}{\hat{g}(x)} = \frac{\delta^2(x^3/3 - x + 2/3)}{(x^2 + a_1)x}.$$

Then,

$$\frac{d}{dx} \left(\frac{(\hat{F}(x) - \hat{F}(1))f(x)}{g(x)} \right) = \frac{\delta^2 \kappa(x)}{3x^2(x^2 + a_1)^2},$$

where $\kappa(x) = (2a_1 + 6)x^3 - 6x^2 - 2a_1$. Since $\kappa'(x) = 6(a_1 + 3)x^2 - 12x > \kappa'(1) = 6 + 6a_1 \geq 0$, we have $\min \kappa(x) = \kappa(1) = 0$ for $x > 1$. Consequently, $(\hat{F}(x) - \hat{F}(1))\hat{f}(x)/\hat{g}(x)$ is increasing.

Let $y = \tilde{y}_2(w)$ and $z = \tilde{z}_2(w)$ represent respectively $\widehat{B_1O}$ and $\widehat{C_1O}$. By the proof of Theorem 2.1 of [11] or Lemma 4.5 of [24, Chapter 4], it follows that

$$(24) \quad \int_{\widehat{B_1OC_1}} \hat{f}(x)dt - \int_{\widehat{B_1H_1C_1}} \hat{f}(x)dt < 0.$$

On the other hand, we have

$$(25) \quad \begin{aligned} \int_{\widehat{B_1O}} \hat{f}(x)dt - \int_{\widehat{B_1A_1}} \hat{f}(x)dt &= \int_{\hat{F}(1)}^0 \frac{dw}{\tilde{y}_2 - w} - \int_{\hat{F}(1)}^0 \frac{dw}{y_2 - w} \\ &= \int_{\hat{F}(1)}^0 \frac{(y_2 - \tilde{y}_2)}{(y_2 - w)(\tilde{y}_2 - w)} dw \\ &> 0. \end{aligned}$$

Similarly, we have

$$(26) \quad \int_{\widehat{OC_1}} \hat{f}(x)dt - \int_{\widehat{D_1C_1}} \hat{f}(x)dt > 0.$$

By (22), (24), (25) and (26), it follows that $\int_{\widehat{A_1B_1D_1}} \hat{f}(x)dt > 0$ and then (21) holds. Therefore, both system (7) and system (4) has a unique large limit cycle when $a_2 = -1$, which is hyperbolic. Combining the nonexistence of small limit cycles, we obtain that system (4) has a unique limit cycle when $a_2 = -1$, where the limit cycle is stable, large and hyperbolic. \square

Proposition 12. *When $a_1 \geq 0$, there exist two continuous functions φ_1 and φ_5 satisfying $-1 < \varphi_1(a_1, \delta) < \varphi_5(a_1, \delta) < -1/3$ and*

- (i): *system (4) has no limit cycles when $\varphi_5(a_1, \delta) < a_2 < 0$;*
- (ii): *system (4) has a unique limit cycle when $a_2 = \varphi_5(a_1, \delta)$, which is semi-stable and large;*
- (iii): *system (4) has two limit cycles when $\varphi_1(a_1, \delta) < a_2 < \varphi_5(a_1, \delta)$, where they are large, the inner one is unstable and the outer one is stable;*
- (iv): *system (4) has one figure-eight loop and one limit cycle when $a_2 = \varphi_1(a_1, \delta)$, where the figure-eight loop is unstable, and the limit cycle is stable and large;*
- (v): *system (4) has two small limit cycles and one large limit cycle when $-1 < a_2 < \varphi_1(a_1, \delta)$, where the small ones are unstable and the large one is stable;*
- (vi): *system (4) has one limit cycle when $a_2 \leq -1$, where the limit cycle is stable and large.*

Proof. By Lemmas 7, 10 and 11, we only need to study the number of limit cycles of system (4) for $a_2 \in (-\infty, -1) \cup (-1, -1/3)$.

For simplicity, we firstly discuss large limit cycles. Assume that system (7) exhibits at least two large limit cycles Γ_1 and Γ_2 for $a_2 < -1$ or $-1 < a_2 < -1/3$, where Γ_1 lies in the interior region surrounded by Γ_2 , as shown in Figure 14. We aim to prove that

$$(27) \quad \oint_{\Gamma_1} \hat{f}(x)dt < \oint_{\Gamma_2} \hat{f}(x)dt,$$

which implies that system (7) has at most two large limit cycles. Firstly, we prove that

$$(28) \quad \int_{\widehat{A_1B_1}} \hat{f}(x)dt < \int_{\widehat{A_2B_2}} \hat{f}(x)dt$$

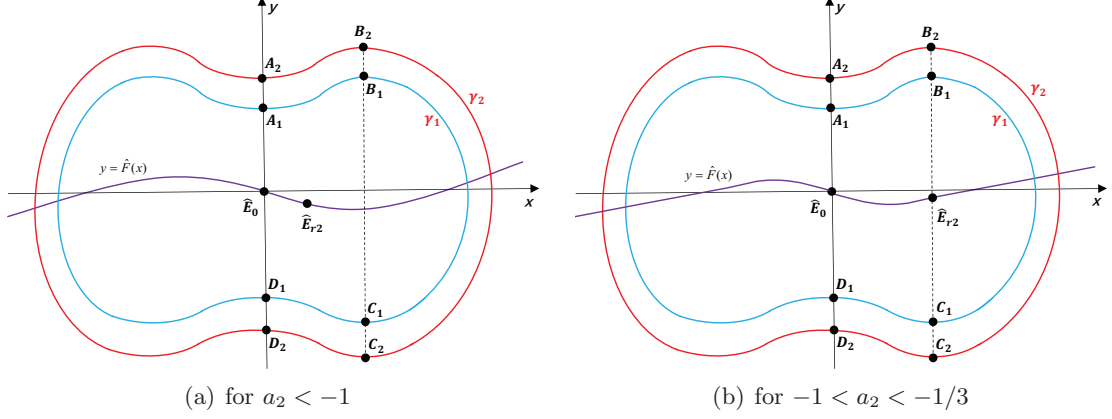


FIGURE 14. Two large limit cycles of (7).

and

$$(29) \quad \int_{\widehat{C_1 D_1}} \hat{f}(x) dt < \int_{\widehat{C_2 D_2}} \hat{f}(x) dt.$$

For each $i = 1, 2$ let y_i represent $\widehat{A_i B_i}$, we can calculate that

$$\begin{aligned}
& \int_{\widehat{A_i B_i}} \hat{f}(x) dt \\
&= - \int_0^1 \frac{\hat{F}'(x)}{\hat{F}(x) - y_i(x)} dx \\
&= - \int_0^1 \frac{\hat{F}'(x) - y_i'(x) + y_i'(x)}{\hat{F}(x) - y_i(x)} dx \\
&= - \int_0^1 \frac{1}{\hat{F}(x) - y_i(x)} d(\hat{F}(x) - y_i(x)) - \int_0^1 \frac{y_i'(x)}{\hat{F}(x) - y_i(x)} dx \\
&= - \ln \left| \frac{\hat{F}(1) - y_i(1)}{\hat{F}(0) - y_i(0)} \right| - \int_0^1 \frac{y_i'(x)}{\hat{F}(x) - y_i(x)} dx \\
&= - \ln \left| \frac{\hat{F}(0) - y_i(1)}{\hat{F}(0) - y_i(0)} \right| - \ln \left| \frac{\hat{F}(1) - y_i(1)}{\hat{F}(0) - y_i(1)} \right| - \int_0^1 \frac{\hat{g}(x)}{(\hat{F}(x) - y_i(x))^2} dx \\
&= - \ln \left| \frac{\hat{F}(1) - y_i(1)}{\hat{F}(0) - y_i(1)} \right| + \int_0^1 \frac{y_i'(x)}{\hat{F}(0) - y_i(x)} dx - \int_0^1 \frac{\hat{g}(x)}{(\hat{F}(x) - y_i(x))^2} dx \\
&= - \ln \left| \frac{\hat{F}(1) - y_i(1)}{\hat{F}(0) - y_i(1)} \right| + \int_0^1 \frac{\hat{g}(x)}{(\hat{F}(0) - y_i(x))(\hat{F}(x) - y_i(x))} dx - \int_0^1 \frac{\hat{g}(x)}{(\hat{F}(x) - y_i(x))^2} dx \\
&= - \ln \left| \frac{y_i(1) - \hat{F}(1)}{y_i(1)} \right| - \int_0^1 \frac{\hat{g}(x) \hat{F}(x)}{y_i(x) (\hat{F}(x) - y_i(x))^2} dx.
\end{aligned}$$

Further, we have

$$\int_{\widehat{A_2 B_2}} \hat{f}(x) dt - \int_{\widehat{A_1 B_1}} \hat{f}(x) dt = \ln \left| \frac{y_1(1) - \hat{F}(1)}{y_1(1)} \right| - \ln \left| \frac{y_2(1) - \hat{F}(1)}{y_2(1)} \right| + \int_0^1 H(x) dx,$$

where

$$H(x) = \frac{\hat{g}(x) \hat{F}(x)}{y_1(x) (\hat{F}(x) - y_1(x))^2} - \frac{\hat{g}(x) \hat{F}(x)}{y_2(x) (\hat{F}(x) - y_2(x))^2}.$$

Evidently, $y_2(x) - \hat{F}(x) > y_1(x) - \hat{F}(x) > 0$, $y_2(x) > y_1(x) > 0$, $\hat{g}(x) < 0$ and $\hat{F}(x) < 0$ for every $x \in (0, 1)$ because of $a_2 < -1$ or $-1 < a_2 < -1/3$. It follows that

$$\frac{y_1(1) - \hat{F}(1)}{y_1(1)} > \frac{y_2(1) - \hat{F}(1)}{y_2(1)} > 1 \text{ and } H(x) > 0,$$

which implies that (28) holds. It is similar to prove that (29) holds. On the other hand, we can prove that

$$(30) \quad \int_{\widehat{B_1C_1}} \hat{f}(x) dt < \int_{\widehat{B_2C_2}} \hat{f}(x) dt.$$

It is not difficult to compute that

$$\frac{[\hat{F}(x) - \hat{F}(1)]\hat{f}(x)}{\hat{g}(x)} = \frac{\delta^2}{3} \cdot \frac{(x^2 + x + 1 + 3a_2)}{x^2 + x} \cdot \frac{(x^2 + a_2)}{(x^2 + a_1)}.$$

When $a_2 < -1$ or $-1 < a_2 < -1/3$,

$$(31) \quad \frac{d[(x^2 + x + 1 + 3a_2)/(x^2 + x)]}{dx} = -\frac{(1 + 3a_2)(1 + 2x)}{(x^2 + x)^2} > 0$$

and

$$(32) \quad \frac{d[(x^2 + a_2)/(a_1 + x^2)]}{dx} = \frac{2(a_1 - a_2)x}{(a_1 + x^2)^2} > 0$$

for $x > 0$. It follows from (31) and (32) that $[\hat{F}(x) - \hat{F}(1)]\hat{f}(x)/\hat{g}(x)$ is increasing for $x \in (1, +\infty)$. Therefore, according to the proof of Theorem 2.1 of [11] or Lemma 4.5 of [24, Chapter 4], we obtain (30). In conclusion, (27) holds by (28), (29) and (30). Therefore, both system (7) and system (4) have at most two large limit cycles when $a_2 < -1$ or $-1 < a_2 < -1/3$.

We secondly discuss small limit cycles for the case $a_2 \in (-\infty, -1) \cup (-1, -1/3)$. As proved in Lemma 3.3 of [4], x_A decreases continuously and x_B increases continuously as $\beta := \delta a_2$ decreases. So, we still get $x_A < x_B$ when $a_2 < -1$, which is same as the case $a_2 = -1$ (see Figure 13(a)). Assume that system (4) exhibits small limit cycles surrounding \hat{E}_{r_2} when $a_2 = \alpha < -1$, where α is fixed. Since the vector field of system (4) is rotated on β , there is an annulus region of Poincaré-Bendixson for $a_2 = -1$, which contradicts the nonexistence of small limit cycles surrounding \hat{E}_{r_2} in this case. Therefore, system (4) has no small limit cycles when $a_2 < -1$. Combining the nonexistence of small limit cycles for $a_2 < -1$ and the statement (iii) of Proposition 5, system (4) has a unique small limit cycle surrounding \hat{E}_{r_2} for arbitrarily fixed δ when $-1 < a_2 < -1 + \varepsilon$ and $\varepsilon > 0$ is sufficiently small.

With the help of the above analysis results, in the following we give the proof of the statements (i)-(vi) of Proposition 12.

Firstly, we prove statement (vi). When $a_2 < -1$, system (4) has at least one large limit cycle by $x_A < x_B$, Proposition 6 and Poincaré-Bendixson Theorem. We know that system (4) has at most two large limit cycles and has no small limit cycles when $a_2 < -1$ by above analysis. We claim that system (4) has a unique limit cycle in the case $a_2 < -1$, that is stable and large. Otherwise, this contradicts (27). When $a_2 = -1$, system (4) has also a unique limit cycle that is stable and large by Lemma 11. This proves statement (vi).

Secondly, we prove statement (iv). System (4) has no small limit cycles when $a_2 \leq -1$, see the statement (vi). It implies that $x_A < x_B$. Besides, by above analysis system (4) has no limit cycles as $-1/3 \leq a_2 < 0$, which means $x_A > x_B$. Moreover, as proved in Lemma 3.3 of [4], x_A decreases continuously and x_B increases continuously as a_2 decreases for arbitrarily fixed δ . Therefore, there is a unique function $\varphi_1(a_1, \delta)$ such that $x_A - x_B = 0$ if and only if $a_2 = \varphi_1(a_1, \delta)$ for system (4), which implies the existence of a figure-eight homoclinic loop. Regarding the saddle \hat{E}_0 of system (4), its eigenvalues are denoted by λ_- and λ_+ , where $\lambda_- + \lambda_+ = -\beta$. Since $a_2 < 0$, the homoclinic loop of system (4) is unstable by Theorem 3.3 of [8]. We claim that there exist no small limit cycles in the interior of the homoclinic loop. Otherwise, this contradicts the

uniqueness of small limit cycles for $-1 < a_2 < -1 + \varepsilon$. By the stability of the homoclinic loop, Proposition 6 and Poincaré-Bendixson Theorem, we can prove that there is a unique large limit cycle surrounding the figure-eight homoclinic loop, which is stable. This proves statement (iv).

Thirdly, statement (v) directly holds from statements (vi) and (iv) by the rotated properties of the vector field.

Then, we prove statement (ii). Combining the statements (v) and (iv), we obtain that system (4) has two limit cycles that are large, when $\varphi_1(a_1, \delta) < a_2 < \varphi_1(a_1, \delta) + \varepsilon$ and $\varepsilon > 0$ is sufficiently small. We have known that system (4) has no limit cycles when $-1/3 \leq a_2 < 0$ by above proof. Since the vector field of system (4) is rotated on β , there is a function $\varphi_5(a_1, \delta)$ such that system (4) has a unique limit cycle if and only if $a_2 = \varphi_5(a_1, \delta)$, which is semi-stable and large. This proves statement (ii).

Statement (iii) can be obtained by statements (v), (iv) and (ii).

At last, statement (i) follows from statement (ii) and the nonexistence of limit cycles for $-1/3 \leq a_2 < 0$ by Lemma 10. The proof is completed. \square

3.3. System (2) with five equilibria. By Lemma 4, system (4) has exactly five equilibria if and only if $-1 < a_1 < 0$. E_{l2} , E_{l1} , E_0 , E_{r1} and E_{r2} of system (2) become $\hat{E}_{l2} := (-1, 0)$, $\hat{E}_{l1} := (-\sqrt{-a_1}, 0)$, $\hat{E}_0 := (0, 0)$, $\hat{E}_{r1} := (\sqrt{-a_1}, 0)$ and $\hat{E}_{r2} := (1, 0)$ of system (4) respectively.

By Lemma 4, the equilibria \hat{E}_{l1} and \hat{E}_{r1} of system (4) are saddles. Moreover, the vector field of system (4) is symmetric about the origin. Therefore, it suffices to give the existence of small limit cycles of system (4) surrounding \hat{E}_0 or \hat{E}_{r2} .

Lemma 13. *System (4) has no small limit cycles surrounding \hat{E}_0 when $a_2 \leq a_1/3$, at most one small limit cycle surrounding \hat{E}_0 when $a_2 > a_1/3$, no small limit cycles surrounding \hat{E}_{r2} when $a_2 \leq -1$ or $a_2 \geq (a_1 - 1 - \sqrt{-a_1})/3$, and at most one small limit cycle surrounding \hat{E}_{r2} when $-1 < a_2 < (a_1 - 1 - \sqrt{-a_1})/3$.*

Proof. It suffices to study small limit cycles of system (7). When $a_2 \leq a_1/3$, assume that system (7) exhibits a small limit cycle Γ_0 surrounding the origin, i.e., Γ_0 lies in the zone $|x| < \sqrt{-a_1}$. Let $E(x, y)$ be defined in (8). For $|x| < \sqrt{-a_1}$ and $a_2 \leq a_1/3$, it is clear that $\hat{g}(x)\hat{F}(x) \leq 0$. Associated with (9), we get $\oint_{\Gamma_0} dE = \oint_{\Gamma_0} -\hat{g}(x)\hat{F}(x)dt > 0$. This contradicts $\oint_{\Gamma_0} dE = 0$. Thus, system (7) has no small limit cycles surrounding the origin when $a_2 \leq a_1/3$.

When $a_2 > a_1/3$, as proven in Lemma 9, we can obtain that system (7) has at most one small limit cycle surrounding the origin.

In the following paragraphs, we distinguish four cases to discuss the existence of small limit cycles of system (4) surrounding \hat{E}_{r2} .

Consider $a_2 = -1$. With transformation (16), we move $(1, \hat{F}(1))$ of system (7) to the origin of system (17). It is clear that $\tilde{F}(0) = 0$, $x\tilde{g}(x) > 0$ for $x \in (\sqrt{-a_1} - 1, 0) \cup (0, +\infty)$, $\tilde{f}(x) < 0$ for $\sqrt{-a_1} - 1 < x < 0$ and $\tilde{f}(x) > 0$ for $x > 0$. Therefore, the conditions (i-iii) of Proposition 9 of [7] hold. Assume that there exist x_1 and x_2 such that (18) holds, where $\sqrt{-a_1} - 1 < x_1 < 0 < x_2$. It follows from the first equality of (18) that

$$(33) \quad x_1^2 + x_2^2 + x_1x_2 + 3x_1 + 3x_2 = 0.$$

By the second equality of (18),

$$(34) \quad a_1 + (x_1 + 1)^2 + (x_1 + 1)(x_2 + 1) + (x_2 + 1)^2 = 0.$$

By (33) and (34), it follows that $a_1 = -3$, which contradicts $-1 < a_1 < 0$. By Corollary 10 of [7], system (17) has no limit cycles in the zone $x > \sqrt{-a_1} - 1$. In other words, system (4) has no small limit cycles surrounding \hat{E}_{r2} when $a_2 = -1$.

Consider $a_2 < -1$. By Lemma 4, we know that \hat{E}_{r2} of system (4) is a source when $a_2 < -1$ or an unstable weak foci of order one when $a_2 = -1$. Assume that system (4) has at least one small limit cycle surrounding \hat{E}_{r2} when $a_2 = \lambda < -1$ and Γ_1 is the innermost small limit cycle

surrounding \hat{E}_{r2} , where λ is fixed. Since the vector field of system (4) is rotated on a_2 , there is an annulus region of Poincaré-Bendixson for $a_2 \in (\lambda, -1]$, which contradicts the nonexistence of small limit cycles surrounding \hat{E}_{r2} when $a_2 = -1$. Thus, system (4) has no small limit cycles surrounding \hat{E}_{r2} when $a_2 < -1$.

Consider $a_2 \geq (a_1 - 1 - \sqrt{-a_1})/3$. Let

$$\tilde{E}(x, y) := \int_1^x \hat{g}(s)ds + \frac{(y - \hat{F}(1))^2}{2}.$$

Then

$$\frac{d\tilde{E}}{dt}|_{(7)} = -\hat{g}(x)(\hat{F}(x) - \hat{F}(1)) \leq 0$$

for $x > \sqrt{-a_1}$. Assume that system (7) exhibits a small limit cycle Γ_2 surrounding $(1, \hat{F}(1))$, i.e., Γ_2 lies in the zone $x > \sqrt{-a_1}$. Then, we have $\oint_{\Gamma_2} d\tilde{E} = \oint_{\Gamma_2} -\hat{g}(x)(\hat{F}(x) - \hat{F}(1))dt < 0$, which contradicts $\oint_{\Gamma_2} dE = 0$. Thus, system (7) has no small limit cycles surrounding $(1, \hat{F}(1))$ when $a_2 \geq (a_1 - 1 - \sqrt{-a_1})/3$.

Consider $-1 < a_2 < (a_1 - 1 - \sqrt{-a_1})/3$. Assume that system (4) has at most two small limit cycles surrounding \hat{E}_{r2} when $-1 < a_2 < (a_1 - 1 - \sqrt{-a_1})/3$, where $\hat{\Gamma}_1, \hat{\Gamma}_2$ are the such innermost two limit cycles and $\hat{\Gamma}_1$ lies in the interior of $\hat{\Gamma}_2$. As proven in Lemma 9, we have $\oint_{\hat{\Gamma}_1} d\tilde{E} < \oint_{\hat{\Gamma}_2} d\tilde{E}$, which contradicts $\oint_{\hat{\Gamma}_1} d\tilde{E} = \oint_{\hat{\Gamma}_2} d\tilde{E} = 0$. Thus, system (4) has at most one small limit cycle surrounding \hat{E}_{r2} when $-1 < a_2 < (a_1 - 1 - \sqrt{-a_1})/3$. The proof is completed. \square

In the following three lemmas, in order to give the exact number of limit cycles for system (4), we study the existence of large limit cycles. Since the vector field of system (4) is symmetric about the origin, the existence of large limit cycles is only meaningful for a large limit cycle surrounding all equilibria.

Lemma 14. *System (4) has a unique limit cycle when $a_2 \leq -1$, which is stable and large.*

Proof. By Lemma 4, $\hat{E}_0, \hat{E}_{l2}, \hat{E}_{r2}$ of system (4) are unstable and $\hat{E}_{l1}, \hat{E}_{r1}$ of system (4) are saddles when $a_2 \leq -1$. From Lemma 13, system (4) has no small limit cycles when $a_2 \leq -1$. Therefore, the stable and unstable manifolds of \hat{E}_{l1} and \hat{E}_{r1} of system (4) are shown in Figure 15(a). Moreover, since equilibria at infinity of system (4) are repelling by Proposition 6, system (4) has at least one large limit cycle by the Poincaré-Bendixson Theorem. So does system (7).

When $a_2 = -1$, assume that system (7) exhibits a large limit cycle γ_1 , as shown in Figure 15(b). For the statement $\oint_{\gamma_1} \hat{f}(x)dt > 0$, the proof is the same as the proof of Proposition 12. The details are omitted. It means that system (7) has at most one large limit cycle, which is stable. Combining the existence of large limit cycles and the nonexistence of small limit cycles, we directly obtain that system (7) has a unique limit cycle when $a_2 = -1$, which is stable and large.

When $a_2 < -1$, suppose that system (7) exhibits at least two large limit cycles, where Γ_1, Γ_2 are the two innermost limit cycles, and Γ_1 lies in the interior of Γ_2 , see Figure 15(c). As proven in Proposition 12, we get

$$\oint_{\Gamma_1} \hat{f}(x)dt > \oint_{\Gamma_2} \hat{f}(x)dt.$$

Moreover, since the outmost limit cycle is externally stable and the innermost one is internally stable, system (7) has also at most one large limit cycle, which is stable. Based on the existence of large limit cycles and the nonexistence of small limit cycles, system (7) has a unique limit cycle when $a_2 < -1$, which is stable and large. The proof is completed. \square

Lemma 15. *System (4) has at most two large limit cycles when $-1 < a_2 \leq (a_1 - 1 - \sqrt{-a_1})/3$, and at most one large limit cycle when $a_1/3 \leq a_2 < 0$.*

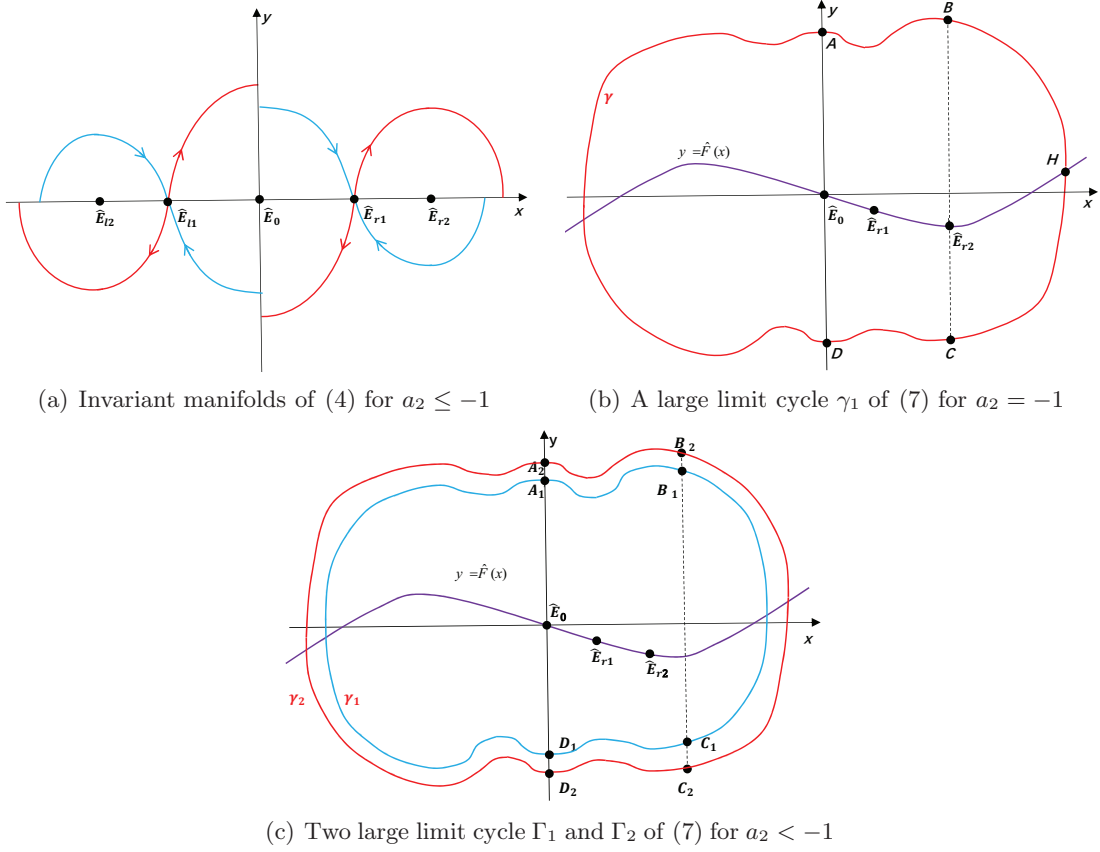


FIGURE 15. The discussion of large limit cycles of (4) for $a_2 \leq -1$.

Proof. When $-1 < a_2 \leq (a_1 - 1 - \sqrt{-a_1})/3$, suppose that system (7) exhibits at least two large limit cycles Γ_1 and Γ_2 , where Γ_1 lies in the interior of Γ_2 , as shown in Figure 16(a). Our task now is to prove

$$(35) \quad \oint_{\Gamma_1} \hat{f}(x) dt < \oint_{\Gamma_2} \hat{f}(x) dt,$$

which implies that system (7) has at most two large limit cycles. Let $y = y_1(x)$ and $y = y_2(x)$ be respectively $\widehat{A_1B_1}$ and $\widehat{A_2B_2}$. Then, we have

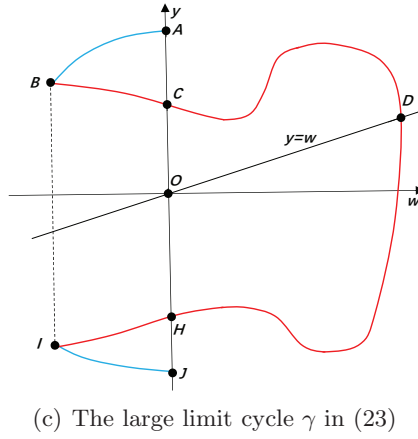
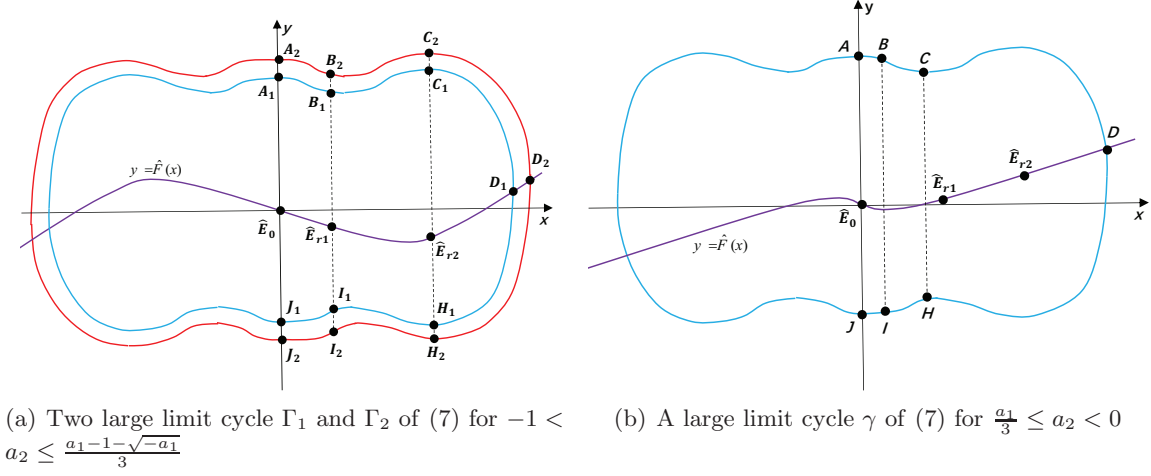
$$(36) \quad \begin{aligned} \int_{\widehat{A_1B_1}} \hat{f}(x) dt - \int_{\widehat{A_2B_2}} \hat{f}(x) dt &= \int_0^{\sqrt{-a_1}} \frac{\hat{f}(x)}{y_1 - \hat{F}(x)} dx - \int_0^{\sqrt{-a_1}} \frac{\hat{f}(x)}{y_2 - \hat{F}(x)} dx \\ &= \int_0^{\sqrt{-a_1}} \frac{\hat{f}(x)(y_2 - y_1)}{(y_1 - \hat{F}(x))(y_2 - \hat{F}(x))} dx \\ &< 0, \end{aligned}$$

because $\hat{f}(x) < 0$ for $x \in (0, \sqrt{-\tilde{h}})$ when $-1 < a_2 \leq (a_1 - 1 - \sqrt{-a_1})/3$. Similarly, we obtain

$$(37) \quad \int_{\widehat{I_1J_1}} \hat{f}(x) dt - \int_{\widehat{I_2J_2}} \hat{f}(x) dt < 0.$$

As proven in Lemma 3.4 of [4], we get

$$(38) \quad \int_{\widehat{B_1C_1}} \hat{f}(x) dt < \int_{\widehat{B_2C_2}} \hat{f}(x) dt \quad \text{and} \quad \int_{\widehat{H_1I_1}} \hat{f}(x) dt < \int_{\widehat{H_2I_2}} \hat{f}(x) dt.$$


 FIGURE 16. Discussion of large limit cycles of (7) for $a_2 \in (-1, \frac{a_1 - 1 - \sqrt{-a_1}}{3}] \cup [\frac{a_1}{3}, 0)$.

As proven in Proposition 12, $[\hat{F}(x) - \hat{F}(\sqrt{-h})]\hat{f}(x)/\hat{g}(x)$ is increasing for $x \in (\sqrt{-h}, +\infty)$. Then, by the proof of Theorem 2.1 of [11] or Lemma 4.5 of [24, Chapter 4],

$$(39) \quad \int_{\widehat{C_1 D_1 H_1}} \hat{f}(x) dt - \int_{\widehat{C_2 D_2 H_2}} \hat{f}(x) dt < 0.$$

By (36-39), it follows that (35) holds. Therefore, system (7) has at most two large limit cycles when $-1 < a_2 \leq (a_1 - 1 - \sqrt{-a_1})/3$. So does system (4).

When $a_1/3 \leq a_2 < 0$, assume that system (7) exhibits a large limit cycle γ , as shown in Figure 16(b). Similarly, γ of system (7) in the positive half-plane is changed into the orbit segments $\widehat{BA} \cup \widehat{BDI} \cup \widehat{IJ}$ of equations (23), where $\lambda_i(w) = \hat{g}(x_i(w))/\hat{f}(x_i(w))$ and $i = 1, 2$, as shown in Figure 16(c). Letting $y = \hat{y}_1(w)$ and $y = \hat{y}_2(w)$ represent respectively the orbit segments \widehat{BA} and \widehat{BC} in the wy -plane, we get $\hat{y}_1(w) > \hat{y}_2(w)$. On the one hand,

$$(40) \quad \begin{aligned} \int_{\widehat{BC}} \hat{f}(x) dt - \int_{\widehat{BA}} \hat{f}(x) dt &= \int_{\frac{2\delta a_2 \sqrt{-a_2}}{3}}^0 \frac{dw}{y_2 - w} - \int_{\frac{2\delta a_2 \sqrt{-a_2}}{3}}^0 \frac{dw}{y_1 - w} \\ &= \int_{\frac{2\delta a_2 \sqrt{-a_2}}{3}}^0 \frac{(\hat{y}_1 - \hat{y}_2)}{(\hat{y}_1 - w)(\hat{y}_2 - w)} dw \\ &> 0. \end{aligned}$$

Similarly, we can obtain

$$(41) \quad \int_{\widehat{HI}} \hat{f}(x) dt - \int_{\widehat{JI}} \hat{f}(x) dt > 0.$$

On the other hand, it is clear that

$$(42) \quad \int_{\widehat{CDH}} \hat{f}(x) dt > 0.$$

By (40-42), $\oint_{\gamma} \hat{f}(x) dt > 0$. Thus, system (7) has at most one large limit cycle for $a_1/3 \leq a_2 < 0$. So does system (4). The proof is completed. \square

Lemma 16. *System (4) has no large limit cycles when $-1/3 \leq a_1 < 0$ and $-1/3 \leq a_2 < 0$, at most one large limit cycle when $a_1 \leq a_2 < a_1/3$ and $-1 < a_1 < -1/3$.*

Proof. Firstly, assume that system (4) has a large limit cycle Γ for $a_1 = a_2 = -1/3$, as shown in Figure 17(a). We claim that $\lambda_1(w) \equiv \lambda_2(w)$ in (23), where $w = F(x)$ for $x > 0$. On the one hand, when $\hat{F}(x_1) = \hat{F}(x_2)$, we have $x_1^2 + x_1x_2 + x_2^2 = 1$, where $0 < x_1 < \sqrt{3}/3 < x_2 < 1$. On the other hand, when the second equation of (18) holds, we also have $x_1^2 + x_1x_2 + x_2^2 = 1$. Then, the assertion is proven. Thus, the two equations in (23) are same. Letting $y = \hat{y}_1(w)$ and $y = \hat{y}_2(w)$ represent respectively the orbit segments \widehat{BA} and \widehat{BC} in the wy -plane, it follows from (23) that $\hat{y}_1(w) \equiv \hat{y}_2(w)$. In the wy -plane, the two orbit segments \widehat{BA} and \widehat{BC} coincide, and the two orbit segments \widehat{IH} and \widehat{IJ} coincide, as shown in Figure 17(b). By the Green's formula,

$$\begin{aligned} \oint_{\Gamma} (y - \hat{F}(x)) dy + g(x) dx &= 2 \iint_{\mathcal{S}} \hat{f}(x) dx dy \\ &= 2 \left(\iint_{\mathcal{S}_1} dw dy - \iint_{\mathcal{S}_2} dw dy \right) \\ &= 2(\Omega(\mathcal{S}_1) - \Omega(\mathcal{S}_2)) = 2\Omega(\mathcal{S}_3) > 0, \end{aligned}$$

where \mathcal{S} is the domain between the y -axis and the orbit segment \widehat{ADJ} in the xy -plane, \mathcal{S}_1 is the domain between $w = \hat{F}(\sqrt{3}/3)$ and the orbit segment \widehat{BDI} in the wy -plane, \mathcal{S}_2 is the domain between the y -axis, $w = \hat{F}(\sqrt{3}/3)$ and the orbit segments \widehat{BA} , \widehat{IH} in the wy -plane, \mathcal{S}_3 is the domain between the y -axis and the orbit segment \widehat{CDH} in the wy -plane. This contradicts $\oint_{\Gamma} (y - \hat{F}(x)) dy + g(x) dx = 0$. Thus, system (4) has no large limit cycles for $a_1 = a_2 = -1/3$.

Secondly, assume that system (4) has a large limit cycle Γ for $-1/3 < a_1 < 0$ and $a_2 = -1/3$, as shown in Figure 18(a). When $\hat{F}(x_1) = \hat{F}(x_2)$, we have $x_1^2 + x_1x_2 + x_2^2 = 1$, where $0 < x_1 < \sqrt{3}/3 < x_2 < 1$. Further, when the second equality of (18) holds, by $x_1^2 + x_1x_2 + x_2^2 = 1$ we also have $x_1x_2(x_1x_2 + 1) = 0$, which contradicts $0 < x_1 < \sqrt{3}/3 < x_2 < 1$. Then, we can obtain

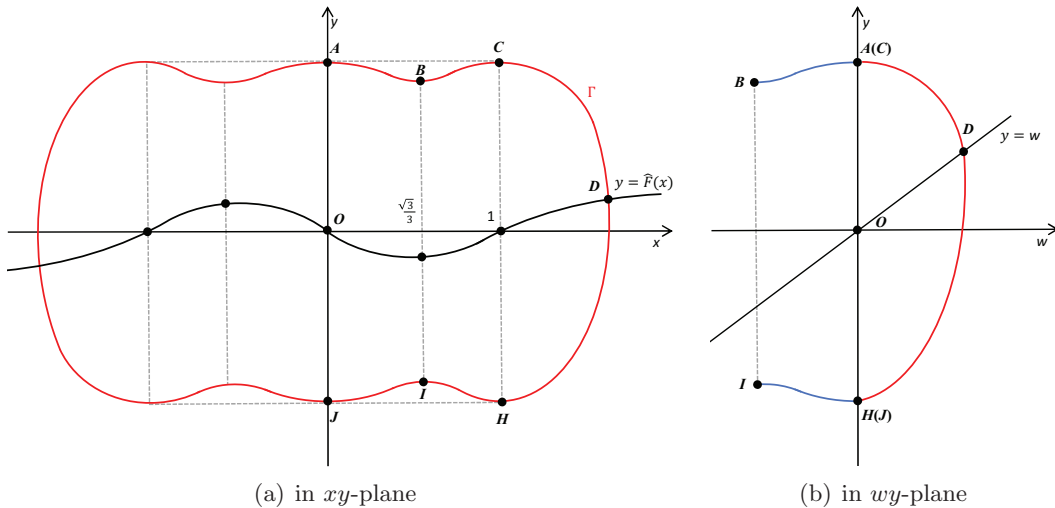


FIGURE 17. A large limit cycle Γ of (7) for $a_1 = a_2 = -1/3$.

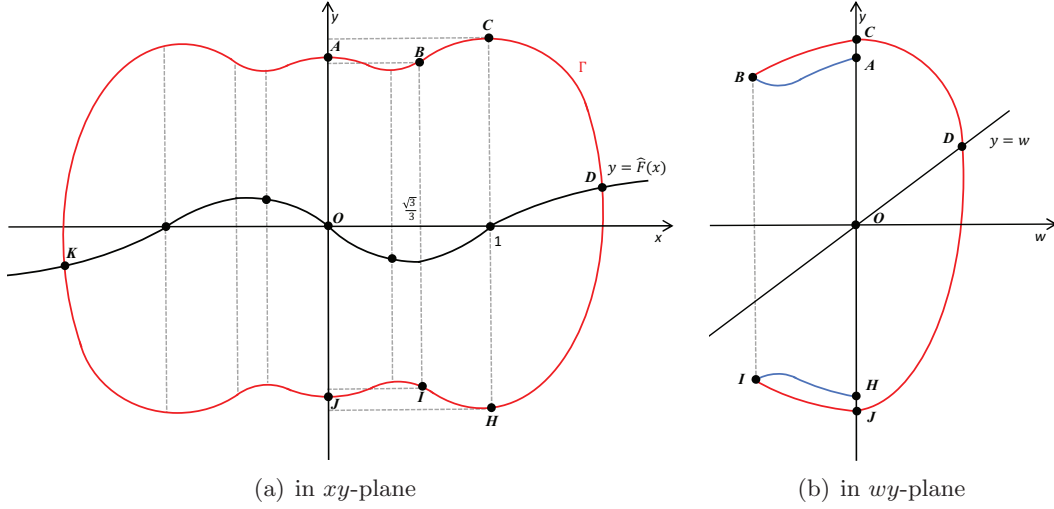


FIGURE 18. A large limit cycle Γ of (7) for $-1/3 < a_1 < 0$ and $a_2 = -1/3$.

that $\lambda_1(w) < \lambda_2(w)$ in (23). Letting $y = \hat{y}_1(w)$ and $y = \hat{y}_2(w)$ represent respectively the orbit segments \widehat{BA} and \widehat{BC} in the wy -plane, it follows from (23) and the Comparison Theorem that $\hat{y}_1(w) < \hat{y}_2(w)$. See Figure 18(b). Then, \mathcal{S}_2 is a subset of \mathcal{S}_1 . By the Green's formula,

$$\begin{aligned} \oint_{\Gamma} (y - \hat{F}(x))dy + g(x)dx &= 2 \iint_{\mathcal{S}} \hat{f}(x) dx dy \\ &= 2 \left(\iint_{\mathcal{S}_1} dw dy - \iint_{\mathcal{S}_2} dw dy \right) \\ &= 2(\Omega(\mathcal{S}_1) - \Omega(\mathcal{S}_2)) > 0, \end{aligned}$$

which contradicts $\oint_{\Gamma} (y - \hat{F}(x))dy + g(x)dx = 0$. Thus, system (4) has no large limit cycles for $-1/3 < a_1 < 0$ and $a_2 = -1/3$.

Thirdly, assume that system (4) has a large limit cycle for $(a_1, a_2) = (a^*, b^*)$, where $-1/3 \leq a^* < 0$, $-1/3 < b^* < 0$, and Γ is the outermost large limit cycle. Since the vector field of system (4) is rotated on a_2 , Γ is broken when $(a_1, a_2) = (a^*, -1/3)$, as shown Figure 19. By the annulus region of Poincaré-Bendixson Theorem, there is a stable limit cycle surrounding γ when $(a_1, a_2) = (a^*, -1/3)$, which contradicts the nonexistence of large limit cycles.

Finally, assume that system (4) has a large limit cycle Γ for $a_1 \leq a_2 < a_1/3$ and $-1 < a_1 < -1/3$, as shown in Figure 20(a). We claim that $\lambda_1(w) > \lambda_2(w)$ in (23), where $w = F(x)$ for

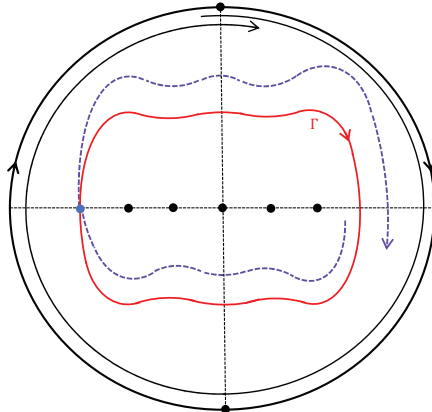


FIGURE 19. Discussion on large limit cycles of (7) for $-1/3 < a_2 < a_1 < 0$.

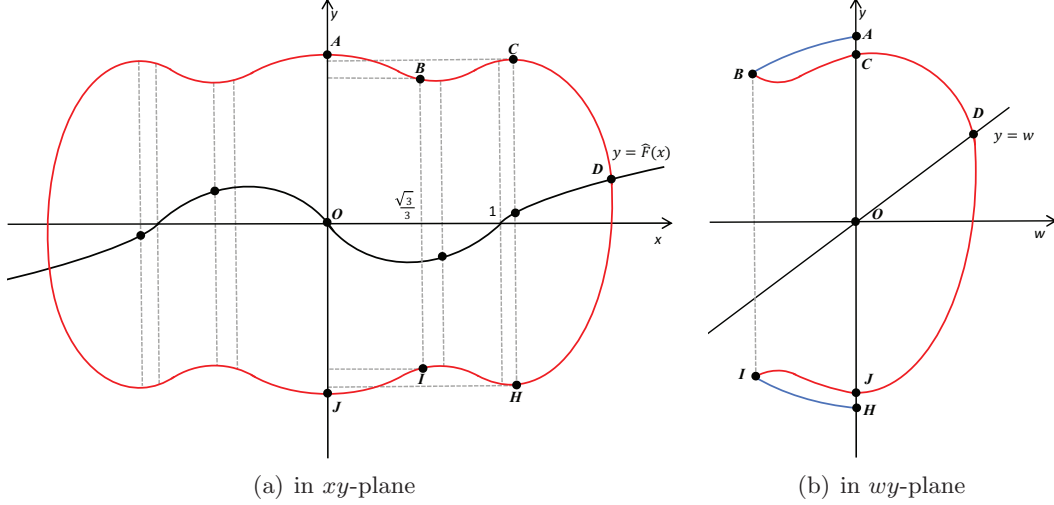


FIGURE 20. A large limit cycle Γ of (7) for $a_1 \leq a_2 < a_1/3$ and $-1 < a_1 < -1/3$.

$x > 0$. When (18) holds, we have

$$x_1^2 + x_1x_2 + x_2^2 = -3a_2, \quad \frac{x_1^2x_2^2 + x_1x_2 - a_2(3a_2 + 1)}{(x_1^2 + a_2)(x_2^2 + a_2)} + \frac{3a_2 + 1}{a_2 - a_1} = 0,$$

where $0 < x_1 < \sqrt{-a_1} < x_2 < 1$. Let $\kappa := x_1 + x_2$. Then, $x_1x_2 = \kappa^2 + 3a_2 > 0$ and $(x_1^2 + a_2)(x_2^2 + a_2) < 0$, implying that $\kappa \in (\sqrt{-3a_2}, 2\sqrt{-a_2})$. Define $h(\sigma) := (2a_2 + 1 - a_1)\sigma^2 + ((a_2 - a_1)(6a_2 + 1) + 5a_2(3a_2 + 1))\sigma + 2a_2(3a_2 + 1)(3a_2 - a_1)$. Notice that

$$-\frac{(a_2 - a_1)(6a_2 + 1) + 5a_2(3a_2 + 1)}{2(2a_2 + 1 - a_1)} + 4a_2 = \frac{(a_2 - a_1)(2a_2 - 11) - 7a_2^2 - a_2}{2(2a_2 + 1 - a_1)} < 0.$$

We check that $h(-4a_2) = 2a_2(1 + a_2)(a_1 - a_2) > 0$, implying $h(\kappa^2) > 0$ for $\kappa \in (\sqrt{-3a_2}, 2\sqrt{-a_2})$. Then, the assertion is proven. Letting $y = \hat{y}_1(w)$ and $y = \hat{y}_2(w)$ represent respectively the orbit segments \overline{BA} and \overline{BC} in the wy -plane, it follows from (23) and the Comparison Theorem that $\hat{y}_1(w) > \hat{y}_2(w)$. We also claim that $y_D > 0$, where y_D is the ordinate of D . See Figure 20(b). Otherwise, \mathcal{S}_1 is a subset of \mathcal{S}_2 , implying similarly the nonexistence of large limit cycles. As proven in the case of $a_1/3 \leq a_2 < 0$ of Lemma 15, we can similarly obtain that system (4) has at most one large limit cycle for $a_1 \leq a_2 < a_1/3$ and $-1 < a_1 < -1/3$. Moreover, the limit cycle is stable and hyperbolic if it exists. \square

Lemma 17. *System (4) has at most four large limit cycles when $(a_1 - 1 - \sqrt{-a_1})/3 < a_2 < \min\{a_1, -1/3\}$ and $-1 < a_1 < 0$.*

Proof. Firstly, we consider that $\delta > 0$ is sufficiently small. By Appendix C, system (4) has at most four large limit cycles.

Secondly, we consider that $\delta > 0$ is not small and let $\beta := \delta a_2$. Assume that system (4) has at least five large limit cycles for $(a_1, \beta, \delta) = (\alpha_0, \beta_0, \delta_0)$, where $(\alpha_0 - 1 - \sqrt{-\alpha_0})/3 < \beta_0 < \min\{\alpha_0, -1/3\}$ and $-1 < \alpha_0 < 0$. Let $\Gamma_1, \dots, \Gamma_5$ be the outermost five limit cycles in order, where Γ_1 lies in the interior regions surrounded by Γ_2 and Γ_5 is externally stable. Notice that the vector field of system (4) is rotated with respect to β and δ . Then, we can obtain that stable limit cycles expand and unstable ones contract as one of β, δ decreases. Next, we adapt the following steps.

- (i): When $a_1 := \alpha_0$ and $\beta := \beta_0$ are fixed, we lessen δ and claim that there exists $\delta_1 \in (0, \delta_0)$ such that either Γ_1 and Γ_2 coincide, or Γ_3 and Γ_4 coincide, or Γ_1 and an interior limit cycle coincide, and

$$(\alpha_0 - 1 - \sqrt{-\alpha_0})\delta_1/3 < \beta_0 < \min\{\alpha_0\delta_1, -\delta_1/3\}.$$

Otherwise, this is a contradiction since system (4) has at most one large limit cycles when $\beta_0 \geq \min\{\alpha_0\delta_1, -\delta_1/3\}$ by Lemma 16.

- (ii): When $a_1 := \alpha_0$ and $\delta = \delta_1$ are fixed, we increase β and can find a value $\beta = \beta_1 \in ((\alpha_0 - 1 - \sqrt{-\alpha_0})\delta_1/3, \beta_0)$ such that either Γ_2 and Γ_3 coincide, or Γ_4 and Γ_5 coincide. Otherwise, if

$$\beta_1 \leq (\alpha_0 - 1 - \sqrt{-\alpha_0})\delta_1/3$$

this is a contradiction since system (4) has at most two large limit cycles by Lemma 15.

- (iii): When $a_1 := \alpha_0$ and $\beta := \beta_1$ are fixed, we lessen δ and claim that there is a value $\delta = \delta_2 \in (0, \delta_1)$ such that either Γ_2 and Γ_3 coincide, or Γ_1 and an interior limit cycle coincide, and

$$(\alpha_0 - 1 - \sqrt{-\alpha_0})\delta_2/3 < \beta_1 < \min\{\alpha_0\delta_2, -\delta_2/3\}.$$

Otherwise, this is a contradiction since system (4) has at most one large limit cycle when $\beta_1 \leq -\alpha_0 - \delta_2$ by Lemma 14.

- (iv): Repeating the aforementioned steps, there is an integer n such that δ_n is small in the $2n + 1$ -th step. Moreover, system (4) has at least four large limit cycles in the moment and one of them is semi-stable. However, when there is a semi-stable large limit cycle, system (4) has at most three large limit cycles with sufficiently small $\delta > 0$ by Appendix C. It induces a contradiction.

Therefore, system (4) cannot have five large limit cycles for $(a_1 - 1 - \sqrt{-a_1})/3 < a_2 < \min\{a_1, -1/3\}$ and $-1 < a_1 < 0$. \square

By Lemmas 13 and 17, there are at most four large limit cycles and no small limit cycles for $(a_1 - 1 - \sqrt{-a_1})/3 < a_2 < \min\{a_1, -1/3\}$ and $-1 < a_1 < 0$. By the analysis of Appendix C and numerical simulations, we conjecture that there are at most two large limit cycles for $(a_1 - 1 - \sqrt{-a_1})/3 < a_2 < \min\{a_1, -1/3\}$ and $-1 < a_1 < 0$. Based on the conjecture and other results, we can obtain the following proposition.

Proposition 18. *There are four continuous functions $\varphi_2(a_1, \delta), \varphi_3(a_1, \delta), \varphi_4(a_1, \delta), \varphi_5(a_1, \delta)$ such that the following statements hold:*

- (i): *system (4) has a unique limit cycle when $a_2 \leq -1$, which is stable and large;*
- (ii): *system (4) has two homoclinic loops and one large limit cycle when $a_2 = \varphi_2(a_1, \delta)$ and $-1 < a_1 < 0$, where the homoclinic loops are unstable and the large limit cycle is stable;*
- (iii): *system (4) has two small limit cycles and one large limit cycle when $-1 < a_2 < \varphi_2(a_1, \delta)$, where the small ones are unstable and the large one is stable;*
- (iv): *system (4) has one stable two-saddle loop surrounding all of $\hat{E}_0, \hat{E}_{l_2}, \hat{E}_{r_2}$ and no limit cycles when $a_2 = \varphi_3(a_1, \delta)$ and $-1 < a_1 \leq a^*$;*
- (v): *system (4) has one unstable two-saddle loop surrounding all of $\hat{E}_0, \hat{E}_{l_2}, \hat{E}_{r_2}$ and exactly one stable large limit cycle when $a_2 = \varphi_3(a_1, \delta)$ and $a^* < a_1 < 0$;*
- (vi): *system (4) has two large limit cycles when $\varphi_2(a_1, \delta) < a_2 < \varphi_3(a_1, \delta)$ and $-1 < a_1 < 0$, where the homoclinic loops are unstable and the large limit cycle is stable;*
- (vii): *system (4) has two limit cycle when $\varphi_2(a_1, \delta) < a_2 < \varphi_5(a_1, \delta)$ and $a^* < a_1 < 0$, where they are large, the inner one is unstable and the outer one is stable;*
- (viii): *system (4) has a unique limit cycle when $a_2 = \varphi_5(a_1, \delta)$ and $a^* < a_1 < 0$, which is semi-stable and large;*
- (ix): *system (4) has no limit cycles when $\varphi_3(a_1, \delta) < a_2 < \varphi_4(a_1, \delta)$ and $-1 < a_1 \leq a^*$ or $\varphi_5(a_1, \delta) < a_2 < \varphi_4(a_1, \delta)$ and $a^* < a_1 < 0$;*
- (x): *system (4) has one two-saddle loop only surrounding \hat{E}_0 if and only if $a_2 = \varphi_4(a_1, \delta)$, which is stable ;*
- (xi): *system (4) has two limit cycle when $\varphi_4(a_1, \delta) < a_2 < 0$ and $-1 < a_1 < 0$, where they are small and stable;*

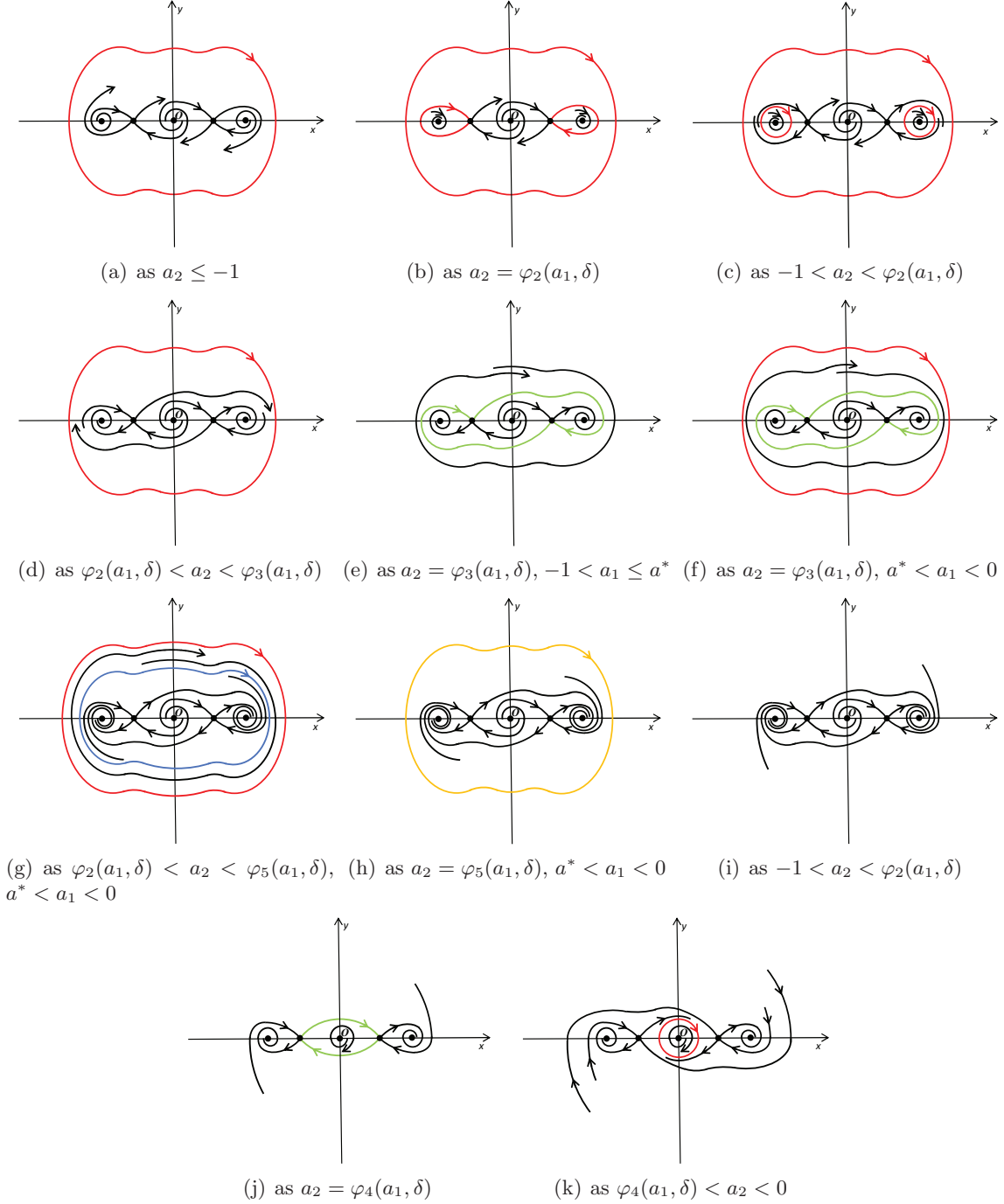


FIGURE 21. All phase portraits of (4) when $-1 < a_1 < 0$ and $a_2 < 0$.

where $\varphi_3(a^*, \delta) = a^*$, $-1 < \varphi_2(a_1, \delta) < \varphi_3(a_1, \delta) < \varphi_4(a_1, \delta) < 0$ and $\varphi_2(a_1, \delta) < -1/3 < \varphi_4(a_1, \delta)$ for $-1 < a_1 < 0$ and $\varphi_3(a_1, \delta) < \varphi_5(a_1, \delta) < -1/3$ for $a^* < a_1 < 0$. See Figure 21.

Proof. Firstly, by Lemma 14, the statement (i) follows, as shown in Figure 21 (a).

Denote $P := (x_P, 0)$ and $Q := (x_Q, 0)$ be respectively the first intersection points of the stable and unstable manifold of the right-hand side of \hat{E}_{r_1} and the x -axis. By Lemma 4 and the statement (i), we know that \hat{E}_{r_2} of system (4) are unstable and system (4) has no small limit cycles when $a_2 \leq -1$. It implies that $x_P < x_Q$ when $a_2 \leq -1$ since system (4) has small limit cycles for $x_P > x_Q$ and $a_2 \leq -1$ by the annulus region of Poincaré-Bendixson

Theorem and system (4) has a homoclinic loop only surrounding \hat{E}_{r2} for $x_P = x_Q$. By Lemmas 4 and 13, we know that \hat{E}_{r2} of system (4) are stable and system (4) has no small limit cycles surrounding \hat{E}_{r2} when $a_2 \geq (a_1 - 1 - \sqrt{-a_1})/3$. It implies that $x_P > x_Q$ when $a_2 \geq (a_1 - 1 - \sqrt{-a_1})/3$. Furthermore, as proved in Lemma 3.3 of [4], x_P increases continuously and x_B decreases continuously as a_2 increases since the vector field of system (4) is rotated on a_2 . Therefore, there is a unique function $\varphi_2(a_1, \delta) \in (-1, (a_1 - 1 - \sqrt{-a_1})/3)$ such that $x_P - x_Q = 0$ if and only if $a_2 = \varphi_2(a_1, \delta)$ as shown in Figure 21 (b). Since the saddle quantities at \hat{E}_{r1} and \hat{E}_{l1} are $\delta(a_1 - a_2) > 0$ for $a_1 > a_2$, the small homoclinic loop only surrounding \hat{E}_{r1} and the small homoclinic loop only surrounding \hat{E}_{l1} are unstable by [8, Theorem 3.3, Chapter 3]. In other words, $x_P < x_Q$ if and only if $a_2 < \varphi_2(a_1, \delta)$, and $x_P > x_Q$ if and only if $a_2 > \varphi_2(a_1, \delta)$. Then, the statements **(ii)** and **(iii)** hold.

Denote $Q := (0, y_Q)$ and $S := (0, y_S)$ be respectively the first intersection points of the stable and unstable manifold of the right-hand side of \hat{E}_{l1} and the y -axis. On the one hand, when $a_2 = 0$ and $-1 < a_1 < 0$, since system (4) has no limit cycles and the origin is stable, we obtain $y_Q + y_S < 0$. Otherwise, system (4) has no small closed orbits surrounding \hat{E}_0 for $y_Q + y_S \geq 0$. This is a contradiction. On the other hand, when $a_2 = a_1/3$ and $-1 < a_1 < 0$, since system (4) has no limit cycles and the origin is unstable, we obtain $y_Q + y_S > 0$. Otherwise, system (4) has no small closed orbits surrounding \hat{E}_0 for $y_Q + y_S \leq 0$. This is a contradiction. When $a_1 \in (-1, 0)$ is fixed, since the vector field of system (4) is rotated on a_2 , there is a unique value $a_2 = \varphi_4(a_1, \delta) \in (a_1/3, 0)$ such that $y_Q + y_S = 0$, i.e., system (4) has a small homoclinic loop surrounding \hat{E}_0 . Since the sum of saddle quantities at \hat{E}_{r1} and \hat{E}_{l1} is $\delta(a_1 - a_2)$ and negative for $a_1 < a_2$, the small homoclinic loop only surrounding \hat{E}_0 is stable by [8, Theorem 3.3, Chapter 3]. Then, the statement **(x)** holds.

Denote $M := (x_M, 0)$ be the first intersection points of the unstable manifold of the right-hand side of \hat{E}_{l1} and the x -axis. It is clear that $x_M > x_P$ for $a_2 = \varphi_2(a_1, \delta)$. By Lemmas 4 and 13, E_0 of system (2) are unstable and there is no small limit cycles surrounding \hat{E}_0 when $a_2 \leq -a_1/3$. It implies that $x_M < x_N$ when $a_2 \leq -a_1/3$. By Lemmas 4 and 7, E_0 of system (2) are stable and there is no small limit cycles when $a_2 = 0$. It implies that $x_M > x_P$ when $a_2 = 0$. Furthermore, as proved in Lemma 3.3 of [4], x_M increases continuously and x_P decreases continuously as a_2 increases. Therefore, there is a unique function $\varphi_3(a_1, \delta)$ such that $x_M - x_P = 0$ if and only if $a_2 = \varphi_3(a_1, \delta)$. Since the sum of saddle quantities at \hat{E}_{r1} and \hat{E}_{l1} is $\delta(a_1 - a_2)$ and positive (resp. negative) for $a_1 > a_2$ (resp. $a_1 < a_2$), a heteroclinic loop is unstable (resp. stable) by [8, Theorem 3.3, Chapter 3]. In other words, $x_M < x_P$ if and only if $a_2 < \varphi_3(a_1, \delta)$, and $x_M > x_P$ if and only if $a_2 > \varphi_3(a_1, \delta)$. By Lemma 6 and the Poincaré-Bendixson Theorem, system (2) has at least one large limit cycle for $a_2 = \varphi_3(a_1, \delta)$ and $a_1 > a_2$. Associated with that system (2) has at most two large limit cycles, system (2) has exactly one large limit cycle for $a_2 = \varphi_3(a_1, \delta)$ and $a_1 > a_2$. Assume that system (2) has at least one large limit cycle for $a_2 = \varphi_3(a_1, \delta)$ and $a_1 \leq a_2$. By Lemma 6 and the stability of heteroclinic loop, there are at least two large limit cycles for $a_2 = \varphi_3(a_1, \delta)$ and $a_1 \leq a_2$. By the heteroclinic bifurcation, there are at least three large limit cycles for $a_2 = \varphi_3(a_1, \delta) + \varepsilon$ and $a_1 \leq a_2$, where $0 < \varepsilon \ll 1$. This is a contradiction. Then, the statements **(iv)** and **(v)** hold. Furthermore, there is a continuous function $a_2 = \varphi_5(a_1, \delta) \in (\varphi_3(a_1, \delta), \min\{a_2, -1/3\})$ such that system (2) has a semi-stable large limit cycle. Then, the statement **(viii)** holds. Since the remainder statements can be similarly proved, we omit them. \square

4. PROOFS OF THEOREMS 1-3 AND SIMULATIONS

Proof of Theorem 1. By Lemmas 4, 8, 9, Proposition 6, the proof can be obtained directly. \square

Proof of Theorem 2. By Proposition 5, statements **(i)-(v)** hold. By Proposition 6, statement **(vi)** holds. By Proposition 18, statements **(vii)-(x)** hold. When system (4) has neither large limit cycles nor large singular closed orbits (including large heteroclinic loops and figure-eight

loops), the orbit connections between equilibria at finity and equilibria at infinity have many cases since the vector field of system (4) is rotated on a_2 . Statements (xi) holds. Finally, according to those bifurcation sets, we give the complete bifurcation diagram in Figure 2. \square

Proof of Theorem 3. The parameter plane $\delta = \delta_0 \in (0, 2\sqrt{3})$ (resp. $\delta = \delta_0 \in [2\sqrt{3}, +\infty)$) are divided into the parameter regions I, II, \dots, XI (resp., R_1, \dots, R_{11}) by these bifurcation surfaces. Moreover, the corresponding global phase portraits in the Poincaré disc can be obtained according to lemmas and propositions in Sections 3 and 4. By Proposition 18, there are at most three limit cycles for $a_2 \in (-\infty, (a_1 - 1 - \sqrt{-a_1})/3] \cup [\min\{a_1, -1/3\}, 0)$ and $-1 < a_1 < 0$. By Lemmas 13 and 17, there are at most four large limit cycles and no small limit cycles for $(a_1 - 1 - \sqrt{-a_1})/3 < a_2 < \min\{a_1, -1/3\}$ and $-1 < a_1 < 0$. Thus we get an upper bound 4 of the number of limit cycles. \square

In the following, we illustrate our theoretical results with some numerical examples.

Example 1. Consider $(a_1, a_2, \delta) = (0.5, -0.1, 1)$. The numerical phase portrait shows that system (4) has no limit cycles and three equilibria in the parameter region I , as shown in Figure 22 (a).

Example 2. Consider $(a_1, a_2, \delta) = (0.5, -0.7, 1)$. The numerical phase portrait shows that system (4) has exactly two large limit cycles and three equilibria in the parameter region II , as shown in Figure 22 (b).

Example 3. Consider $(a_1, a_2, \delta) = (0.5, -0.9, 1)$. The numerical phase portrait shows that system (4) has exactly two small limit cycles, one large limit cycle and three equilibria in the parameter region III , as shown in Figure 22 (c).

Example 4. Consider $(a_1, a_2, \delta) = (0.5, -1.1, 1)$. The numerical phase portrait shows that system (4) has exactly one large limit cycle and three equilibria in the parameter region IV , as shown in Figure 22 (d).

Example 5. Consider $(a_1, a_2, \delta) = (-0.5, -1.1, 1)$. The numerical phase portrait shows that system (4) has exactly one large limit cycle and five equilibria in the parameter region V , as shown in Figure 22 (e).

Example 6. Consider $(a_1, a_2, \delta) = (-0.5, -0.95, 1)$. The numerical phase portrait shows that system (4) has exactly two small limit cycles, one large limit cycle and five equilibria in the parameter region VI , as shown in Figure 22 (f).

Example 7. Consider $(a_1, a_2, \delta) = (-0.5, -0.85, 1)$. The numerical phase portrait shows that system (4) has exactly one large limit cycle and five equilibria in the parameter region VII , as shown in Figure 23 (a).

Example 8. Consider $(a_1, a_2, \delta) = (-0.02, -0.63, 1)$. The numerical phase portrait shows that system (4) has exactly two large limit cycles and five equilibria in the parameter region $VIII$, as shown in Figure 23 (b).

Example 9. Consider $(a_1, a_2, \delta) = (-0.5, -0.1, 1)$. The numerical phase portrait shows that system (4) has no limit cycles and five equilibria in the parameter region IX , as shown in Figure 23 (c).

Example 10. Consider $(a_1, a_2, \delta) = (-0.5, -0.05, 1)$. The numerical phase portrait shows that system (4) has exactly one small limit cycle surrounding \hat{E}_0 and five equilibria in the parameter region X , as shown in Figure 23 (d).

Example 11. Consider $(a_1, a_2, \delta) = (-0.5, 0.5, 1)$. The numerical phase portrait shows that system (4) has no limit cycles and five equilibria in the parameter region XI , as shown in Figure 23 (e).

ACKNOWLEDGEMENTS

We sincerely thank Prof. Xiuli Cen for her useful suggestions and valuable comments on Appendix C.

This work is financially supported by the National Key R&D Program of China (No. 2022YFA1005900). The first author is supported by the National Natural Science Foundation of China

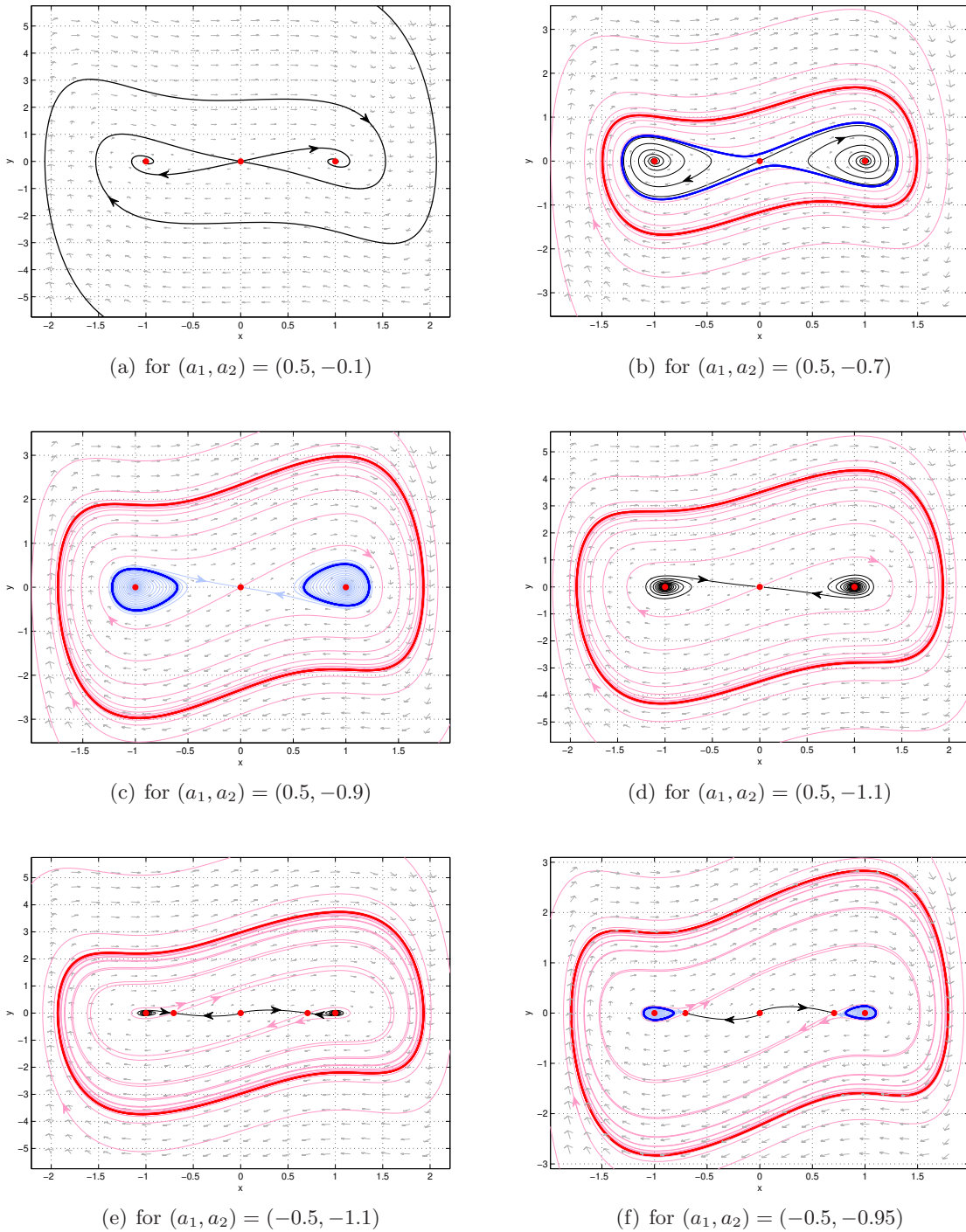


FIGURE 22. Numerical phase portraits of (2) when $\delta = 1$.

(Nos. 12322109, 12171485) and Science and Technology Innovation Program of Hunan Province (No. 2023RC3040). The second author is supported by the National Natural Science Foundation of China (No. 12271378) and Sichuan Science and Technology Program (No. 2024NS-FJQ0008). The third author is supported by the China Postdoctoral Science Foundation (No. 2023M743969) and Postdoctoral Fellowship Program of CPSF (No. GZC20233195). The fourth author is supported by the National Natural Science Foundation of China (Nos. 11931016,

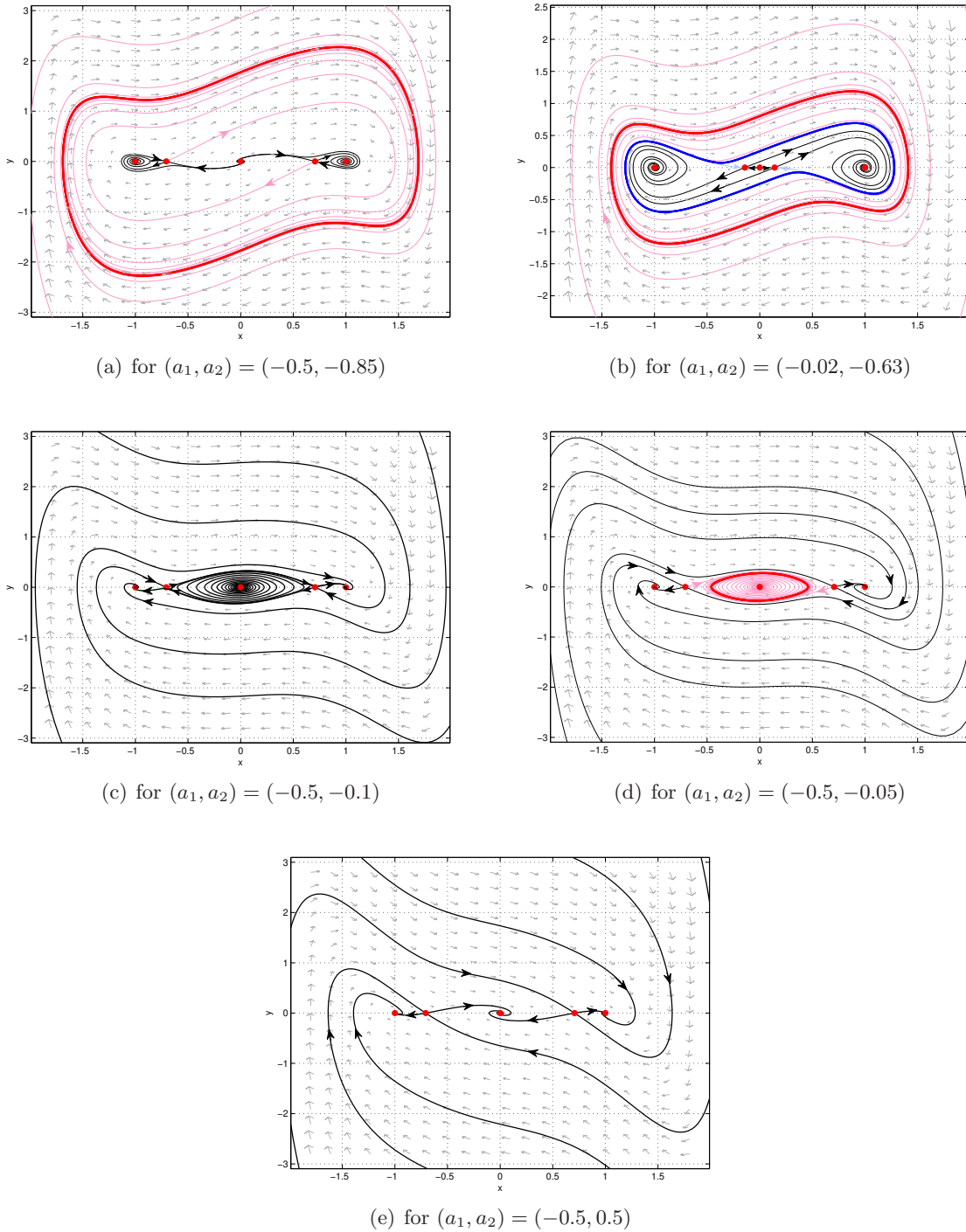


FIGURE 23. Numerical phase portraits of (2) when $\delta = 1$.

12271355, 12161131001), Science and Technology Innovation Action Plan of Science and Technology Commission of Shanghai Municipality (STCSM, No. 20JC1413200) and Innovation Program of Shanghai Municipal Education Commission (No. 2021-01-07-00-02-E00087).

REFERENCES

- [1] Q. Cao, Y. Han, T. Liang, M. Wiercigroch, S. Piskarev, Multiple buckling and codimension-three bifurcation phenomena of a nonlinear oscillator, *Int. J. Bifur. Chaos* **24** (2014), 1430005–1–17.

- [2] R. W. Carroll, A. J. Glick, On the Ginzburg-Landau equations, *Arch. Rational Mech. Anal.* **16** (1964), 373-384.
- [3] H. Chen, X. Chen, J. Xie, Global phase portrait of a degenerate Bogdanov-Takens system with symmetry, *Discrete Contin. Dyn. Syst. (Series B)* **22** (2017), 1273-1293.
- [4] H. Chen, X. Chen, Global phase portraits of a degenerate Bogdanov-Takens system with symmetry (II), *Discrete Contin. Dyn. Syst. (Series B)* **23** (2018), 4141-4170.
- [5] H. Chen, X. Chen, M. Jia, Y. Tang, A quintic \mathbb{Z}_2 -equivariant Liénard system arising from the complex Ginzburg-Landau equation, *SIAM J. Math. Anal.* **55** (2023), 5993-6038.
- [6] H. Chen, M. Jia, Y. Tang, A degenerate planar piecewise linear differential system with three zones, *J. Differential Equations* **297** (2021) 433-468.
- [7] H. Chen, J. Llibre, Y. Tang, Global dynamics of a SD oscillator, *Nonlinear Dyn.* **91** (2018), 1755-1777.
- [8] S. N. Chow, C. Li, D. Wang, *Normal Forms and Bifurcation of Planar Vector Fields*, Cambridge. Press, 1994.
- [9] G. Dangelmayr, D. Armbruster, M. Neveling, A codimension three bifurcation for the laser with saturable absorber, *Z. Phys. B* **59** (1985), 365-370.
- [10] F. Dumortier, C. Herssens, Polynomial Liénard equations near infinity, *J. Differential Equations* **153** (2000), 1-29.
- [11] F. Dumortier, C. Rousseau, Cubic Liénard equations with linear damping, *Nonlinearity* **3** (1990), 1015-1039.
- [12] Z. Feng, A nonconvex dissipative system and its applications (I), *J. Glob. Optim.* **40** (2008), 623-636.
- [13] Z. Feng, D. Y. Gao A nonconvex dissipative system and its applications (II), *J. Glob. Optim.* **40** (2008), 637-651.
- [14] R. Goh, B. de Rijk, Spectral stability of pattern-forming fronts in the complex Ginzburg-Landau equation with a quenching mechanism, *Nonlinearity* **35** (2022), 170-244.
- [15] B. Guo, B. Wang, Finite-dimensional behaviour for the derivative Ginzburg-Landau equation in two spatial dimensions, *Phys. D* **89** (1995), 83-99.
- [16] Y. Han, Q. Cao, Y. Chen, M. Wiercigroch, A novel mass-spring based smooth and discontinuous oscillator with strongly irrational nonlinearities, *Sci. China-Phys. Mech. Astron.* **55** (2012), 1832-1843.
- [17] L. Katzarkov, M. Kontsevich, T. Pantev, Bogomolov-Tian-Todorov Theorems for Landau-Ginzburg models, *J. Differential Geometry* **105** (2017), 55-117.
- [18] N. Levinson, O. K. Smith, A general equation for relaxation oscillations, *Duke Math. J.* **9** (1942), 382-403.
- [19] S. Li, H. Wen, On the L^2 -Hodge theory of Landau-Ginzburg models, *Adv. Math.* **396** (2022), 108165.
- [20] K. Lu, X. Pan, Ginzburg-Landau equation with DeGennes boundary condition, *J. Differential Equations* **129** (1996), 136-165.
- [21] T. Ogawa, T. Yokota, Uniqueness and inviscid limits of solutions for the complex Ginzburg-Landau equation in a two-dimensional domain, *Comm. Math. Phys.* **245** (2004), 105-121.
- [22] F. Verhulst, *Nonlinear Differential Equations and Dynamical Systems*, Universitext, Springer, 1991.
- [23] B. Wang, The limit behavior of solutions for the Cauchy problem of the complex Ginzburg-Landau equation, *Comm. Pure Appl. Math.* **55** (2002), 481-508.
- [24] Z. Zhang, T. Ding, W. Huang, Z. Dong, *Qualitative Theory of Differential Equations*, Transl. Math. Monogr., Amer. Math. Soc., Providence, RI, 1992.

APPENDIX A

$$\begin{aligned}
I &:= \{(a_1, a_2, \delta) \in \Omega \mid a_2 > \varphi_5(a_1, \delta), a_1 \geq 0, 0 < \delta < 2\sqrt{3}\}, \\
II &:= \{(a_1, a_2, \delta) \in \Omega \mid \varphi_1(a_1, \delta) < a_2 < \varphi_5(a_1, \delta), a_1 \geq 0, 0 < \delta < 2\sqrt{3}\}, \\
III &:= \{(a_1, a_2, \delta) \in \Omega \mid -1 < a_2 < \varphi_1(a_1, \delta), a_1 \geq 0, 0 < \delta < 2\sqrt{3}\}, \\
IV &:= \{(a_1, a_2, \delta) \in \Omega \mid a_2 \leq -1, a_1 \geq 0, 0 < \delta < 2\sqrt{3}\}, \\
V &:= \{(a_1, a_2, \delta) \in \Omega \mid a_2 \leq -1, -1 < a_1 < 0, 0 < \delta < 2\sqrt{3}\}, \\
VI &:= \{(a_1, a_2, \delta) \in \Omega \mid -1 < a_2 < \varphi_2(a_1, \delta), -1 < a_1 < 0, 0 < \delta < 2\sqrt{3}\}, \\
VII &:= \{(a_1, a_2, \delta) \in \Omega \mid \varphi_2(a_1, \delta) < a_2 < \varphi_3(a_1, \delta), -1 < a_1 < 0, 0 < \delta < 2\sqrt{3}\}, \\
VIII &:= \{(a_1, a_2, \delta) \in \Omega \mid \varphi_3(a_1, \delta) < a_2 < \varphi_5(a_1, \delta), a^* < a_1 < 0, 0 < \delta < 2\sqrt{3}\}, \\
IX &:= \{(a_1, a_2, \delta) \in \Omega \mid \varphi_5(a_1, \delta) < a_2 < \varphi_4(a_1, \delta), a^* < a_1 < 0, 0 < \delta < 2\sqrt{3}\} \cup \\
&\quad \{(a_1, a_2, \delta) \in \Omega \mid \varphi_3(a_1, \delta) < a_2 < \varphi_4(a_1, \delta), -1 < a_1 \leq a^*, 0 < \delta < 2\sqrt{3}\}, \\
X &:= \{(a_1, a_2, \delta) \in \Omega \mid \varphi_4(a_1, \delta) < a_2 < 0, -1 < a_1 < 0, 0 < \delta < 2\sqrt{3}\},
\end{aligned}$$

$$\begin{aligned}
XI &:= \{(a_1, a_2, \delta) \in \Omega \mid a_2 \geq 0, -1 < a_1 < 0, 0 < \delta < 2\sqrt{3}\}, \\
DL_1 &:= \{(a_1, a_2, \delta) \in \Omega \mid a_2 = \varphi_5(a_1, \delta), a_1 \geq 0, 0 < \delta < 2\sqrt{3}\}, \\
DL_2 &:= \{(a_1, a_2, \delta) \in \Omega \mid a_2 = \varphi_5(a_1, \delta), a^* < a_1 < 0, 0 < \delta < 2\sqrt{3}\}, \\
HE_{11} &:= \{(a_1, a_2, \delta) \in \Omega \mid a_2 = \varphi_3(a_1, \delta), -1 < a_1 < a^*, 0 < \delta < 2\sqrt{3}\}, \\
HE_{12} &:= \{(a_1, a_2, \delta) \in \Omega \mid a_2 = \varphi_3(a_1, \delta), a^* \leq a_1 < 0, 0 < \delta < 2\sqrt{3}\}, \\
SL_1 &:= \{(a_1, a_2, \delta) \in \Omega \mid a_2 = \varphi_3(-1, \delta), a_1 = -1, \delta > 0\}, \\
SL_2 &:= \{(a_1, a_2, \delta) \in \Omega \mid a_2 = \varphi_4(-1, \delta), a_1 = -1, 0 < \delta < 2\sqrt{3}\}, \\
T_1 &:= \{(a_1, a_2, \delta) \in \Omega \mid a_2 < -1, a_1 = -1, \delta > 0\}, \\
T_2 &:= \{(a_1, a_2, \delta) \in \Omega \mid -1 < a_2 < \varphi_3(-1, \delta), a_1 = -1, \delta > 0\}, \\
T_3 &:= \{(a_1, a_2, \delta) \in \Omega \mid \varphi_3(-1, \delta) < a_2 < \varphi_4(-1, \delta), a_1 = -1, 0 < \delta < 2\sqrt{3}\}, \\
T_4 &:= \{(a_1, a_2, \delta) \in \Omega \mid \varphi_4(-1, \delta) < a_2 < 0, a_1 = -1, 0 < \delta < 2\sqrt{3}\}, \\
T_5 &:= \{(a_1, a_2, \delta) \in \Omega \mid a_2 \geq 0, a_1 = -1, 0 < \delta < 2\sqrt{3}\}, \\
R_{11i} &:= \{(a_1, a_2, \delta) \in \Omega \mid a_2 = \phi_{1,i}(a_1, \delta), a_1 \geq 0, \delta \geq 2\sqrt{3}\}, \\
R_{12i} &:= \{(a_1, a_2, \delta) \in \Omega \mid a_2 = \phi_{2,i}(a_1, \delta), a_1 \geq 0, \delta \geq 2\sqrt{3}\}, \\
R_{13i} &:= \{(a_1, a_2, \delta) \in \Omega \mid \phi_{2,i}(a_1, \delta) < a_2 < \phi_{1,i}(a_1, \delta), a_1 \geq 0, \delta \geq 2\sqrt{3}\}, \\
R_{14i} &:= \{(a_1, a_2, \delta) \in \Omega \mid \phi_{1,i+1}(a_1, \delta) < a_2 < \phi_{2,i}(a_1, \delta), a_1 \geq 0, \delta \geq 2\sqrt{3}\}, \\
R_2 &:= \{(a_1, a_2, \delta) \in \Omega \mid \varphi_1(a_1, \delta) < a_2 < \varphi_5(a_1, \delta), a_1 \geq 0, \delta \geq 2\sqrt{3}\}, \\
R_3 &:= \{(a_1, a_2, \delta) \in \Omega \mid -1 < a_2 < \varphi_1(a_1, \delta), a_1 \geq 0, \delta \geq 2\sqrt{3}\}, \\
R_4 &:= \{(a_1, a_2, \delta) \in \Omega \mid a_2 \leq -1, a_1 \geq 0, \delta \geq 2\sqrt{3}\}, \\
R_5 &:= \{(a_1, a_2, \delta) \in \Omega \mid a_2 \leq -1, -1 < a_1 < 0, \delta \geq 2\sqrt{3}\}, \\
R_6 &:= \{(a_1, a_2, \delta) \in \Omega \mid -1 < a_2 < \varphi_2(a_1, \delta), -1 < a_1 < 0, \delta \geq 2\sqrt{3}\}, \\
R_7 &:= \{(a_1, a_2, \delta) \in \Omega \mid \varphi_2(a_1, \delta) < a_2 < \varphi_3(a_1, \delta), -1 < a_1 < 0, \delta \geq 2\sqrt{3}\}, \\
R_8 &:= \{(a_1, a_2, \delta) \in \Omega \mid \varphi_3(a_1, \delta) < a_2 < \varphi_5(a_1, \delta), a^* < a_1 < 0, \delta \geq 2\sqrt{3}\}, \\
R_{91i} &:= \{(a_1, a_2, \delta) \in \Omega \mid \varphi_5(a_1, \delta) < a_2 = \phi_{5,i}(a_1, \delta) < \varphi_4(a_1, \delta), a^* < a_1 < 0, \delta \geq 2\sqrt{3}\} \cup \\
&\quad \{(a_1, a_2, \delta) \in \Omega \mid \varphi_3(a_1, \delta) < a_2 = \phi_{5,i}(a_1, \delta) < \varphi_4(a_1, \delta), -1 < a_1 \leq a^*, \delta \geq 2\sqrt{3}\}, \\
R_{92i} &:= \{(a_1, a_2, \delta) \in \Omega \mid \varphi_5(a_1, \delta) < a_2 = \phi_{6,i}(a_1, \delta) < \varphi_4(a_1, \delta), a^* < a_1 < 0, \delta \geq 2\sqrt{3}\} \cup \\
&\quad \{(a_1, a_2, \delta) \in \Omega \mid \varphi_3(a_1, \delta) < a_2 = \phi_{6,i}(a_1, \delta) < \varphi_4(a_1, \delta), -1 < a_1 \leq a^*, \delta \geq 2\sqrt{3}\}, \\
R_{93i} &:= \{(a_1, a_2, \delta) \in \Omega \mid \max\{\varphi_5(a_1, \delta), \phi_{6,i}(a_1, \delta)\} < a_2 < \min\{\varphi_4(a_1, \delta), \phi_{5,i}(a_1, \delta)\}, \\
&\quad a^* < a_1 < 0, \delta \geq 2\sqrt{3}\} \cup \{(a_1, a_2, \delta) \in \Omega \mid \max\{\varphi_3(a_1, \delta), \phi_{6,i}(a_1, \delta)\} < a_2 \\
&\quad < \min\{\varphi_4(a_1, \delta), \phi_{5,i}(a_1, \delta)\}, -1 < a_1 \leq a^*, \delta \geq 2\sqrt{3}\}, \\
R_{94i} &:= \{(a_1, a_2, \delta) \in \Omega \mid \max\{\varphi_5(a_1, \delta), \phi_{5,i+1}(a_1, \delta)\} < a_2 < \min\{\varphi_4(a_1, \delta), \phi_{6,i}(a_1, \delta)\}, \\
&\quad a^* < a_1 < 0, \delta \geq 2\sqrt{3}\} \cup \{(a_1, a_2, \delta) \in \Omega \mid \max\{\varphi_3(a_1, \delta), \phi_{5,i+1}(a_1, \delta)\} < a_2 \\
&\quad < \min\{\varphi_4(a_1, \delta), \phi_{6,i}(a_1, \delta)\}, -1 < a_1 \leq a^*, \delta \geq 2\sqrt{3}\}, \\
R_{101i} &:= \{(a_1, a_2, \delta) \in \Omega \mid \varphi_4(a_1, \delta) < a_2 = \phi_{3,i}(a_1, \delta) < 0, -1 < a_1 < 0, \delta \geq 2\sqrt{3}\}, \\
R_{102i} &:= \{(a_1, a_2, \delta) \in \Omega \mid \varphi_4(a_1, \delta) < a_2 = \phi_{4,i}(a_1, \delta) < 0, -1 < a_1 < 0, \delta \geq 2\sqrt{3}\}, \\
R_{103i} &:= \{(a_1, a_2, \delta) \in \Omega \mid \varphi_4(a_1, \delta) < a_2 = \phi_{5,i}(a_1, \delta) < 0, -1 < a_1 < 0, \delta \geq 2\sqrt{3}\}, \\
R_{104i} &:= \{(a_1, a_2, \delta) \in \Omega \mid \varphi_4(a_1, \delta) < a_2 = \phi_{6,i}(a_1, \delta) < 0, -1 < a_1 < 0, \delta \geq 2\sqrt{3}\}, \\
R_{105i} &:= \{(a_1, a_2, \delta) \in \Omega \mid \max\{\varphi_4(a_1, \delta), \phi_{4,i}(a_1, \delta)\} < a_2 < \min\{0, \phi_{3,i}(a_1, \delta)\}, \\
&\quad -1 < a_1 < 0, \delta \geq 2\sqrt{3}\},
\end{aligned}$$

$$\begin{aligned}
R_{106i} &:= \{(a_1, a_2, \delta) \in \Omega \mid \max\{\varphi_4(a_1, \delta), \phi_{5,i}(a_1, \delta)\} < a_2 < \min\{0, \phi_{4,i}(a_1, \delta)\}, \\
&\quad -1 < a_1 < 0, \delta \geq 2\sqrt{3}\}, \\
R_{107i} &:= \{(a_1, a_2, \delta) \in \Omega \mid \max\{\varphi_4(a_1, \delta), \phi_{6,i}(a_1, \delta)\} < a_2 < \min\{0, \phi_{5,i}(a_1, \delta)\}, \\
&\quad -1 < a_1 < 0, \delta \geq 2\sqrt{3}\}, \\
R_{108i} &:= \{(a_1, a_2, \delta) \in \Omega \mid \max\{\varphi_4(a_1, \delta), \phi_{3,i+1}(a_1, \delta)\} < a_2 < \min\{0, \phi_{6,i}(a_1, \delta)\}, \\
&\quad -1 < a_1 < 0, \delta \geq 2\sqrt{3}\}, \\
R_{111i} &:= \{(a_1, a_2, \delta) \in \Omega \mid a_2 = \phi_{3,i}(a_1, \delta) > 0, -1 < a_1 < 0, \delta \geq 2\sqrt{3}\}, \\
R_{112i} &:= \{(a_1, a_2, \delta) \in \Omega \mid a_2 = \phi_{4,i}(a_1, \delta) > 0, -1 < a_1 < 0, \delta \geq 2\sqrt{3}\}, \\
R_{113i} &:= \{(a_1, a_2, \delta) \in \Omega \mid a_2 = \phi_{5,i}(a_1, \delta) > 0, -1 < a_1 < 0, \delta \geq 2\sqrt{3}\}, \\
R_{114i} &:= \{(a_1, a_2, \delta) \in \Omega \mid a_2 = \phi_{6,i}(a_1, \delta) > 0, -1 < a_1 < 0, \delta \geq 2\sqrt{3}\}, \\
R_{115i} &:= \{(a_1, a_2, \delta) \in \Omega \mid \max\{0, \phi_{4,i}(a_1, \delta)\} < a_2 < \phi_{3,i}(a_1, \delta), -1 < a_1 < 0, \delta \geq 2\sqrt{3}\}, \\
R_{116i} &:= \{(a_1, a_2, \delta) \in \Omega \mid \max\{0, \phi_{5,i}(a_1, \delta)\} < a_2 < \phi_{4,i}(a_1, \delta), -1 < a_1 < 0, \delta \geq 2\sqrt{3}\}, \\
R_{117i} &:= \{(a_1, a_2, \delta) \in \Omega \mid \max\{0, \phi_{6,i}(a_1, \delta)\} < a_2 < \phi_{5,i}(a_1, \delta), -1 < a_1 < 0, \delta \geq 2\sqrt{3}\}, \\
R_{118i} &:= \{(a_1, a_2, \delta) \in \Omega \mid \max\{0, \phi_{3,i+1}(a_1, \delta)\} < a_2 < \phi_{6,i}(a_1, \delta), -1 < a_1 < 0, \delta \geq 2\sqrt{3}\}, \\
\widehat{DL}_1 &:= \{(a_1, a_2, \delta) \in \Omega \mid a_2 = \varphi_5(a_1, \delta), a_1 \geq 0, \delta \geq 2\sqrt{3}\}, \\
\widehat{DL}_2 &:= \{(a_1, a_2, \delta) \in \Omega \mid a_2 = \varphi_5(a_1, \delta), a^* < a_1 < 0, \delta \geq 2\sqrt{3}\}, \\
\widehat{HE}_{11} &:= \{(a_1, a_2, \delta) \in \Omega \mid a_2 = \varphi_3(a_1, \delta), -1 < a_1 < a^*, \delta \geq 2\sqrt{3}\}, \\
\widehat{HE}_{12} &:= \{(a_1, a_2, \delta) \in \Omega \mid a_2 = \varphi_3(a_1, \delta), a^* \leq a_1 < 0, \delta \geq 2\sqrt{3}\}, \\
HE_{21i} &:= \{(a_1, a_2, \delta) \in \Omega \mid a_2 = \varphi_4(a_1, \delta) = \phi_{5,i}(a_1, \delta), -1 < a_1 < 0, \delta \geq 2\sqrt{3}\}, \\
HE_{22i} &:= \{(a_1, a_2, \delta) \in \Omega \mid a_2 = \varphi_4(a_1, \delta) = \phi_{6,i}(a_1, \delta), -1 < a_1 < 0, \delta \geq 2\sqrt{3}\}, \\
HE_{23i} &:= \{(a_1, a_2, \delta) \in \Omega \mid \phi_{6,i}(a_1, \delta) < a_2 = \varphi_4(a_1, \delta) < \phi_{5,i}(a_1, \delta), -1 < a_1 < 0, \delta \geq 2\sqrt{3}\}, \\
HE_{24i} &:= \{(a_1, a_2, \delta) \in \Omega \mid \phi_{5,i+1}(a_1, \delta) < a_2 = \varphi_4(a_1, \delta) < \phi_{6,i}(a_1, \delta), -1 < a_1 < 0, \delta \geq 2\sqrt{3}\}, \\
SL_{21i} &:= \{(a_1, a_2, \delta) \in \Omega \mid a_2 = \varphi_4(-1, \delta) = \phi_{5,i}(a_1, \delta), a_1 = -1, \delta \geq 2\sqrt{3}\}, \\
SL_{22i} &:= \{(a_1, a_2, \delta) \in \Omega \mid a_2 = \varphi_4(-1, \delta) = \phi_{6,i}(a_1, \delta), a_1 = -1, \delta \geq 2\sqrt{3}\}, \\
SL_{23i} &:= \{(a_1, a_2, \delta) \in \Omega \mid \phi_{6,i}(a_1, \delta) < a_2 = \varphi_4(-1, \delta) = \phi_{5,i}(a_1, \delta), a_1 = -1, \delta \geq 2\sqrt{3}\}, \\
SL_{24i} &:= \{(a_1, a_2, \delta) \in \Omega \mid \phi_{5,i+1}(a_1, \delta) < a_2 = \varphi_4(-1, \delta) = \phi_{6,i}(a_1, \delta), a_1 = -1, \delta \geq 2\sqrt{3}\}, \\
T_{31i} &:= \{(a_1, a_2, \delta) \in \Omega \mid \varphi_3(-1, \delta) < a_2 = \phi_{5,i}(a_1, \delta) < \varphi_4(-1, \delta), a_1 = -1, \delta \geq 2\sqrt{3}\}, \\
T_{32i} &:= \{(a_1, a_2, \delta) \in \Omega \mid \varphi_3(-1, \delta) < a_2 = \phi_{6,i}(a_1, \delta) < \varphi_4(-1, \delta), a_1 = -1, \delta \geq 2\sqrt{3}\}, \\
T_{33i} &:= \{(a_1, a_2, \delta) \in \Omega \mid \max\{\varphi_5(-1, \delta), \phi_{6,i}(-1, \delta)\} < a_2 < \min\{\varphi_4(-1, \delta), \phi_{5,i}(-1, \delta)\}, \\
&\quad a_1 = -1, \delta \geq 2\sqrt{3}\}, \\
T_{34i} &:= \{(a_1, a_2, \delta) \in \Omega \mid \max\{\varphi_5(-1, \delta), \phi_{5,i+1}(-1, \delta)\} < a_2 < \min\{\varphi_4(-1, \delta), \phi_{6,i}(-1, \delta)\}, \\
&\quad a_1 = -1, \delta \geq 2\sqrt{3}\}, \\
T_{41i} &:= \{(a_1, a_2, \delta) \in \Omega \mid \varphi_4(-1, \delta) < a_2 = \phi_{3,i}(a_1, \delta) < 0, a_1 = -1, \delta \geq 2\sqrt{3}\}, \\
T_{42i} &:= \{(a_1, a_2, \delta) \in \Omega \mid \varphi_4(-1, \delta) < a_2 = \phi_{4,i}(a_1, \delta) < 0, a_1 = -1, \delta \geq 2\sqrt{3}\}, \\
T_{43i} &:= \{(a_1, a_2, \delta) \in \Omega \mid \varphi_4(-1, \delta) < a_2 = \phi_{5,i}(a_1, \delta) < 0, a_1 = -1, \delta \geq 2\sqrt{3}\}, \\
T_{44i} &:= \{(a_1, a_2, \delta) \in \Omega \mid \varphi_4(-1, \delta) < a_2 = \phi_{6,i}(a_1, \delta) < 0, a_1 = -1, \delta \geq 2\sqrt{3}\}, \\
T_{45i} &:= \{(a_1, a_2, \delta) \in \Omega \mid \max\{\varphi_4(-1, \delta), \phi_{4,i}(-1, \delta)\} < a_2 < \min\{0, \phi_{3,i}(-1, \delta)\}, \\
&\quad a_1 = -1, \delta \geq 2\sqrt{3}\}, \\
T_{46i} &:= \{(a_1, a_2, \delta) \in \Omega \mid \max\{\varphi_4(-1, \delta), \phi_{5,i}(-1, \delta)\} < a_2 < \min\{0, \phi_{4,i}(-1, \delta)\},
\end{aligned}$$

$$\begin{aligned}
& a_1 = -1, \delta \geq 2\sqrt{3}, \\
T_{47i} & := \{(a_1, a_2, \delta) \in \Omega \mid \max\{\varphi_4(-1, \delta), \phi_{6,i}(-1, \delta)\} < a_2 < \min\{0, \phi_{5,i}(-1, \delta)\}, \\
& \quad a_1 = -1, \delta \geq 2\sqrt{3}\}, \\
T_{48i} & := \{(a_1, a_2, \delta) \in \Omega \mid \max\{\varphi_4(-1, \delta), \phi_{3,i+1}(-1, \delta)\} < a_2 < \min\{0, \phi_{6,i}(-1, \delta)\}, \\
& \quad a_1 = -1, \delta \geq 2\sqrt{3}\}, \\
T_{51i} & := \{(a_1, a_2, \delta) \in \Omega \mid a_2 = \phi_{3,i}(a_1, \delta) \geq 0, a_1 = -1, \delta \geq 2\sqrt{3}\}, \\
T_{52i} & := \{(a_1, a_2, \delta) \in \Omega \mid a_2 = \phi_{4,i}(a_1, \delta) \geq 0, a_1 = -1, \delta \geq 2\sqrt{3}\}, \\
T_{53i} & := \{(a_1, a_2, \delta) \in \Omega \mid a_2 = \phi_{5,i}(a_1, \delta) \geq 0, a_1 = -1, \delta \geq 2\sqrt{3}\}, \\
T_{54i} & := \{(a_1, a_2, \delta) \in \Omega \mid a_2 = \phi_{6,i}(a_1, \delta) \geq 0, a_1 = -1, \delta \geq 2\sqrt{3}\}, \\
T_{55i} & := \{(a_1, a_2, \delta) \in \Omega \mid \phi_{4,i}(-1, \delta) < a_2 < \phi_{3,i}(-1, \delta), a_2 \geq 0, a_1 = -1, \delta \geq 2\sqrt{3}\}, \\
T_{56i} & := \{(a_1, a_2, \delta) \in \Omega \mid \phi_{5,i}(-1, \delta) < a_2 < \phi_{4,i}(-1, \delta), a_2 \geq 0, a_1 = -1, \delta \geq 2\sqrt{3}\}, \\
T_{57i} & := \{(a_1, a_2, \delta) \in \Omega \mid \phi_{6,i}(-1, \delta) < a_2 < \phi_{5,i}(-1, \delta), a_2 \geq 0, a_1 = -1, \delta \geq 2\sqrt{3}\}, \\
T_{58i} & := \{(a_1, a_2, \delta) \in \Omega \mid \phi_{3,i+1}(-1, \delta) < a_2 < \phi_{6,i}(-1, \delta), a_2 \geq 0, a_1 = -1, \delta \geq 2\sqrt{3}\}.
\end{aligned}$$

APPENDIX B

Proof of Lemma 4. It is easy to check that the number and abscissas of equilibria of system (2) are determined by the equation $x(x^4 + \mu_2 x^2 + \mu_1) = 0$. Notice that the number of roots of the equation $x(x^4 + \mu_2 x^2 + \mu_1) = 0$ is determined by the relationship between $\Delta := \mu_2^2 - 4\mu_1$ and 0 and the relationship between μ_2 and $\sqrt{\Delta}$. Thus, we show the number of equilibria of system (2) by the following nine cases:

Case (I): System (2) has five equilibria $\hat{E}_{l2}, \hat{E}_{l1}, \hat{E}_0, \hat{E}_{r1}, \hat{E}_{r2}$ when $\Delta > 0$ and $\mu_2 < -\sqrt{\Delta}$, that is, $\mu_1 > 0$ and $\mu_2 < -2\sqrt{\mu_1}$.

Case (II): System (2) has three equilibria $\hat{E}_{l2}, \hat{E}_0, \hat{E}_{r2}$ when $\Delta > 0$ and $\mu_2 = -\sqrt{\Delta}$, that is, $\mu_1 = 0$ and $\mu_2 < 0$.

Case (III): System (2) has three equilibria $\hat{E}_{l2}, \hat{E}_0, \hat{E}_{r2}$ when $\Delta > 0$ and $-\sqrt{\Delta} < \mu_2 < \sqrt{\Delta}$, that is, $\mu_1 < 0$ and $\mu_2 \in \mathbb{R}$.

Case (IV): System (2) has one equilibrium \hat{E}_0 when $\Delta > 0$ and $\mu_2 = \sqrt{\Delta}$, that is, $\mu_1 = 0$ and $\mu_2 > 0$.

Case (V): System (2) has one equilibrium \hat{E}_0 when $\Delta > 0$ and $\mu_2 > \sqrt{\Delta}$, that is, $\mu_1 > 0$ and $\mu_2 > 2\sqrt{\mu_1}$.

Case (VI): System (2) has three equilibria $\hat{E}_{l2}, \hat{E}_0, \hat{E}_{r2}$ when $\Delta = 0$ and $\mu_2 < 0$, that is, $\mu_1 > 0$ and $\mu_2 = -2\sqrt{\mu_1}$.

Case (VII): System (2) has one equilibrium \hat{E}_0 when $\Delta = 0$ and $\mu_2 = 0$, that is, $\mu_1 = \mu_2 = 0$.

Case (VIII): System (2) has one equilibrium \hat{E}_0 when $\Delta = 0$ and $\mu_2 > 0$, that is, $\mu_1 > 0$ and $\mu_2 = 2\sqrt{\mu_1}$.

Case (IX): System (2) has one equilibrium \hat{E}_0 when $\Delta < 0$, that is, $\mu_1 > 0$ and $-2\sqrt{\mu_1} < \mu_2 < 2\sqrt{\mu_1}$.

As a consequence, we obtain the location of equilibria of system (2), as illustrated in Table 1. We now study the qualitative properties of $\hat{E}_{l2}, \hat{E}_{l1}, \hat{E}_0, \hat{E}_{r1}, \hat{E}_{r2}$ of system (2) in turn.

The Jacobian matrix at \hat{E}_0 is the following form

$$J_{E_0} := \begin{pmatrix} 0 & 1 \\ -\mu_1 & -\mu_3 \end{pmatrix}.$$

According to $\det J_{E_0} = \mu_1$ and $\text{tr} J_{E_0} = -\mu_3$, it follows that \hat{E}_0 is a saddle for $\mu_1 < 0$, a sink for $\mu_1 > 0$ and $\mu_3 > 0$, and a source for $\mu_1 > 0$ and $\mu_3 < 0$. When $\mu_1 > 0$ and $\mu_3 = 0$, with the

scaling transformation

$$(y, t) \rightarrow (\sqrt{\mu_1}y, \frac{t}{\sqrt{\mu_1}}),$$

system (2) becomes

$$(43) \quad \begin{aligned} \dot{x} &= y, \\ \dot{y} &= -x - \frac{\mu_2}{\mu_1}x^3 - \frac{1}{\mu_1}x^5 - \frac{b}{\sqrt{\mu_1}}x^2y. \end{aligned}$$

By [8, p.211], we calculate the first focal value for system (43) and get that at the origin

$$g_3 = -\frac{b}{8\sqrt{\mu_1}} < 0$$

because of $b > 0$. Therefore, the origin of system (43) is a stable weak focus of order one and so is \hat{E}_0 . As $\mu_1 = \mu_3 = 0$, system (2) is simplified as

$$(44) \quad \begin{aligned} \dot{x} &= y, \\ \dot{y} &= -\mu_2x^3 - x^5 - bx^2y. \end{aligned}$$

It follows from [24, Theorem 7.2 of Chapter 2] that \hat{E}_0 of system (44) is a degenerate saddle for $\mu_2 < 0$, a degenerate center or focus for $\mu_2 > 0$, a degenerate center or focus for $\mu_2 = 0$ and $b \in (0, 2\sqrt{3})$, and a degenerate node for $\mu_2 = 0$ and $b \in [2\sqrt{3}, +\infty)$. Letting

$$H(x, y) = \frac{\mu_2x^3}{3} + \frac{x^5}{5} + \frac{y^2}{2},$$

we have

$$\frac{dH(x, y)}{dt} \Big|_{(44)} = -bx^2y^2 \leq 0,$$

implying that a stable focus for $\mu_2 > 0$, or $\mu_2 = 0$ and $b \in (0, 2\sqrt{3})$. Furthermore, for $\mu_1 = 0$ and $\mu_3 \neq 0$, using the translation transformation

$$(x, y) \rightarrow (x - \frac{y}{\mu_3}, y),$$

system (2) is changed into

$$(45) \quad \begin{aligned} \dot{x} &= -\frac{\mu_2}{\mu_3}(x - \frac{y}{\mu_3})^3 - \frac{1}{\mu_3}(x - \frac{y}{\mu_3})^5 - \frac{b}{\mu_3}(x - \frac{y}{\mu_3})^2y, \\ \dot{y} &= -\mu_3y - \mu_2(x - \frac{y}{\mu_3})^3 - (x - \frac{y}{\mu_3})^5 - b(x - \frac{y}{\mu_3})^2y. \end{aligned}$$

Solving $\dot{y} = 0$ of system (45), we obtain

$$(46) \quad y = -\frac{\mu_2}{\mu_3}x^3 + \frac{-\mu_3^2 + b\mu_2\mu_3 - 3\mu_2^2}{\mu_3^3}x^5 + O(x^6)$$

by the Implicit Function Theorem. Substituting (46) into the first equation of system (45), we have

$$\frac{dx}{dt} = -\frac{\mu_2}{\mu_3}x^3 + \frac{-\mu_3^2 + b\mu_2\mu_3 - 3\mu_2^2}{\mu_3^3}x^5 + O(x^6).$$

According to [24, Theorem 7.1 of Chapter 2], it follows that the origin of system (45) is a stable degenerate node for $\mu_2 \geq 0$ and $\mu_3 > 0$, an unstable degenerate node for $\mu_2 \geq 0$ and $\mu_3 < 0$, and a degenerate saddle for $\mu_2 < 0$ and $\mu_3 \neq 0$. So is \hat{E}_0 .

The Jacobian matrices at both \hat{E}_{l_2} and \hat{E}_{r_2} are of the following form

$$J_{\hat{E}_{l_2}} = J_{\hat{E}_{r_2}} := \begin{pmatrix} 0 & 1 \\ -\Delta + \mu_2\sqrt{\Delta} & -\mu_3 - \frac{b(-\mu_2 + \sqrt{\Delta})}{2} \end{pmatrix}.$$

By **Cases (I), (II), (III)** and **(VI)**, we know that the necessary conditions of the existence of \hat{E}_{l_2} and \hat{E}_{r_2} are $\Delta \geq 0$ and $\mu_2 < \sqrt{\Delta}$. Therefore, we obtain $\det J_{\hat{E}_{l_2}} = \det J_{\hat{E}_{r_2}} = \sqrt{\Delta}(\sqrt{\Delta} - \mu_2) > 0$ for $\Delta > 0$ and $\det J_{\hat{E}_{l_2}} = \det J_{\hat{E}_{r_2}} = 0$ for $\Delta = 0$. It is easy to check that $\text{tr} J_{\hat{E}_{l_2}} =$

$\text{tr}J_{\hat{E}_{r_2}} = -\mu_3 - b(-\mu_2 + \sqrt{\Delta})/2 < 0$ for $\mu_3 > -b(-\mu_2 + \sqrt{\Delta})/2$ and $\text{tr}J_{\hat{E}_{l_2}} = \text{tr}J_{\hat{E}_{r_2}} > 0$ for $\mu_3 < -b(-\mu_2 + \sqrt{\Delta})/2$. It follows that both \hat{E}_{l_2} and \hat{E}_{r_2} are sinks for $\Delta > 0$ and $\mu_3 > -b(-\mu_2 + \sqrt{\Delta})/2$, and sources for $\Delta > 0$ and $\mu_3 < -b(-\mu_2 + \sqrt{\Delta})/2$. When $\Delta > 0$ and $\mu_3 = -b(-\mu_2 + \sqrt{\Delta})/2$, by the following translation transformation

$$(x, y) \rightarrow \left(x + \sqrt{\frac{-\mu_2 + \sqrt{\Delta}}{2}}, y \right),$$

system (2) becomes

$$(47) \quad \begin{aligned} \dot{x} &= y, \\ \dot{y} &= (-\Delta + \mu_2\sqrt{\Delta})x + \sqrt{\frac{-\mu_2 + \sqrt{\Delta}}{2}}(2\mu_2 - 5\sqrt{\Delta})x^2 + (4\mu_2 - 5\sqrt{\Delta})x^3 \\ &\quad - 5\sqrt{\frac{-\mu_2 + \sqrt{\Delta}}{2}}x^4 - x^5 - bx^2y - 2b\sqrt{\frac{-\mu_2 + \sqrt{\Delta}}{2}}xy, \end{aligned}$$

implying that \hat{E}_{r_2} becomes the origin of system (47). Under the scaling transformation

$$(y, t) \rightarrow \left(\sqrt{\Delta - \mu_2\sqrt{\Delta}}y, \frac{t}{\sqrt{\Delta - \mu_2\sqrt{\Delta}}} \right),$$

system (47) can be written as

$$(48) \quad \begin{aligned} \dot{x} &= y, \\ \dot{y} &= -x + \frac{\sqrt{-\mu_2 + \sqrt{\Delta}}}{\sqrt{2\Delta - \mu_2\sqrt{2\Delta}}}(2\mu_2 - 5\sqrt{\Delta})x^2 + \frac{4\mu_2 - 5\sqrt{\Delta}}{\Delta - \mu_2\sqrt{\Delta}}x^3 - 5\frac{\sqrt{-\mu_2 + \sqrt{\Delta}}}{\sqrt{2\Delta - \mu_2\sqrt{2\Delta}}}x^4 \\ &\quad - \frac{1}{\Delta - \mu_2\sqrt{\Delta}}x^5 - \frac{b}{\sqrt{\Delta - \mu_2\sqrt{\Delta}}}x^2y - \sqrt{2}b\frac{\sqrt{-\mu_2 + \sqrt{\Delta}}}{\sqrt{\Delta - \mu_2\sqrt{\Delta}}}xy. \end{aligned}$$

From [8, p.211], we calculate the first focal value for system (48) and get that at the origin

$$g_3 = \frac{b(2\sqrt{\Delta} - \mu_2)}{4\sqrt{\Delta}\sqrt{\Delta - \mu_2\sqrt{\Delta}}} > 0$$

because of $\mu_2 < \sqrt{\Delta}$. Hence the origin of system (48) is an unstable weak focus of order one and so is \hat{E}_{r_2} . By the symmetry of system (2) about the origin, \hat{E}_{l_2} is an unstable weak focus of order one.

As $\Delta = 0$ and $\mu_3 = b\mu_2/2$, by the following translation transformation

$$(x, y) \rightarrow \left(x + \sqrt{\frac{-\mu_2}{2}}, y \right),$$

system (2) becomes

$$(49) \quad \begin{aligned} \dot{x} &= y, \\ \dot{y} &= \mu_2\sqrt{-2\mu_2}x^2 + 4\mu_2x^3 - 5\sqrt{\frac{-\mu_2}{2}}x^4 - x^5 - b\sqrt{-2\mu_2}xy - bx^2y \end{aligned}$$

implying that \hat{E}_{r_2} becomes the origin of system (49). It follows from [24, Theorem 7.3 of Chapter 2] that the origin of system (49) is a cusp and so is \hat{E}_{r_2} . By the symmetry of system (2) about the origin, \hat{E}_{l_2} is a cusp for $\Delta = 0$ and $\mu_3 = b\mu_2/2$.

When $\Delta = 0$ and $\mu_3 \neq b\mu_2/2$, using the translation transformation $(x, y) \rightarrow (x + \sqrt{-\mu_2/2}, y)$, system (2) can be rewritten as

$$(50) \quad \begin{aligned} \dot{x} &= y, \\ \dot{y} &= \mu_2\sqrt{-2\mu_2}x^2 + 4\mu_2x^3 - 5\sqrt{\frac{-\mu_2}{2}}x^4 - x^5 + (-\mu_3 + \frac{b\mu_2}{2})y - b\sqrt{-2\mu_2}xy - bx^2y \end{aligned}$$

meaning that \hat{E}_{r2} becomes the origin of system (50). For simplicity, denote $k =: \mu_3 - b\mu_2/2$. Then, using the translation transformation $(x, y) \rightarrow (x - y/k, y)$, system (50) is changed into

$$(51) \quad \begin{aligned} \dot{x} &= \frac{\mu_2\sqrt{-2\mu_2}}{k}(x - \frac{y}{k})^2 + \frac{4\mu_2}{k}(x - \frac{y}{k})^3 - \frac{5}{k}\sqrt{\frac{-\mu_2}{2}}(x - \frac{y}{k})^4 - \frac{1}{k}(x - \frac{y}{k})^5 \\ &\quad - \frac{b}{k}\sqrt{-2\mu_2}(x - \frac{y}{k})y - \frac{b}{k}(x - \frac{y}{k})^2y, \\ \dot{y} &= \mu_2\sqrt{-2\mu_2}(x - \frac{y}{k})^2 + 4\mu_2(x - \frac{y}{k})^3 - 5\sqrt{\frac{-\mu_2}{2}}(x - \frac{y}{k})^4 - (x - \frac{y}{k})^5 \\ &\quad - b\sqrt{-2\mu_2}(x - \frac{y}{k})y - b(x - \frac{y}{k})^2y - ky. \end{aligned}$$

Solving $\dot{y} = 0$ of system (51), we get

$$(52) \quad y = \frac{\mu_2\sqrt{-2\mu_2}}{k}x^2 + O(x^3)$$

by the Implicit Function Theorem. Substituting (52) into the first equation of (51), we have

$$\frac{dx}{dt} = \frac{\mu_2\sqrt{-2\mu_2}}{k}x^2 + O(x^3).$$

We know $\mu_2 = -2\sqrt{\mu_1}$ by **Case (VI)**. It can easily be checked that $k > 0$ for $\mu_3 > b\mu_2/2$ and $k < 0$ for $\mu_3 < b\mu_2/2$. Based on [24, Theorem 7.1 of Chapter 2], it follows that the origin of system (51) is a saddle-node with one stable nodal sector for $\mu_3 > b\mu_2/2$ or a saddle-node with unstable nodal sector for $\mu_3 < b\mu_2/2$. So is \hat{E}_{r2} . By the symmetry of system (2) about the origin, \hat{E}_{l2} is a saddle-node with one stable nodal sector for $\mu_3 > b\mu_2/2$ or a saddle-node with unstable nodal sector for $\mu_3 < b\mu_2/2$ when $\Delta = 0$.

The Jacobian matrices at both \hat{E}_{l1} and \hat{E}_{r1} are the following form

$$J_{\hat{E}_{l1}} = J_{\hat{E}_{r1}} := \begin{pmatrix} 0 & 1 \\ -\Delta - \mu_2\sqrt{\Delta} & -\mu_3 - \frac{b(-\mu_2 - \sqrt{\Delta})}{2} \end{pmatrix}.$$

By **Case (I)**, we know that the necessary conditions of the existence of \hat{E}_{l1} and \hat{E}_{r1} are $\Delta > 0$ and $\mu_2 < -\sqrt{\Delta}$. Then, we have $\det J_{\hat{E}_{l1}} = \det J_{\hat{E}_{r1}} = \Delta + \mu_2\sqrt{\Delta} < 0$. Therefore, both \hat{E}_{l1} and \hat{E}_{r1} are saddles. The proof of Lemma 4 is complete. \square

APPENDIX C

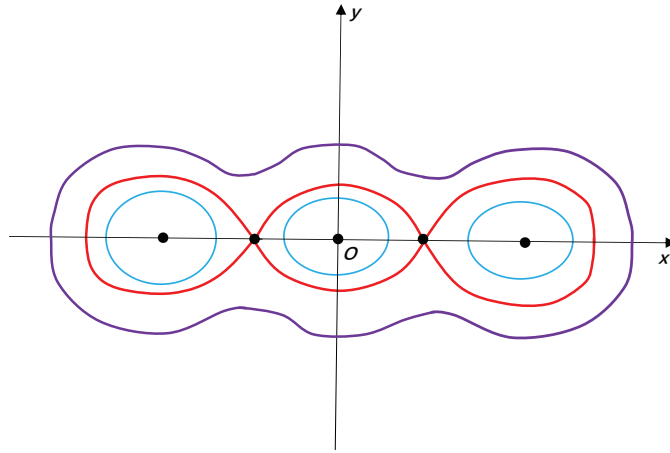


FIGURE 24. The phase portrait of (53).

When $\delta = 0$, system (4) is a Hamiltonian system

$$(53) \quad \begin{aligned} \dot{x} &= y, \\ \dot{y} &= -x(a_1 + x^2)(-1 + x^2), \end{aligned}$$

which has the first integral (8). The level curves $\{E(x, y) = e, e \geq e_1\}$ are shown in Figure 24, where $e_1 := \min\{0, -a_1/4 - 1/12\}$. In this proof, we only care these closed orbits surrounding five equilibria, i.e., $\{E(x, y) = e, e > e_2\}$, where $e_2 := a_1^2/4 + a_1^3/12$. Let $L := \{(x, y) | x = 0, y > \sqrt{2e_2}\}$. Then, the large closed level curve intersects L at exactly one point $(0, \alpha(e))$. Thus, L can be parameterized by e . For every $e \in (e_2, +\infty)$, consider the orbit of system (53) passing through $P_e \in L$. When the orbit goes forward and backward from P_e , it has respectively two intersection points Q_1 and Q_2 with the positive x -axis. Let the piece of orbit from Q_1 to Q_2 denote by $\gamma(e, \delta, a_2)$. Clearly, $\gamma(e, \delta, a_2)$ is an orbit if and only if $Q_1 = Q_2$. Moreover, $Q_1 = Q_2$ if and only if $E(Q_1) = E(Q_2)$. It is to notice that

$$\frac{dE}{dt} \Big|_{(2)} dt = -\delta(a_2 + x^2)y^2 dt = -\delta(a_2 + x^2)y dx,$$

implying that

$$E(Q_2) - E(Q_1) = \int_{t(Q_1)}^{t(Q_2)} \frac{dE}{dt} \Big|_{(2)} dt = - \int_{\gamma} \delta(a_2 + x^2)y dx.$$

Thus, $\gamma(e, \delta, a_2)$ is a closed orbit if and only if $\int_{\gamma} (a_2 + x^2)y dx = 0$. Let

$$F(e, \delta, \zeta) = \int_{\gamma} (a_2 + x^2)y dx.$$

By the same way as Lemma 1.5 of [8, Chapter 4], we can prove that the function $F(e, \delta, a_2)$ is continuous and C^∞ in δ and a_2 on a set

$$U = \{(e, a_2) | e_2 \leq e < +\infty, 0 \leq \delta \leq \delta_0, \zeta_1 \leq a_2 \leq \zeta_2\},$$

where δ_0 is positive and $\zeta_1 < \zeta_2$ are constants. Moreover, $F \in C^\infty$ in h on the set

$$V = \{(e, b, \zeta) | e_2 < e < +\infty, 0 \leq \delta \leq \delta_0, \zeta_1 \leq a_2 \leq \zeta_2\}.$$

By Taylor expansion, it follows that

$$F(e, \delta, \zeta) = F(e, 0, \zeta) + O(\delta),$$

where

$$F(e, 0, \zeta) = \oint_{\Gamma_e} (a_2 + x^2)y dx = a_2 I_0(e) + I_2(e),$$

$I_i(e) = \oint_{\Gamma_e} x^i y dx$ for $i = 0, 2$ and Γ_e is the large closed orbit of system (53). Let

$$P(h) = \frac{I_2(e)}{I_0(e)},$$

where $e \geq e_2$. By

$$y = \sqrt{2e + a_1 x^2 - \frac{(a_1 - 1)x^4}{2} - \frac{x^6}{3}},$$

it follows that

$$(54) \quad I'_i(e) = \oint_{\Gamma_e} \frac{x^i}{y} dx, \quad \text{for } i \in \mathbb{N}.$$

On the one hand, it follows from (54) that

$$(55) \quad I_i(e) = 2 \int_{-\eta(e)}^{\eta(e)} \frac{x^i y^2}{y} dx = 2e I'_i(e) + a_1 I'_{i+2}(e) - \frac{a_1 - 1}{2} I'_{i+4}(e) - \frac{1}{3} I'_{i+6}(e).$$

On the other hand, by an integration by parts, we have

$$(56) \quad I_i(e) = 2 \left(\frac{x^{i+1} y}{i+1} \Big|_{-\eta(e)}^{\eta(e)} - \frac{1}{i+1} \int_{-\eta(e)}^{\eta(e)} \frac{x^{i+1} (a_1 x - (a_1 - 1)x^3 - x^5)}{y} dx \right).$$

By $y(-\eta(e), e) = y(\eta(e), e) = 0$ and (56), it follows that

$$(57) \quad I_i(e) = -\frac{a_1 I'_{i+2}(e)}{i+1} + \frac{(a_1 - 1)I'_{i+4}(e)}{i+1} + \frac{I'_{i+6}(e)}{i+1}.$$

Taking $i = 0, 2, 4$ in (57) and solving $I'_6(e), I'_8(e), I'_{10}(e)$, we obtain

$$(58) \quad \begin{aligned} I'_6(e) &= I_0(e) + a_1 I'_2(e) - (a_1 - 1)I'_4(e), \\ I'_8(e) &= (1 - a_1)I_0(e) + 3I_2(e) - (a_1 - 1)a_1 I'_2(e) + (a_1^2 - a_1 + 1)I'_4(e), \\ I'_{10}(e) &= (a_1^2 - a_1 + 1)I_0(e) - 3(a_1 - 1)I_2(e) + 5I_4(e) + a_1(a_1^2 - a_1 + 1)I'_2(e) \\ &\quad - (a_1 - 1)(1 + a_1^2)I'_4(e). \end{aligned}$$

Taking $i = 0, 2, 4$ in (55) and using (58), we obtain that

$$(59) \quad \begin{aligned} I_0(e) &= \frac{3e}{2}I'_0(e) + \frac{a_1}{2}I'_2(e) + \frac{1 - a_1}{8}I'_4(e), \\ I_2(e) &= \frac{(1 - a_1)e}{8}I'_0(e) + \frac{a_1 - a_1^2 + 8e}{8}I'_2(e) + \frac{9 + 14a_1 + 9a_1^2}{96}I'_4(e), \\ I_4(e) &= \frac{3(5 + 6a_1 + 5a_1^2)e}{128}I'_0(e) + \frac{3(5a_1 + 6a_1^2 + 5a_1^3 + 8e - 8a_1e)}{128}I'_2(e) \\ &\quad + \frac{45 + 73a_1 - 73a_1^2 - 45a_1^3 + 384e}{512}I'_4(e). \end{aligned}$$

Letting $V = (I_0(e), I_2(e), I_4(e))^T$, then by (59), we have

$$(60) \quad (12Ie + C)V' = RV,$$

where I is a unit matrix of order 3, and

$$(61) \quad C = \begin{pmatrix} 0 & 4a_1 & 1 - a_1 \\ 0 & a_1(1 - a_1) & (1 + a_1)^2 \\ 0 & a_1(1 + a_1)^2 & 1 + 2a_1 - 2a_1^2 - a_1^3 \end{pmatrix}, \quad R = \begin{pmatrix} 8 & 0 & 0 \\ a_1 - 1 & 12 & 0 \\ -(1 + a_1)^2 & 3(a_1 - 1) & 16 \end{pmatrix}.$$

Taking

$$(62) \quad Z(e) = \frac{3}{4}(a_1 - 1)I_2(e) + I_4(e)$$

and using (60), we have

$$(63) \quad D(e) \begin{pmatrix} I''_0(e) \\ I''_2(e) \\ Z''(e) \end{pmatrix} = \begin{pmatrix} a_{11}(e) & a_{12}(e) \\ a_{21}(e) & a_{22}(e) \\ a_{31}(e) & a_{32}(e) \end{pmatrix} \begin{pmatrix} I'_0(e) \\ Z'(e) \end{pmatrix},$$

where

$$(64) \quad \begin{aligned} D(e) &= 3e(3a_1 + 12e + 1)(-a_1^3 - 3a_1^2 + 12e), \\ a_{11}(e) &= -3e(3 + 7a_1 - 7a_1^2 - 3a_1^3 + 48e), \\ a_{12}(e) &= 10a_1^2 + 3a_1^3 - 12e + 3a_1(1 + 4e), \\ a_{21}(e) &= 3e(10a_1^2 + 3a_1^3 - 12e + 3a_1(1 + 4e)), \\ a_{22}(e) &= -12(1 + a_1)^2e, \\ a_{31}(e) &= -\frac{9}{4}e(-7a_1^3 - 3a_1^4 + 4e + a_1^2(7 + 4e) + a_1(3 + 56e)), \\ a_{32}(e) &= -3(-3 - 7a_1 + 7a_1^2 + 3a_1^3 - 48e)e. \end{aligned}$$

Let $M(e) = a_2 I_0(e) + I_2(e)$. By (62) and (63),

$$(65) \quad \begin{aligned} M''(e) &= \frac{(a_2 a_{11}(e) + a_{21}(e))I_0'(e) + (a_2 a_{12}(e) + a_{22}(e))Z'(e)}{D(e)} \\ &= \frac{I_0'(e)}{D(e)} (a_2 a_{11}(e) + a_{21}(e) + (a_2 a_{12}(e) + a_{22}(e))w(e)), \end{aligned}$$

where

$$(66) \quad w(e) = \frac{Z'(e)}{I_0'(e)}$$

satisfies the differential equation

$$(67) \quad \begin{aligned} \dot{e} &= 12e(1 + 3a_1 + 12e)(-3a_1^2 - a_1^3 + 12e), \\ \dot{w} &= v_0(e) + v_1(e)w + v_2(e)w^2, \end{aligned}$$

and

$$(68) \quad \begin{aligned} v_0(e) &= -9e(3a_1 + 7a_1^2 - 7a_1^3 - 3a_1^4 + 4e + 56a_1e + 4a_1^2e), \\ v_1(e) &= 24e(3 + 7a_1 - 7a_1^2 - 3a_1^3 + 48e), \\ v_2(e) &= -4(3a_1 + 10a_1^2 + 3a_1^3 - 12e + 12a_1e). \end{aligned}$$

In the following, we will split some cases to study the number of zeros of $M''(e)$ in (65) for $e > e_2$.

First, we consider $a_1 = -1/3$. In the case, $e_2 = 2/81$, and

$$M''(e) = -\frac{(3a_2 + 1)(w(e) + 9e)I_0'(e)}{e(81e - 2)}, \quad e > e_2.$$

Notice that $a_2 < \min\{a_1, -1/3\} = -1/3$. Thus, the number of zeros of $M''(e)$ in $(e_2, +\infty)$ equals the number of intersection points of the curve $\Gamma = \{(e, w) \mid w = w(e), e \in (e_2, \infty)\}$ and the straight line $\mathcal{L} = \{(e, w) \mid w + 9e = 0, e \in (e_2, \infty)\}$ in the (e, w) plane.

Using (63), we have the asymptotic expansion of $w(e)$ near $e \rightarrow e_2^+$

$$(69) \quad w(e) = -\frac{2}{9} - \frac{2}{3 \log(e - e_2)} + o\left(\frac{1}{\log(e - e_2)}\right),$$

and the asymptotic expansion of $w(e)$ when $e \rightarrow +\infty$

$$w(e) = c_0 e^{\frac{2}{3}} + o\left(e^{\frac{2}{3}}\right),$$

where c_0 is a positive constant. In this case, $w(e)$ satisfies the differential equation

$$(70) \quad \begin{aligned} \dot{e} &= e(81e - 2), \\ \dot{w} &= 3(w^2 + 18ew + 2e). \end{aligned}$$

Notice that the horizontal isocline of this system has two branches

$$w^+(e) = -9e + \sqrt{81e^2 - 2e}, \quad w^-(e) = -9e - \sqrt{81e^2 - 2e}.$$

Moreover, $w^+(e)$ has the asymptotic expansion near $e \rightarrow e_2^+$

$$(71) \quad w^+(e) = -\frac{2}{9} + \sqrt{2}\sqrt{e - e_2} - 9(e - e_2) + o(e - e_2).$$

Comparing (69) with (71), we have

$$w(e) > w^+(e), \quad e \rightarrow e_2.$$

It follows from system (70) that

$$\frac{dw}{de} > 0, \quad \text{for } w > w^+(e), \quad e > e_2.$$

Thus, we have $w(e) > w^+(e)$ for all $e \in (e_2, +\infty)$. Further, we obtain

$$w(e) > w^+(e) > -9e, \quad e \in (e_2, +\infty).$$

This implies that the curve Γ and the straight line \mathcal{L} have no intersection points in the (e, w) plane. Hence, the function $M''(e)$ has no zeros in $(e_2, +\infty)$. And we obtain that $M(e)$ has at most two zeros in $(e_2, +\infty)$.

When $a_1 \neq -\frac{1}{3}$, denote

$$A(e) = a_2 a_{11}(e) + a_{21}(e), \quad \text{and} \quad B(e) = a_2 a_{12}(e) + a_{22}(e),$$

where a_{ij} 's are given in (64). Obviously, $B(e)$ is a polynomial of e with degree at most 1. And it is not identically zero. Thus, the number of zeros of $M''(e)$ in $(e_2, +\infty)$ equals the number of intersection points of the curve $\Gamma = \{(e, w) \mid w = w(e), e \in (e_2, \infty)\}$ and the curve $\mathcal{C} = \{(e, w) \mid A(e) + B(e)w = 0, e \in (e_2, \infty)\}$ in the (e, w) plane.

Using (63), we have the asymptotic expansion of $w(e)$ near $e \rightarrow e_2^+$

$$(72) \quad w(e) = \frac{1}{4}a_1(3 + a_1) + \frac{3a_1(1 + a_1)}{\log(e - e_2)} + o\left(\frac{1}{\log(e - e_2)}\right),$$

and the asymptotic expansion of $w(e)$ when $e \rightarrow +\infty$

$$(73) \quad w(e) = c_1 e^{\frac{2}{3}} + o\left(e^{\frac{2}{3}}\right), \quad c_1 > 0.$$

Note that the horizontal isocline of system (67) has two branches

$$w^+(e) = \frac{-v_1(e) + \sqrt{v_1(e)^2 - 4v_0(e)v_2(e)}}{2v_2(e)}, \quad w^-(e) = \frac{-v_1(e) - \sqrt{v_1(e)^2 - 4v_0(e)v_2(e)}}{2v_2(e)},$$

where $v_i(e), i = 0, 1, 2$ are given in (68), and for $e > e_2$

$$v_2(e) > v_2(e_2) = -4a_1(1 + a_1)^2(3 + a_1) > 0,$$

$$v_1^2(e) - 4v_0(e)v_2(e) = 144e(3a_1^3 + 7a_1^2 - 7a_1 - 64e - 3)(a_1^3 + 3a_1^2 - 12e)(3a_1 + 12e + 1) > 0.$$

Moreover, $w^+(e)$ has the asymptotic expansion

$$(74) \quad w^+(e) = \frac{1}{4}a_1(a_1 + 3) + \frac{\sqrt{3}}{2} \sqrt{\frac{7a_1^2 + 6a_1 + 3}{a_1 + 1}} \sqrt{e - e_2} + \frac{3(4a_1^2 + 3a_1 + 1)(e - e_2)}{a_1(a_1 + 1)^2} + o(e - e_2).$$

Comparing (72) with (74), we have $w(e) > w^+(e)$ as $e \rightarrow e_2$. It follows from system (67) that

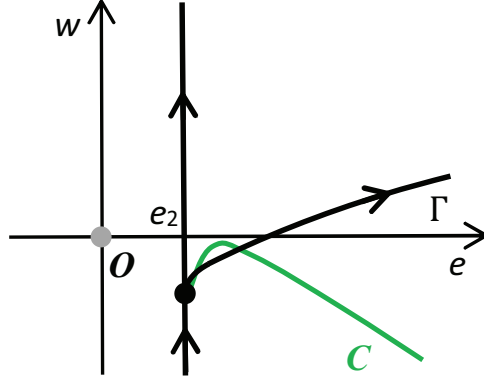
$$\frac{dw}{de} > 0, \quad \text{for } w > w^+(e), \quad e > e_2.$$

Thus, we have $w(e) > w^+(e)$ for all $e \in (e_2, +\infty)$.

For the curve \mathcal{C} , denote $w_{\mathcal{C}}(e) = -\frac{A(e)}{B(e)}$. Moreover, denote by l_1 the curve $a_2 = -\frac{(1+a_1)^2}{1-a_1}$. It is easy to verify that $\frac{da_2}{da_1} = \frac{(-3+a_1)(1+a_1)}{(-1+a_1)^2} < 0$ for $-1 < a_1 < 0$, and $a_2 = 0$ when $a_1 = -1$, $a_2 = -\frac{1}{3}$ when $a_1 = -\frac{1}{3}$ and $a_2 = -1$ when $a_1 = 0$. That is, the curve l_1 passing through $(-1, 0)$, $(-\frac{1}{3}, -\frac{1}{3})$ and $(0, -1)$ is decreasing on $(-1, 0)$. Thus, the curve l_1 intersects the line $a_2 = a_1$ at $A = (-\frac{1}{3}, -\frac{1}{3})$ and is above the line $a_2 = a_1$ when $-1 < a_1 < -\frac{1}{3}$, and the curve l_1 intersects the curve $a_2 = \frac{a_1 - 1 - \sqrt{-a_1}}{3}$ with $B = (a_1^*, a_2^*)$ with $a_1^* = \frac{1}{16}(-33 - \sqrt{97} + \sqrt{930 + 66\sqrt{97}}) \approx -0.19$, such that $\frac{a_1 - 1 - \sqrt{-a_1}}{3} < -\frac{(1+a_1)^2}{1-a_1} < -\frac{1}{3}$ when $-\frac{1}{3} < a_1 < a_1^*$ and the curve l_1 is below the curve $a_2 = \frac{a_1 - 1 - \sqrt{-a_1}}{3}$ when $a_1^* < a_1 < 0$, see Figure 25.

When $a_2 = -\frac{(1+a_1)^2}{1-a_1}$,

$$w_{\mathcal{C}}(e) = \frac{3e(12e - a_1^3 - 2a_1^2 + 2a_1 + 1)}{a_1(a_1 + 1)^2}.$$

FIGURE 25. The graphs of the curves of \mathcal{C} and Γ .

Since $w_{\mathcal{C}}(e_2) = \frac{1}{4}a_1(a_1 + 3)$ and

$$w'_{\mathcal{C}}(e) = \frac{3(24e - a_1^3 - 2a_1^2 + 2a_1 + 1)}{a_1(a_1 + 1)^2} < \frac{3(a_1^3 + 4a_1^2 + 2a_1 + 1)}{a_1(a_1 + 1)^2} < 0, \quad e > e_2.$$

Thus, $w_{\mathcal{C}}(e) < w_{\mathcal{C}}(e_2) < w(e)$, when $e > e_2$. For this case, the function $M''(e)$ has no zeros in $(e_2, +\infty)$. When $a_2 \neq -\frac{(1+a_1)^2}{1-a_1}$,

$$w_{\mathcal{C}}(e) = \frac{3(-1 + a_1 - 4a_2)e(e - \bar{e}_1)}{(1 + 2a_1 + a_1^2 + a_2 - a_1a_2)(e - \bar{e}_2)}, \quad w'_{\mathcal{C}}(e) = \frac{3(-1 + a_1 - 4a_2)(e^2 - 2\bar{e}_2e + \bar{e}_1\bar{e}_2)}{(1 + 2a_1 + a_1^2 + a_2 - a_1a_2)(e - \bar{e}_2)^2},$$

where

$$\bar{e}_1 = -\frac{(3 + a_1)(1 + 3a_1)(a_1 - a_2 + a_1a_2)}{12(-1 + a_1 - 4a_2)}, \quad \bar{e}_2 = \frac{a_1(3 + a_1)(1 + 3a_1)a_2}{12(1 + 2a_1 + a_1^2 + a_2 - a_1a_2)}.$$

Notice that $\frac{a_1 - 1 - \sqrt{-a_1}}{3} < a_2 < \min\{a_1, -\frac{1}{3}\}$ with $-1 < a_1 < 0$. Thus, $a_2 < a_1$ and $-1 + a_1 - 4a_2 > -1 - 3a_2 > 0$, implying that

$$(75) \quad \begin{aligned} \bar{e}_1 &> 0, \quad \text{for } -1 < a_1 < -\frac{1}{3}, \\ \bar{e}_1 &< 0, \quad \text{for } -\frac{1}{3} < a_1 < 0, \\ e_2 - \bar{e}_1 &= \frac{(1 + a_1)^2(3 + a_1)(a_1 - a_2)}{12(-1 + a_1 - 4a_2)} > 0. \end{aligned}$$

Moreover, we have

$$e_2 - \bar{e}_2 = \frac{a_1(1 + a_1)^2(3 + a_1)(a_1 - a_2)}{12(1 + 2a_1 + a_1^2 + a_2 - a_1a_2)} > 0$$

if $a_2 < -\frac{(1+a_1)^2}{1-a_1}$, and

$$(76) \quad e_2 - \bar{e}_2 = \frac{a_1(1 + a_1)^2(3 + a_1)(a_1 - a_2)}{12(1 + 2a_1 + a_1^2 + a_2 - a_1a_2)} < 0$$

if $a_2 > -\frac{(1+a_1)^2}{1-a_1}$. It follows that when $a_2 < -\frac{(1+a_1)^2}{1-a_1}$, only the right half branch of the curve $w_{\mathcal{C}}(e)$ is located at $e > e_2$ and

$$w_{\mathcal{C}}(e) = \frac{3(-1 + a_1 - 4a_2)e(e - \bar{e}_1)}{(1 + 2a_1 + a_1^2 + a_2 - a_1a_2)(e - \bar{e}_2)} < 0,$$

while when $a_2 > -\frac{(1+a_1)^2}{1-a_1}$, the curve $w_{\mathcal{C}}(e)$ has two branches for $e > e_2$ and

$$w_{\mathcal{C}}(e) = \frac{3(-1 + a_1 - 4a_2)e(e - \bar{e}_1)}{(1 + 2a_1 + a_1^2 + a_2 - a_1a_2)(e - \bar{e}_2)} < 0, \quad \text{if } e_2 < e < \bar{e}_2,$$

and

$$w_C(e) = \frac{3(-1 + a_1 - 4a_2)e(e - \bar{e}_1)}{(1 + 2a_1 + a_1^2 + a_2 - a_1a_2)(e - \bar{e}_2)} > 0, \text{ if } e > \bar{e}_2 > e_2.$$

Moreover, since

$$\bar{e}_2^2 - \bar{e}_1\bar{e}_2 = \frac{a_1a_2(1 + a_1)^2(3 + a_1)^2(1 + 3a_1)^2(a_1 - a_2)(1 + a_2)}{144(-1 + a_1 - 4a_2)(1 + 2a_1 + a_1^2 + a_2 - a_1a_2)^2} > 0$$

when $a_2 < -\frac{(1+a_1)^2}{1-a_1}$, we obtain that the curve $w_C(e)$ is increasing on the interval $(\bar{e}_2, \bar{e}_2 + \sqrt{\bar{e}_2^2 - \bar{e}_1\bar{e}_2})$ and decreasing on the interval $(\bar{e}_2 + \sqrt{\bar{e}_2^2 - \bar{e}_1\bar{e}_2}, +\infty)$. When $a_2 > -\frac{(1+a_1)^2}{1-a_1}$, we have that the curve $w_C(e)$ is decreasing on the interval $(\bar{e}_2 - \sqrt{\bar{e}_2^2 - \bar{e}_1\bar{e}_2}, \bar{e}_2) \cup (\bar{e}_2, \bar{e}_2 + \sqrt{\bar{e}_2^2 - \bar{e}_1\bar{e}_2})$ and increasing on the interval $(\bar{e}_2 + \sqrt{\bar{e}_2^2 - \bar{e}_1\bar{e}_2}, +\infty)$.

When $a_2 < -\frac{(1+a_1)^2}{1-a_1}$, compare e_2 with $\bar{e}_2 + \sqrt{\bar{e}_2^2 - \bar{e}_1\bar{e}_2}$. A direct computation shows that

$$(77) \quad \bar{e}_2^2 - \bar{e}_1\bar{e}_2 - (e_2 - \bar{e}_2)^2 = \frac{a_1(1 + a_1)^2(3 + a_1)^2(a_1 - a_2)(1 + 3a_1 + 4a_1^2)}{144(-1 + a_1 - 4a_2)(1 + 2a_1 + a_1^2 + a_2 - a_1a_2)} \left(a_2 - \frac{(-1 + a_1)a_1^2}{1 + 3a_1 + 4a_1^2} \right).$$

Denote by l_2 the curve $a_2 = \frac{(-1+a_1)a_1^2}{1+3a_1+4a_1^2}$. It is easy to verify that $\frac{da_2}{da_1} = \frac{2a_1(1+a_1)^2(2a_1-1)}{(1+3a_1+4a_1^2)^2} > 0$ for $-1 < a_1 < 0$, and $a_2 = -1$ when $a_1 = -1$, $a_2 = -\frac{1}{3}$ when $a_1 = -\frac{1}{3}$ and $a_2 = 0$ when $a_1 = 0$. That is, the curve l_2 passing through $(-1, -1)$, $(-\frac{1}{3}, -\frac{1}{3})$ and $(0, 0)$ is increasing on $(-1, 0)$. Owing to

$$\left. \frac{da_2}{da_1} \right|_{a_1=-1} = 0 \quad \text{and} \quad \left. \frac{d}{da_1} \left(\frac{a_1 - 1 - \sqrt{-a_1}}{3} \right) \right|_{a_1=-1} = \frac{1}{2},$$

we obtain that the curve l_2 intersects the curve $a_2 = \frac{a_1 - 1 - \sqrt{-a_1}}{3}$ at $C = (a_1^{**}, a_2^{**})$ with $a_1^{**} \approx -0.49$ and intersects the line $a_2 = a_1$ at A , see Figure 25. Two cases are considered.

(i) When $a_2 \leq \frac{(-1+a_1)a_1^2}{1+3a_1+4a_1^2}$, $\bar{e}_2^2 - \bar{e}_1\bar{e}_2 - (e_2 - \bar{e}_2)^2 \leq 0$ from (77), thus we have

$$\bar{e}_2 + \sqrt{\bar{e}_2^2 - \bar{e}_1\bar{e}_2} - e_2 = \sqrt{\bar{e}_2^2 - \bar{e}_1\bar{e}_2} - (e_2 - \bar{e}_2) \leq 0.$$

Hence, the curve $w_C(e)$ is decreasing on the interval $(e_2, +\infty)$. Combing with

$$w_C(e_2) = \frac{1}{4}a_1(a_1 + 3),$$

it follows that for $e > e_2$,

$$w_C(e) < w_C(e_2) < w(e),$$

which implies that the function $M''(e)$ has no zeros in $(e_2, +\infty)$ when $(a_1, a_2) \in G_1$. And we obtain that $M(e)$ has at most two zeros in $(e_2, +\infty)$.

(ii) When $a_2 > \frac{(-1+a_1)a_1^2}{1+3a_1+4a_1^2}$, $\bar{e}_2^2 - \bar{e}_1\bar{e}_2 - (e_2 - \bar{e}_2)^2 > 0$ from (77), thus we have

$$\bar{e}_2 + \sqrt{\bar{e}_2^2 - \bar{e}_1\bar{e}_2} - e_2 = \sqrt{\bar{e}_2^2 - \bar{e}_1\bar{e}_2} - (e_2 - \bar{e}_2) > 0.$$

Hence, the function $w(e)$ is increasing on the interval $(e_2, \bar{e}_2 + \sqrt{\bar{e}_2^2 - \bar{e}_1\bar{e}_2})$ and is decreasing on the interval $(\bar{e}_2 + \sqrt{\bar{e}_2^2 - \bar{e}_1\bar{e}_2}, +\infty)$. Notice that near $e \rightarrow e_2^+$

$$(78) \quad w_C(e) = \frac{1}{4}a_1(a_1 + 3) + \frac{3((-1 + a_1)a_1^2 - (1 + 3a_1 + 4a_1^2)a_2)}{a_1(1 + a_1)^2(a_1 - a_2)}(e - e_2) + o(e - e_2),$$

and

$$(79) \quad w_C(e) \rightarrow -\infty, \text{ when } e \rightarrow +\infty.$$

Comparing the results in (72), (73), (78) and (79), we have

$$(80) \quad \begin{aligned} w_{\mathcal{C}}(e) &< w(e), \text{ when } e \rightarrow e_2^+, \\ w_{\mathcal{C}}(e) &< w(e), \text{ when } e \rightarrow +\infty. \end{aligned}$$

We claim that the function $M''(e)$ has at most two zeros in $(e_2, +\infty)$ when $(a_1, a_2) \in G_2$. To prove this, we show that there exists exactly one point of the curve \mathcal{C} at which the vector field (67) is tangent on the curve \mathcal{C} . We call it the contact point. A direct computation gives that

$$(81) \quad \left. \frac{dw_{\mathcal{C}}(e)}{de} - \frac{dw(e)}{de} \right|_{w=w_{\mathcal{C}}(e)} = -\frac{3}{4B^2(e)}\Psi(e),$$

where

$$(82) \quad \begin{aligned} \Psi(e) &= \psi_2 e^2 + \psi_1 e + \psi_0 \\ &= -48(a_1 - 4a_2 - 1)(5a_1^2 - 8a_1 a_2 + 6a_1 + 8a_2 + 5)e^2 + 4(a_1 + 3)(3a_1 + 1) \\ &\quad (6a_1^3 a_2 + 3a_1^3 - 3a_1^2 a_2^2 + 30a_1^2 a_2 + 10a_1^2 - 74a_1 a_2^2 - 30a_1 a_2 + 3a_1 - 3a_2^2 - 6a_2)e \\ &\quad + a_1(a_1 + 3)^2(3a_1 + 1)^2 a_2(3a_1 a_2 + 4a_1 - 3a_2). \end{aligned}$$

Denote by l_3 the curve $a_2 = \frac{5+6a_1+5a_1^2}{8(-1+a_1)}$. It is easy to verify that $\frac{da_2}{da_1} = \frac{-11-10a_1+5a_1^2}{8(-1+a_1)^2} > 0$ for $-1 < a_1 < \frac{5-4\sqrt{5}}{5}$, and $\frac{da_2}{da_1} < 0$ for $\frac{5-4\sqrt{5}}{5} < a_1 < 0$, and $a_2 = -\frac{1}{4}$ when $a_1 = -1$, $a_2 = -\frac{1}{3}$ when $a_1 = -\frac{1}{3}$ and $a_2 = -\frac{5}{8}$ when $a_1 = 0$. That is, the curve l_3 passing through $(-1, -\frac{1}{4})$, $(-\frac{1}{3}, -\frac{1}{3})$ and $(0, -\frac{5}{8})$ is increasing on $(-1, \frac{5-4\sqrt{5}}{5})$ and is decreasing on $(\frac{5-4\sqrt{5}}{5}, 0)$. Thus, we obtain that the curve l_3 intersects the line $a_2 = a_1$ at A , and intersects the curve $a_2 = \frac{a_1-1-\sqrt{-a_1}}{3}$ at $D = (a_1^{***}, a_2^{***})$ with $a_1^{***} = \frac{1}{49} \left(-135 + 36\sqrt{11} + 4\sqrt{802 - 240\sqrt{11}} \right) \approx -0.118$, which locates between the curves l_1 and l_2 when $-\frac{1}{3} < a_1 < 0$, see Figure 25. In the region G_2 , it follows from $a_2 < \frac{5+6a_1+5a_1^2}{8(-1+a_1)}$ that $\psi_2 > 0$. Since

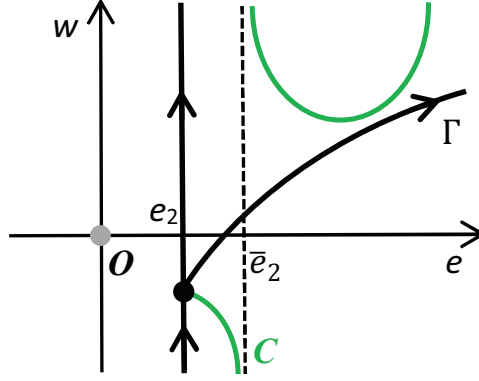
$$(83) \quad \Psi(e_2) = -\frac{1}{3}a_1(1+a_1)^2(3+a_1)^2(a_1-a_2)(-3a_1-18a_1^2+5a_1^3-9a_2-30a_1a_2-41a_1^2a_2),$$

and in the region G_2 , $-1 < a_1 < -\frac{1}{3}$ and $a_2 > \frac{(-1+a_1)a_1^2}{1+3a_1+4a_1^2}$,

$$(84) \quad \begin{aligned} -3a_1 - 18a_1^2 + 5a_1^3 - 9a_2 - 30a_1a_2 - 41a_1^2a_2 &= a_1(-3 - 18a_1 + 5a_1^2) + (-9 - 30a_1 - 41a_1^2)a_2 \\ &< -\frac{a_1(1+a_1)(1+3a_1)(3+6a_1+7a_1^2)}{1+3a_1+4a_1^2} \\ &< 0, \end{aligned}$$

we have $\Psi(e_2) < 0$ from (83) and (84). Further, $\Psi(e)$ has a unique zero in $(e_2, +\infty)$ by $\psi_2 > 0$. This confirms that there are exactly one contact point on the curve \mathcal{C} for $e > e_2$. It follows from the result in (80) that the curve \mathcal{C} and the curve Γ has at most two intersection points when $e > e_2$, otherwise, extra contact points will emerge, which results in a contradiction, see Figure 26. Therefore, the function $M(e)$ has at most four zeros on the interval $(e_2, +\infty)$ when $(a_1, a_2) \in G_2$.

Finally, we study the number of zeros of $M(e)$ on the interval $(e_2, +\infty)$ when (a_1, a_2) locates in the regions G_3 and G_4 and their intersection curve l_3 . Notice that in these regions $-\frac{1}{3} < a_1 < 0$ and $a_2 > -\frac{(1+a_1)^2}{1-a_1}$. For this case, $e_2 < \bar{e}_2$ and $\bar{e}_2 - \sqrt{\bar{e}_2^2 - \bar{e}_1\bar{e}_2} < 0 < e_2$ by (75) and (76). Thus, the function $w_{\mathcal{C}}(e)$ is decreasing on the interval $(e_2, \bar{e}_2) \cup (\bar{e}_2, \bar{e}_2 + \sqrt{\bar{e}_2^2 - \bar{e}_1\bar{e}_2})$ and is increasing on the interval $(\bar{e}_2 + \sqrt{\bar{e}_2^2 - \bar{e}_1\bar{e}_2}, +\infty)$.


 FIGURE 26. The graphs of the curves of \mathcal{C} and Γ .

Notice that near $e \rightarrow e_2^+$, $w_{\mathcal{C}}(e)$ has the asymptotic expansion (78), and

$$(85) \quad \begin{aligned} w_{\mathcal{C}}(e) &\rightarrow -\infty, \text{ when } e \rightarrow \bar{e}_2^-, \\ w_{\mathcal{C}}(e) &\rightarrow +\infty \text{ when } e \rightarrow \bar{e}_2^+, \end{aligned}$$

and when $e \rightarrow +\infty$

$$(86) \quad w_{\mathcal{C}}(e) = \frac{3(-1 + a_1 - 4a_2)}{(1 + 2a_1 + a_1^2 + a_2 - a_1a_2)}e + o(e).$$

Comparing the results in (72), (73), (78), (85) and (86), we have

$$(87) \quad \begin{aligned} w_{\mathcal{C}}(e) &< w(e), \text{ when } e \rightarrow e_2^+, \\ w_{\mathcal{C}}(e) &< w(e), \text{ when } e \rightarrow \bar{e}_2^-, \\ w_{\mathcal{C}}(e) &> w(e), \text{ when } e \rightarrow \bar{e}_2^+, \\ w_{\mathcal{C}}(e) &> w(e), \text{ when } e \rightarrow +\infty. \end{aligned}$$

By the result in (87) and the monotonicity of the function $w_{\mathcal{C}}(e)$ in (e_2, \bar{e}_2) and the function $w(e)$, we know that the curves \mathcal{C} and Γ do not have intersection points when $e \in (e_2, \bar{e}_2)$. In the following, we just need to consider $e > \bar{e}_2$.

For $(a_1, a_2) \in l_3 = \partial G_3 \cup \partial G_4$, $-\frac{1}{3} < a_1 \leq a_1^{***}$ and $a_2 = \frac{5+6a_1+5a_1^2}{8(-1+a_1)}$. One has $\psi_2 = 0$ and $\Psi(e)$ has a unique zero

$$\hat{e} = \frac{(1 - a_1)a_1(3 + a_1)(1 + 3a_1)(5 + 6a_1 + 5a_1^2)}{4(11 - 76a_1 - 126a_1^2 - 76a_1^3 + 11a_1^4)}.$$

Since

$$\hat{e} - e_2 = -\frac{(-5 + a_1)a_1(1 + a_1)^2(3 + a_1)(3 + 2a_1 + 11a_1^2)}{12(11 - 76a_1 - 126a_1^2 - 76a_1^3 + 11a_1^4)} < 0,$$

we have there is no contact point on the curve \mathcal{C} for $e > e_2$ from (81). Thus, by the result in (87), the curve \mathcal{C} and the curve Γ has no intersection points when $e > e_2$, otherwise, an extra contact point will emerge, which results in a contradiction. Therefore, the function $M(e)$ has at most two zeros on the interval $(e_2, +\infty)$ for $(a_1, a_2) \in l_3 = \partial G_3 \cup \partial G_4$.

In the region G_3 , $-\frac{1}{3} < a_1 \leq a_1^{***}$ and $a_2 < \frac{5+6a_1+5a_1^2}{8(-1+a_1)} < -\frac{1}{3}$, one has $\psi_2 > 0$ and

$$\psi_0 = a_1a_2(3 + a_1)^2(1 + 3a_1)^2(4a_1 - 3a_2 + 3a_1a_2) > a_1a_2(3 + a_1)^2(1 + 3a_1)^3 > 0.$$

A direct computation shows that

$$\begin{aligned}\psi_1 \Big|_{a_2 = \frac{5+6a_1+5a_1^2}{8(-1+a_1)}} &= \frac{5(3+a_1)^2(1+3a_1)^2(11-76a_1-126a_1^2-76a_1^3+11a_1^4)}{16(-1+a_1)^2} > 0 \\ \psi_1 \Big|_{a_2 = -\frac{(1+a_1)^2}{1-a_1}} &= \frac{4(3+a_1)^2(1+3a_1)^2(1-19a_1-44a_1^2-19a_1^3+a_1^4)}{(-1+a_1)^2} > 0 \\ \psi_1 \Big|_{a_2 = \frac{a_1-1-\sqrt{-a_1}}{3}} &= \frac{4}{9}(3+a_1)(1+3a_1)(15+12\sqrt{-a_1}+34a_1-52\sqrt{-a_1}a_1+126a_1^2 \\ &\quad + 52\sqrt{-a_1}a_1^2+34a_1^3-12\sqrt{-a_1}a_1^3+15a_1^4) > 0.\end{aligned}$$

It is also easy to verify that $\psi_1 > 0$ by considering the intersection points of the curve $\psi_1 = 0$ and l_1, l_3 and $a_2 = \frac{a_1-1-\sqrt{-a_1}}{3}$ for $a_1 \in (-\frac{1}{3}, 0)$. Thus, the function $\Psi(e)$ has no zero in $(\bar{e}_2, +\infty)$. In other words, there does not exist the contact point on the curve \mathcal{C} for $e > \bar{e}_2$ from (81) when $(a_1, a_2) \in G_3$. Similarly, by the result in (87) the curve \mathcal{C} and the curve Γ has no intersection points when $e > \bar{e}_2$. Otherwise, an extra contact point will emerge, which results in a contradiction. Therefore, the function $M(e)$ has at most two zeros on the interval $(e_2, +\infty)$ for $(a_1, a_2) \in G_3$.

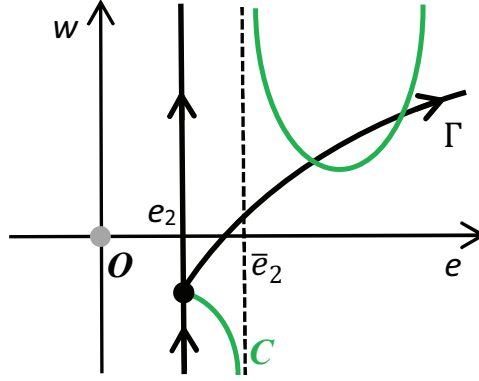


FIGURE 27. The graphs of the curves of \mathcal{C} and Γ .

In the region G_4 , $-\frac{1}{3} < a_1 < 0$ and $\frac{5+6a_1+5a_1^2}{8(-1+a_1)} < a_2 < -\frac{1}{3}$, one has $\psi_2 < 0$ and

$$\psi_0 = a_1 a_2 (3+a_1)^2 (1+3a_1)^2 (4a_1 - 3a_2 + 3a_1 a_2) > a_1 a_2 (3+a_1)^2 (1+3a_1)^3 > 0.$$

A direct computation shows that

$$(88) \quad \Psi(\bar{e}_2) = \frac{a_1(1+a_1)^2(3+a_1)^2(1+3a_1)^2(a_1-a_2)a_2(1+a_2)(15+34a_1+15a_1^2+12a_2-12a_1a_2)}{3(1+2a_1+a_1^2+a_2-a_1a_2)^2},$$

and

$$(89) \quad 15+34a_1+15a_1^2+12a_2-12a_1a_2 > \frac{5}{2}(3+a_1)(1+3a_1) > 0.$$

Hence, we have $\Psi(\bar{e}_2) > 0$ from (88) and (89). Further, $\Psi(e)$ in (82) has a unique zero in $(\bar{e}_2, +\infty)$ by $\psi_2 < 0$. This confirms that there is exactly one contact point on the curve \mathcal{C} for $e > \bar{e}_2$. It follows from the result in (87) that the curve \mathcal{C} and the curve Γ has at most two intersection points when $e > \bar{e}_2$. Otherwise, extra contact points will emerge, which results in a contradiction, see Figure 27. Therefore, the function $M(e)$ has at most four zeros on the interval $(e_2, +\infty)$ when $(a_1, a_2) \in G_4$.

¹ SCHOOL OF MATHEMATICS AND STATISTICS, HNP-LAMA, CENTRAL SOUTH UNIVERSITY, CHANGSHA, HUNAN 410083, CHINA

Email address: chen.hebai@csu.edu.cn

Email address: mathmj@csu.edu.cn, corresponding author

² SCHOOL OF MATHEMATICS, SICHUAN UNIVERSITY, CHENGDU, SICHUAN 610064, CHINA
Email address: `scuxchen@scu.edu.cn`, `xingwu.chen@hotmail.com`, **corresponding author**

³ SCHOOL OF MATHEMATICAL SCIENCES, CMA-SHANGHAI, SHANGHAI JIAO TONG UNIVERSITY, SHANGHAI, 200240, CHINA
Email address: `mathtyl@sjtu.edu.cn`